

Alma Mater Studiorum – Università di Bologna

**DOTTORATO DI RICERCA IN
CHIMICA**

Ciclo XXVI

Settore Concorsuale di afferenza: 03/C2

Settore Scientifico disciplinare: CHIM/04

**A STUDY OF NEW AND MORE SUSTAINABLE CATALYTIC
ROUTES FOR THE SYNTHESIS OF ADIPIC ACID**

Presentata da: Elena Rozhko

Coordinatore Dottorato

Relatore

Prof. Aldo Roda

Prof. Fabrizio Cavani

Esame finale anno 2014

Summary

Summary.....	1
Introduction.....	5
Adipic Acid	8
1. Physical chemical properties	8
2. Uses of Adipic acid	8
3. Production of Adipic Acid	8
3.1. Current industrial processes	9
3.1.1. Oxidation of cyclohexane to KA Oil.....	10
3.1.2. Hydrogenation of phenol to KA Oil.....	12
3.1.3. Hydration of cyclohexene to cyclohexanol.....	12
3.1.4. Oxidation of KA Oil to AA with nitric acid	13
3.1.5. Risks, disadvantages and environmental issues in AA production.....	15
3.1.6. Methods for N ₂ O abatement	16
3.1.6.1. Catalytic abatement.....	16
3.1.6.2. Thermal destruction of N ₂ O.....	17
3.1.6.3. Conversion of N ₂ O into recoverable NO	18
3.2. Alternative ways for the production of AA	19
3.2.1. Oxidation of cyclohexane to KA Oil.....	19
3.2.1.1. Homogeneous oxidation of cyclohexane.....	19
3.2.1.2. Heterogeneous cyclohexane oxidation.....	19
3.2.2. Oxidation of KA oil	20
3.2.2.1. Oxygen as the oxidant	20
3.2.2.2. Hydrogen peroxide as the oxidant.....	21
3.2.3. Direct oxidation of cyclohexane to AA.....	21
3.2.4. Alternative starting materials	23
3.2.4.1. Butadiene	23
3.2.4.2. n-Hexane	24
3.2.4.3. Cyclohexene	24
3.2.4.3.1. Oxidation of cyclohexene with oxygen	25
3.2.4.3.2. Oxidation of cyclohexene with HP or t-BuOOH.....	26
3.2.4.3.2.1. Three-step oxidation of cyclohexene to AA.....	26

3.2.4.3.2.2. Two-step oxidation of cyclohexene to AA.....	26
3.2.4.3.2.3. Single-step oxidation of cyclohexene to AA.....	26
3.2.4.4. D-glucose as a starting compound to produce AA	27
3.3. Conclusions concerning possible synthetic routes to AA.....	28
Baeyer-Villiger reaction: Oxidation of cyclohexanone with hydrogen peroxide	30
4. Baeyer-Villiger reaction	30
5. ϵ -Caprolactone.....	32
6. Experimental Part	34
6.1. Catalysts	34
6.2. Catalytic measurements of cyclohexanone hydroperoxidation	35
6.3. Treatment of the reaction mixture	35
6.4. Analysis of the products	35
6.4.1. HPLC	36
6.4.2. ESI-MS	36
6.4.3. NMR	36
6.5. Computational investigations	37
7. Results and discussion	39
7.1. Kinetic experiments.....	39
7.2. Identification of the reaction products	40
7.3. Study of the mechanism of BV oxidation of cyclohexanone with hydrogen peroxide.....	49
The two-step oxidation cyclohexene to adipic acid via 1,2-cyclohexanediol	70
8. The first step: cyclohexene dihydroxylation.....	71
8.1. Experimental part.....	72
8.1.1. Synthesis of the catalyst	72
8.1.2. Catalytic measurements	72
8.1.3. Treatment of the reaction mixture	72
8.1.4. Analysis of the reaction products	72
8.1.4.1. Ionic chromatography	73
8.1.4.2. Gas chromatography	73
8.2. Results and discussion	74
9. The second step: 1,2-cyclohexanediol oxidation	78

9.1.	Ru-based catalysts.....	78
9.2.	Experimental part.....	79
9.2.1.	Synthesis of the catalyst	79
9.2.2.	Characterization of the catalyst	79
9.2.2.1.	XRD analysis	79
9.2.2.2.	HR-TEM	80
9.2.3.	Catalytic measurements	81
9.2.4.	Treatment of the reaction mixture	82
9.2.5.	Analysis of the reaction products	82
9.3.	Results and Discussion	83
9.3.1.	Influence of pH value	83
9.3.2.	Stability of catalysts under reaction conditions.....	83
9.3.2.1.	Dissolution of the support	84
9.3.2.2.	Leaching experiments.....	84
9.3.2.3.	Recyclability experiments	85
9.3.3.	Reactivity experiments.....	85
9.3.4.	Reactivity of the CHDO and HCHN. Study of the reaction mechanism ..	90
9.4.	Au-based catalysts.....	95
9.5.	Experimental part.....	96
9.5.1.	Synthesis of the catalysts.....	96
9.5.2.	Characterization of the suspension of the gold nanoparticles by means of DLS	97
9.5.3.	Characterization of the catalysts	98
9.5.3.1.	XRD analysis	99
9.5.3.2.	HR-TEM	100
9.5.4.	Catalytic measurements	101
9.5.5.	Treatment of the reaction mixture	101
9.5.6.	Analysis of the reaction products	101
9.6.	Results and discussion	102
9.6.1.	Au/TiO ₂ catalyst	102
9.6.1.1.	Effect of the Au:CHD ratio.....	102
9.6.1.2.	Effect of the NaOH:CHD ratio.....	103

9.6.1.3.	Effect of temperature	105
9.6.1.4.	Stability of the catalyst under reaction conditions.....	106
9.6.1.4.1.	Leaching experiments.....	106
9.6.1.4.2.	Recyclability experiments.....	107
9.6.1.5.	Activity of the catalyst as a function of reaction time	107
9.6.1.6.	Reactivity of the CHDO and HCHN. Study of the reaction mechanism	109
9.6.2.	Au/MgO and Au/Mg(OH) ₂	111
9.6.2.1.	Effect of the NaOH:CHD ratio	111
9.6.2.2.	Effect of the Au:CHD ratio.....	112
9.6.2.3.	Stability of the catalyst under reaction conditions.....	113
9.6.2.3.1.	Leaching experiments.....	113
9.6.2.3.2.	Recyclability experiments.....	114
9.6.2.4.	Activity of the catalyst as a function of reaction time	115
9.7.	Polyoxometalates	118
9.8.	Experimental part.....	120
9.8.1.	Synthesis of the catalyst	120
9.8.2.	Characterization of the catalyst.....	120
9.8.2.1.	FT-IR spectroscopy	120
9.8.3.	Catalytic measurements	122
9.8.4.	Treatment of the reaction mixture	122
9.8.5.	Analysis of the reaction mixture	122
9.8.5.1.	GC-MS	122
9.9.	Results and discussion	124
9.9.1.	Activity of the POMs catalysts	124
9.9.2.	Reactivity of the CHDO and HCHN. Study of the reaction mechanism	125
Conclusions.....		128
References		129

Introduction

This work describes new strategies for the synthesis of adipic acid (AA), which is an emblematic example in the context of a more sustainable chemical industry. In fact, the traditional process for AA synthesis presents some environmental drawbacks; therefore the research in this area is currently attempting to solve these problems by developing more friendly technologies. Moreover, in recent decades, companies have begun to develop a strong awareness of the importance of environmental issues, in part because of reasons related to the need for environment protection, in part because of economic issues.

"Green Chemistry" is a trend in the world of chemistry, whose aim is to develop a more environmentally friendly chemistry, by limit the consumption of non-renewable natural resources, and finally protect human health.

This awareness is also the consequence of practical negative experiences, sometimes catastrophic, when the chemical industry affected people and the environment. This was also caused by the lack of knowledge of the toxicity of some chemicals, of the effect of chemicals accumulation in living bodies, and in general on environment.

Only more recently Green Chemistry turned into a discipline, with the establishment of the "Twelve principles":

- 1) prevent waste rather than to treat at the end of life;
- 2) in a chemical reaction maximize the incorporation of the reactants in the product;
- 3) use as much as possible materials and substances that are not dangerous for the environment and human health;
- 4) produce as much as possible desired and non-toxic materials;
- 5) use catalytic reactions rather than stoichiometric;
- 6) minimize the use of solvents and auxiliary reagents or use of less toxic compounds;
- 7) optimize the energy efficiency of processes;
- 8) use as much as possible renewable raw materials;
- 9) minimize the derivatization of chemicals;
- 10) substances produced must decompose at the end of life, into non-toxic and non-hazardous compounds;
- 11) maximize the control of chemical processes through sampling and control in real time, especially for hazardous substances;
- 12) develop inherently safer processes.

The main problem of Green Chemistry is that it is rarely fully applicable; in fact, some processes follow some of these principles, others cannot follow any of them, because there are no viable alternatives from the point economic and technical standpoint. Moreover, it is not sufficient to develop "Green" technologies, the chemistry within must

be "Sustainable". This term includes aspects which are strictly related: economic, social and environmental development.

The Sustainable development (and chemistry) therefore aims to meet three needs: the needs of society, the best use of scarce resources and the reduction of impact on human health and the environment.

On a practical level, the sustainability of a chemical process can be guided by the twelve principles of green chemistry, but other important factors should also be taken into account, such as the possibility to make profits and provide labor. Currently, risk reduction in chemical processes goes through some basic guidelines that in some cases also help to improve the overall sustainability of the process:

- 1) Intensification: reduce the size of the equipment while maintaining the same productivity (continuous reactors rather than batch), and minimize the use of toxic substances; if necessary it is preferable to produce them and use them in situ.
- 2) Substitution: replacement of solvents, reagents and hazardous substances with less hazardous ones; replacement of dangerous processes with safer ones, use inherently safer processes.
- 3) Restriction: try to limit the potential damage caused by an accident introducing containment structures, diluting the toxic substances or introducing inerts, increasing controls and safety systems of the plant, etc.
- 4) Simplification: eliminate as far as possible, the sources of error.

All these rules and principles fit perfectly with the production of AA, both in terms of pollution abatement systems and implementation of safety devices on existing production processes, and in terms of more sustainable technologies aimed at replacing those currently employed.

The aim of my PhD research project was to investigate new and more sustainable routes, compared to those currently used, for the production of AA. It is very important to choose the "green" oxidant from both the environmental and economic point of view. In my project molecular oxygen and hydrogen peroxide were used as oxidants. When molecular oxygen is used, there are no co-products of oxygen reduction (when O is fully incorporated in the substrate), while in case of hydrogen peroxide the co-product is water. Hydrogen peroxide is an expensive oxidizing agent, if compared to air or other stoichiometric oxidants, but it can be viewed as a green one compared, for instance, to nitric acid or stoichiometric metal ions (Cr, Mn, etc).

Heterogeneous and homogeneous catalytic systems were studied during my research. Both catalyst types have advantages. For example, heterogeneous catalysts can be reused in the reaction after easy separation from the reaction mixture by filtration. Homogeneous catalysts can be highly selective, and do not show mass-transfer limitation problems.

My project was divided into two parts:

1. The two-step oxidation of cyclohexene, where the latter is first oxidized into trans-1,2-cyclohexanediol (CHD) with aqueous hydrogen peroxide, and then the glycol is transformed into AA by reaction with molecular oxygen. Various catalysts were investigated in this process, both heterogeneous and homogeneous. We also studied the mechanism of CHD oxidation with oxygen in the presence of different catalysts.
2. Baeyer-Villiger oxidation of cyclohexanone with aqueous hydrogen peroxide into ϵ -caprolactone, as a first step on the way to produce AA. Study on the mechanism of the uncatalyzed (thermal) oxidation of cyclohexanone were also carried out. Investigation on how the different heterogeneous catalysts affect the formation of the reaction products and their distribution was done.

Adipic Acid

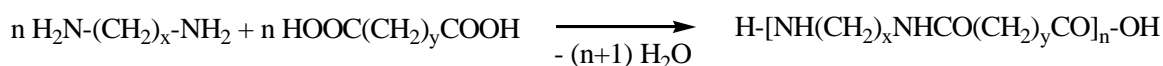
1. Physical chemical properties

At room temperature and atmospheric pressure adipic acid (AA) is an odorless, sour tasting white powder. The melting point is 152°C. AA is soluble in polar solvents; with increasing temperature its solubility in water grows [1].

2. Uses of Adipic acid

AA is a very important chemical intermediate. The main use of AA (63% of its consumption) is the production of Nylon-6,6 fibers (fishing lines, tires, carpets, home furnishing, and in tough fabrics for backpacks, parachutes, luggage and business cases) and resins (electrical connectors, auto parts, and items such as self-lubricating bearings, gears and cams) (Figure 1).

Nylon-6,6 was first synthesized by Wallace Hume Carothers in 1935 in the laboratories of DuPont, and after three years DuPont patented the process [1].



Other uses of AA are in the production of polyesters (25%, for polyurethane resins), plasticizers (7%), as well as resins (2%) and 3% for other applications (cosmetics, pharmaceuticals products, fertilizers, paper, cement, wax, etc.) [2].

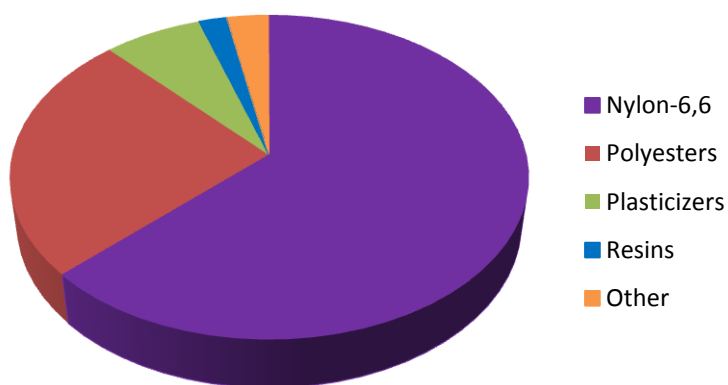


Figure 1. AA application

3. Production of Adipic Acid

The global capacity of AA was around 2.8 million metric tons per year in 2006; the production takes place mainly in Europe and the United States (62%), Asia (18% excluding Japan) and, to a less extent, in Japan and South America. The overall growth for AA is close

to 3% per year. The most rapidly growing sector is the production of nylon, during the past decade it has grown by 8-10% per year.

Table 1 shows the main AA producers and their capacity [2].

Table 1. Main producers of AA

Producer	Capacity (million tons per year)
Inolex Chem (USA)	0.02
Solutia (USA)	0.40
BASF (Germany)	0.26
Asahi Kasei Corporation (Japan)	0.17
Azot Severodonetsk (Ukraine)	0.03
Lanxess AG (Germany)	0.07
Invista (Koch Ind) (USA, Canada, Singapore, UK)	1.09
Rhodia (now Solvay) (France, Brazil, Korea)	0.54
Radici Chimica (Italy, Germany)	0.15
Rivneazot	0.03
China Shenma Group (China)	0.11
PetroChina Liaoyang Petrochemical (China)	0.14
Xinjiang Dushanzi Tianli (China)	0.08
Taiyuan Chemical Industry (China)	0.05
Shandong Bohui Chemical Industry Group (China)	0.08
Shandong Hongye Chemical Industry Group (China)	0.10

3.1. Current industrial processes

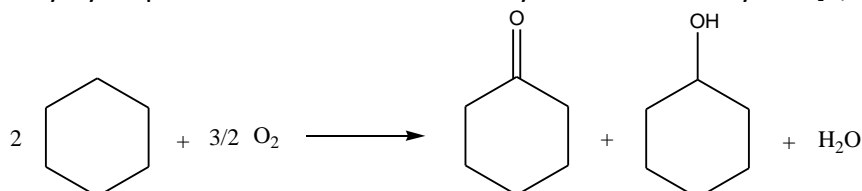
All industrial processes today have in common the final step of oxidation with nitric acid of an intermediate, which can be either a mixture of cyclohexanol and cyclohexanone (KA oil or Ol/One mixture), or cyclohexanol only. Thus, while the oxidative cleavage is

carried out always with the same procedures, the synthesis of the intermediate can be performed following different ways:

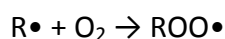
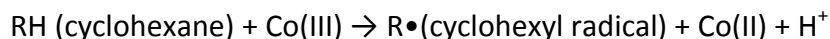
- Oxidation of cyclohexane to KA Oil
- Hydrogenation of phenol to KA Oil
- Hydration of cyclohexene to cyclohexanol, whereby cyclohexene is produced by the selective hydrogenation of benzene.

3.1.1. Oxidation of cyclohexane to KA Oil

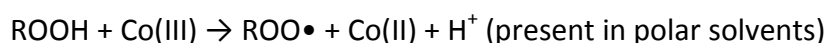
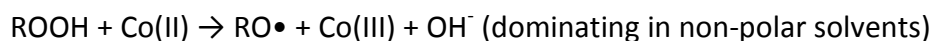
Cyclohexane is usually obtained by hydrogenation of benzene or in small amount from the naphtha fraction. The oxidation of cyclohexane to KA oil was first industrialized by DuPont in the 1940s. The reaction consists of two steps: oxidation and deperoxidation. The first step can be done in the absence of catalyst, whereas for the deperoxidation step a catalyst is needed. The cyclohexane is oxidized into cyclohexylhydroperoxide in passivated reactors to optimize the concentration of the latter and in the absence of transition metal complexes to avoid hydroperoxide decomposition. The deperoxidation is performed in the second reactor where the control of the final OI/One ratio is achieved by control of catalyst amount and reaction conditions. The conversion is kept at 5-7% per-pass, in order to limit the consecutive reactions, because the alcohol and the ketone are more reactive than cyclohexane. Selectivity to KA Oil is 75-80%, the by-products are carboxylic acids (e.g. 6-hydroxyhexanoic, *n*-butyric, *n*-valeric, succinic, glutaric and adipic acids) and cyclohexylhydroperoxide. The unconverted cyclohexane is recycled [3, 4].



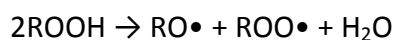
The reaction proceeds by the homolytic autoxidation chemistry. Cyclohexanol is formed from the RO• radical (R=C₆H₁₁).



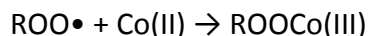
The main role of Co is to accelerate the decomposition of the hydroperoxide, ROOH; it leads to the formation of alkoxy or peroxy radicals (Haber-Weiss mechanism):



which matches with:

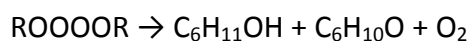
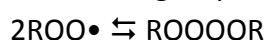


In case of high concentration of Co(II), the latter competes with cyclohexane for the alkylperoxy radical:

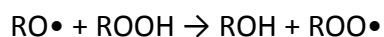
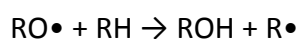


and instead of a propagation step, a termination step would take place. Therefore in this case the catalyst may become an inhibitor.

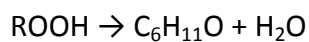
Russell mechanism of secondary cyclohexylperoxy radicals decomposition is a dominating reaction for the formation of cyclohexanol and cyclohexanone. It first leads to the coupling of alkylperoxy radical and then reacts by a six-center 1,5-H-atom shift; it is also a terminating step of the radical chain reaction:



Other ways for radical propagation are:



The cleavage of an α C-H bond can give directly cyclohexanone:



Cyclohexanone can also form from cyclohexanol by oxidation [5, 6].

The scheme of the process for the oxidation of cyclohexane with air is shown in Figure 2. The reaction is performed in three in-series reactors; cyclohexane is fed to the first one, and air is flown to each one of the three reactors. This allows better control of the reaction performance and also improves safety. The products are washed with water and then with caustic solution to decrease the amount of acid impurities. Caustic solution can be recycled during the process.

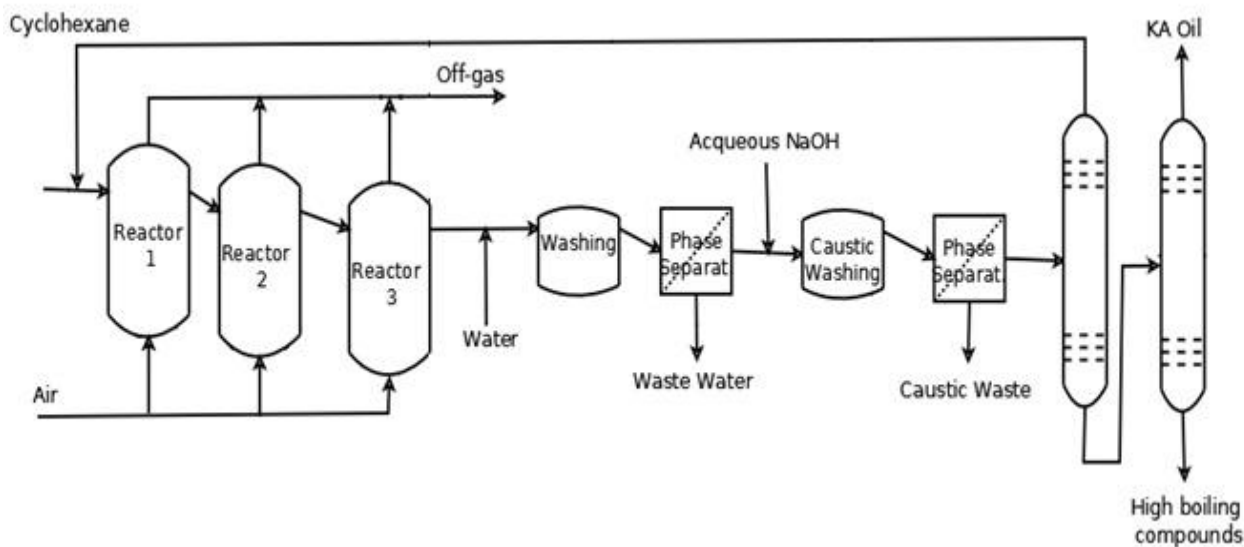


Figure 2. Scheme of the process for the oxidation of cyclohexane with air.

There is also another process for cyclohexane oxidation, nowadays adopted in several plants. The basic principle of this method is the addition of an anhydrous meta-boric acid as a suspension in cyclohexane, for the first step of oxidation. No other catalyst is needed. Boric acid reacts with cyclohexanol yielding a borate ester that stabilizes the product and decreases the possibility to oxidize it into cyclohexanone and degradation compounds. In this case conversion is 10-15% and selectivity is 90%; molar ratio cyclohexanol/cyclohexanone is around 10. The borate ester can be easily hydrolyzed back to boric acid and cyclohexanol with hot water [2].

3.1.2. Hydrogenation of phenol to KA Oil

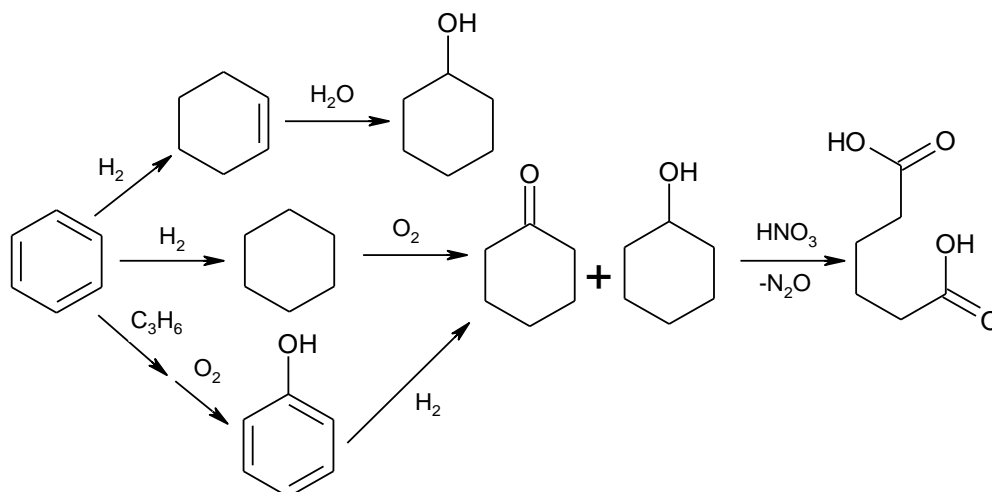
The process of KA Oil production by phenol hydrogenation has been industrialized by Solutia and Radici. It has some advantages, such as a less complex equipment needed for KA production, the possibility to get directly the mixture of the ketone and alcohol and to control the OI/One ratio, the high selectivity to the product and the better safety of the process compared to cyclohexane oxidation, which may reduce investment cost. By increasing the amount of ketone in the mixture, it is possible to save hydrogen during phenol reduction, and nitric acid during the oxidation of KA Oil.

3.1.3. Hydration of cyclohexene to cyclohexanol

Cyclohexene can be synthesized by the hydrogenation of benzene. Thermodynamically this reaction is not favorable. In order to stop the hydrogenation at the mono-olefin it is necessary to carry out the reaction in the presence of Pt or Ru powder, coated with a layer of an aqueous solution of zinc sulfate. The reaction is conducted in benzene, the catalyst is surrounded by the aqueous phase; due to this reason the compounds which are soluble in aqueous phase are hydrogenated. The reaction product,

cyclohexene, is less soluble in the aqueous phase than benzene, and moves to organic phase, an event that allows to avoid further hydrogenation. The selectivity to the reaction product is around 80% with 70–75% benzene conversion [5]. Then cyclohexene is hydrated on a ZSM-5 catalyst.

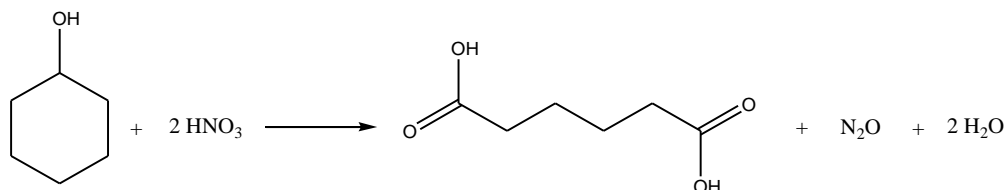
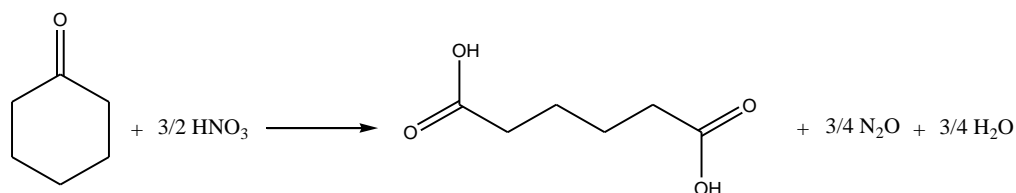
Scheme 1 summarizes the different industrial processes for the AA production starting from benzene.



Scheme 1. Current processes for the AA production starting from benzene

3.1.4. Oxidation of KA Oil to AA with nitric acid

The final oxidation of KA oil or cyclohexanol only is carried out using nitric acid in an excess of at least seven times higher than the stoichiometric molar ratio, in the presence of an homogeneous catalysts based on Cu(II) and ammonium metavanadate [4, 7].



Cyclohexanone \rightarrow AA ΔH_R - 172 kcal/mol

Cyclohexanol \rightarrow AA ΔH_R - 215 kcal/mol

The reaction is performed in two in-series reactors; the temperature in the first reactor is 60-80°C, while in the second one is 90-100 °C with a pressure of 1-4 atm. The yield to AA is 95% with total conversion of KA oil; the by-products are glutaric acid (with

selectivity 3%) and succinic acid (with selectivity 2%). Figure 3 shows the simplified flow sheet of the KA Oil oxidation process with nitric acid.

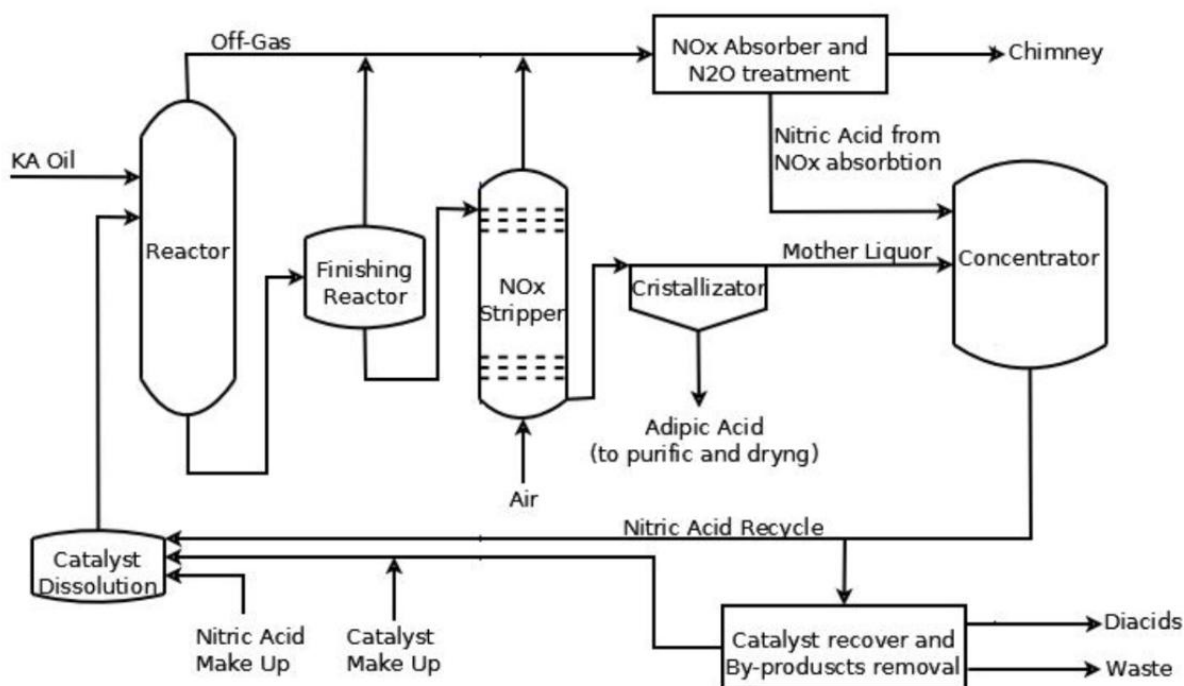
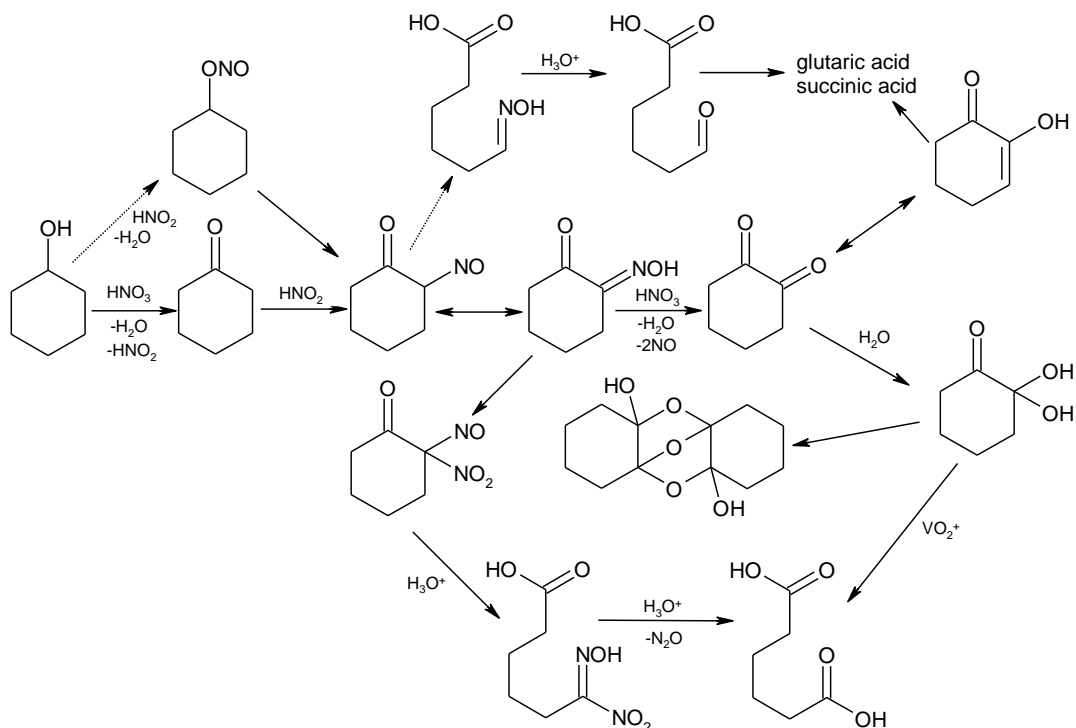


Figure 3. Scheme of the KA Oil oxidation process

The reaction mechanism of KA oil oxidation with nitric acid was investigated in 1963 [8,9] and lately has been revised. The mechanism of the process is shown in Scheme 2. The first step is the oxidation of cyclohexanol to the ketone, then the latter is nitrosated by nitrous acid to give 2-nitrosocyclohexanone. This intermediate can transform by means of different ways. When nitrous acid is present, the nitrosoketone can be hydrolyzed giving α -diketone and hydroxylamine (Claisen-Manasse reaction). Another pathway is when the oxime is oxidized by a stronger oxidant to produce α -diketone and nitrogen oxides. α -Diketone can be further oxidized yielding AA. However, the main pathway is the formation of 2-nitro-2-nitrosocyclohexanone, that is hydrolyzed to 6-nitro-6-hydroximinohexanoic acid. Oxidative hydrolysis of the latter gives AA through the formation of an intermediate adipomonohydroxamic acid. The consumption of HNO_3 in this case is 2 mol per mole of cyclohexanone [2].



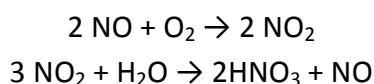
Scheme 2. Main reactions involved in the mechanism of KA Oil oxidation to AA with nitric acid.

3.1.5. Risks, disadvantages and environmental issues in AA production

The hazard of the process derives from the use of nitric acid, as it is a strong acid and a powerful oxidant. For this reason, the plant must be constructed of durable materials, such as titanium or stainless steel, more expensive than normal steels.

The exothermicity of the reaction may give rise to fires and explosions, given the high concentration of organic compounds present in the reactor that requires high attention from the point of view of safety.

From the environmental point of view, the main problem relates to the production of nitrous oxide, N_2O , and nitrogen oxides during the last phase of oxidation with nitric acid. The nitrogen oxides NO and NO_2 are the main causes of acid rain and under suitable atmospheric conditions favor the photochemical smog that leads to the formation of ozone in the troposphere resulting harmful to living beings. However, NO_x can be almost completely recovered by water adsorption in a multistage column, yielding a nitric acid solution.



This route allows regain nitric acid which can be reused within the process itself. The greater cost is in the low temperatures and high pressures needed to maximize the efficiency of the treatment [2].

Nitrous oxide is a greenhouse gas due to its strong IR absorption; its emission is around 300 kg per ton of AA. The estimated atmospheric lifetime of N₂O is 150 years. At the level of the troposphere nitrous oxide acts as a catalyst in the cycles of ozone destruction, contributing to its decline. Today, only a small part of N₂O is produced by human activities (less than 5%), and within the latter that one deriving from the production of AA is very low due, to the abatement systems installed in the plants. Today more than 90% of the N₂O generated at AA plants is decomposed before being released into the environment [2, 10].

3.1.6. Methods for N₂O abatement

There are several N₂O abatement technologies in order to decrease its emission in the AA plants.

- Catalytic dissociation of N₂O to N₂ and O₂;
- Thermal destruction of N₂O;
- Conversion of N₂O into recoverable NO.

3.1.6.1. Catalytic abatement

Catalytic decomposition is the simplest method to remove N₂O because it doesn't need any additional chemical compounds. The reaction is highly exothermic (-19.6 kcal/mol) and includes the following steps:

1. $\text{N}_2\text{O} + * \rightarrow \text{N}_2\text{O}^*$
2. $\text{N}_2\text{O}^* \rightarrow \text{N}_2 + \text{O}^*$
3. $2 \text{O}^* \leftrightarrow \text{O}_2 + 2^*$
4. $\text{N}_2\text{O} + \text{O}^* \rightarrow \text{N}_2 + \text{O}_2 + *$

where * is the active site of the catalyst [11].

There are several classes of catalysts that can be used in this process: noble metals (Pt, Au), pure or mixed metal oxides (spinel, perovskite – types, oxides from hydrotalcites), supported systems (metal or metal oxides on alumina, silica) and zeolites [12].

Since the reaction is highly exothermic, there are several problems to deal with:

- ✓ the sintering of the catalyst;
- ✓ the need for special heat-resistant expensive materials for reactors;
- ✓ troubles regarding the environmental regulation: the NO_x formation increases when the temperature of the catalytic bed is increasing. NO_x concentration is limited by law.

Part of the worked-up and cooled gas is fed back to dilute the N₂O stream stemming from the AA production. This helps to avoid overheating and levels off the heat production over the entire bed. Typically the inlet temperatures in the reactor are around 450-500°C, and 700-800°C at the outlet, taking into account an inlet concentration of nitrous oxide of about 12 %.

Radici developed the process with a multi-bed reactor (Figure 4) in order to improve the process of N₂O catalytic abatement. The gaseous flow with nitrous oxide is divided into three flows, that are fed separately to the three catalytic beds [13,14]. The stream from the third catalytic layer shows residual nitrous oxide content of less than 500 ppm, and is subdivided into two streams; one is fed to the atmosphere and the second is mixed with the feed to the first catalytic layer and re-circulated into the process of N₂O decomposition.

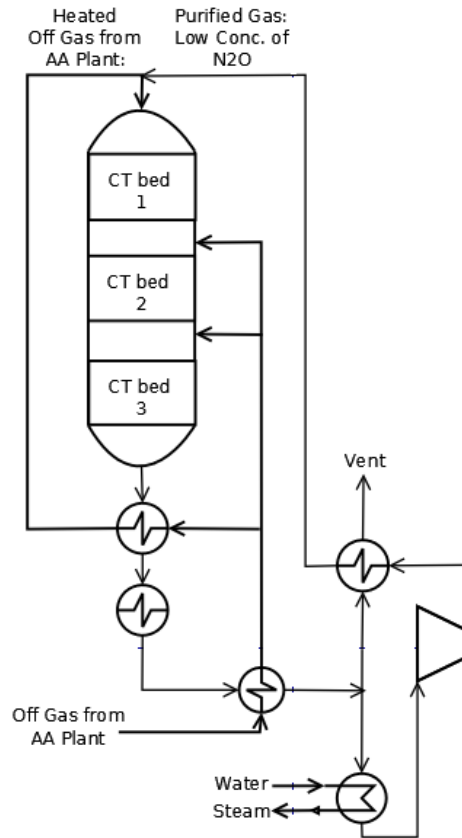
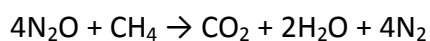
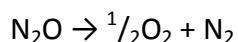
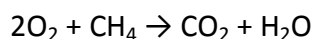
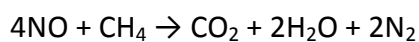


Figure 4. Simplified flow sheet of Radici process for N₂O catalytic abatement

3.1.6.2. Thermal destruction of N₂O

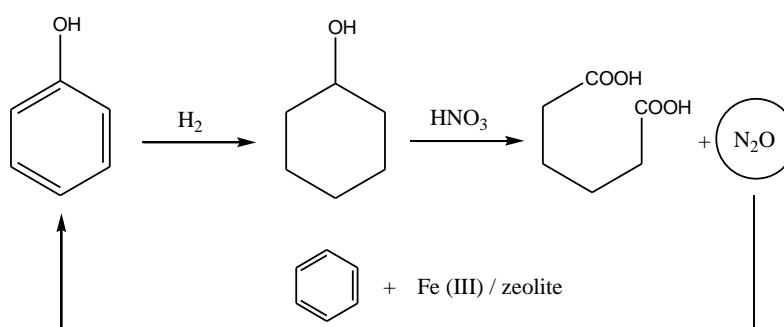
There are two ways to carry out the thermal destruction of N₂O, that differ depending on how the decomposition occurs: either at oxidizing conditions, or as a result of burning in a reducing flame. In the first case, N₂O is oxidized to higher oxides, NO and NO₂, which are then adsorbed in water yielding nitric acid. Nitric acid can be recycled in the process upstream. In the second approach, sub-stoichiometric combustion conditions are used, to minimize the formation of nitrogen oxides. The reducing atmosphere is made by adding an excess of methane to the gas mixture that is fed to the burner (containing O₂ and N₂O). Excess methane gives an unburned part (CO and H₂) that is a reactant for NO_x reduction to nitrogen. The following reactions take place in the reducing method of N₂O thermal abatement.





3.1.6.3. Conversion of N₂O into recoverable NO

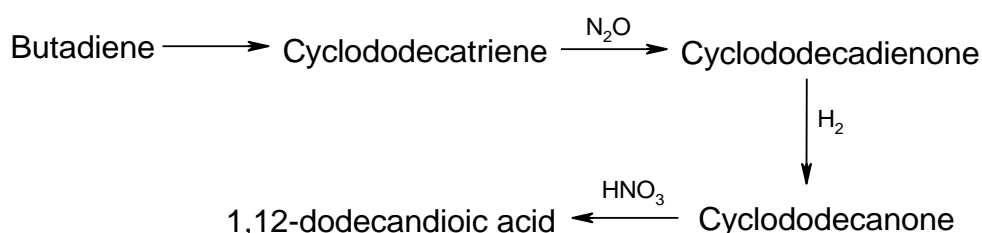
The nitrous oxide can be recovered in pure form in order to be sold or to be used as an oxidant in other downstream processes. The recovery process consists in the absorption and desorption in appropriate solvents or solid carriers. The sale as such is very limited because the majority of the market is covered by nitrous oxide generated from the production of nitric acid, which allows to obtain an even more pure product, with lower costs of purification. A solution would be to find an alternative use in internal processes that produce it. An example of downstream integration with the production of AA has been proposed by Solutia and Boreskov Institute of Catalysis, which involves the use of N₂O as an oxidant for the synthesis of phenol from benzene in the presence of a ZSM-5 zeolite exchanged with Fe (III), giving a selectivity to phenol as high as 95%. Phenol could be further hydrogenated to cyclohexanol and used for the synthesis of AA [15] (Scheme 3).



Scheme 3. Scheme of N₂O integration for the synthesis of phenol

However the process has not been put into commercial operation due to rapid catalyst deactivation, because of tar deposition, low efficiency with regard to N₂O and to the poor economics of the small phenol plants, compared to traditional plants for phenol production.

A solution developed by BASF provides the reuse of nitrous oxide for the production of 1,12-dodecanoic acid, in particular in the step of cyclododecatriene oxidation to cyclododecadienone (Scheme 4).



Scheme 4. Process proposed by BASF

This process, already operating at the industrial level, generates a much higher yield compared to the classical process and constitutes a solution to the disposal of N₂O [16].

3.2. Alternative ways for the production of AA

Because of the disadvantages and risks related to the use of nitric acid as the oxidant in the AA production, there is a great interest to develop alternative methods for AA synthesis. Various substrates can be used as starting reagents for this reaction as well as different oxidizing agents (O₂, hydrogen peroxide - HP, tert-butyl hydroperoxide - TBHP). In this chapter some alternative processes for the AA production are discussed.

3.2.1. Oxidation of cyclohexane to KA Oil

The literature reports numerous studies about the use of different oxidants for cyclohexane oxidation to KA Oil or AA in the presence of homogeneous or heterogeneous catalysts.

3.2.1.1. Homogeneous oxidation of cyclohexane

Many studies regard the use of homogeneous catalysts, alternative to those based on cobalt currently used in the industrial process, with air as the oxidant. For example, Keggin type polyoxometalates, systems based on copper, and salts or complexes of iron or vanadium, have been used. Some of them are able to give cyclohexanol and cyclohexanone with selectivity similar to those of traditional catalysts, but do not allow to reach high conversion of cyclohexane. Some of these catalysts, however, require expensive or less ecological components, others are active only in the presence of certain reagents or co-reductants, or appear to be not stable, and therefore are not usable at an industrial level [17,18,19,20].

3.2.1.2. Heterogeneous cyclohexane oxidation

The use of heterogeneous catalysts, despite their lower activity, allows a simplification and a reduction of the economic and environmental costs, associated to product purification. Numerous studies have been performed with regard to heterogeneous catalytic systems either for the oxidation of cyclohexane to KA Oil or even directly to AA, with different oxidants. Examples are shown below:

a) Gold nanoparticles supported on mesoporous materials, such as SBA-15, MCM-41, are the catalysts for cyclohexane oxidation to KA Oil in the presence of oxygen (93% selectivity to the mixture with 18% of substrate conversion). Similar results were obtained using Au nanoparticles dispersed over the silica, alumina and titania [21,22,23].

b) Cu or Fe phthalocyanines encapsulated in X or Y zeolites catalyze cyclohexane oxidation to either KA Oil or AA with oxygen at near-ambient conditions. The best results were obtained with methanol as the solvent: 12.7% of cyclohexane conversion with 41% of

selectivity to AA in the presence of halogen-substituted phthalocyanine of Fe encapsulated in the X zeolite [24].

c) the use of Ce containing catalysts for cyclohexane oxidation with different oxidants is also reported. Thus, for example, Ce-exchanged Y zeolite catalyzes the cyclohexane oxidation with *t*-BuOOH at 90°C, giving 10% reactant conversion with good selectivity to KA Oil [25]. Alumina-supported Ce(IV) oxide was used in the oxidation of either cyclohexane or the mixture of cyclohexane and cyclohexanone with air at 15 atm pressure and 110°C. AA was obtained with 66% yield, cyclohexane conversion was 38% and cyclohexanone conversion was 41% [26].

d) Ti-based catalysts were investigated in cyclohexane oxidation with hydrogen peroxide (HP), *t*-BuOOH or oxygen. For example, with titanium substituted hexagonal mesoporous aluminophosphate (Ti-HMA) molecular sieves or Ti-MCM-41 similar performances were obtained. In the presence of HP as an oxidant the reactant conversion was 90% with Ti-HMA and 88% with Ti-MCM-41, with selectivity to KA Oil (mainly OI in both cases) equal to 95% and 99%, respectively. But acetic acid was used as a solvent in these reactions, that may favor the leaching of Ti and forms peracetic acid, which acts as the true final oxidant [27].

e) Cr-based catalysts, such as Cr-MCM-41 and Cr-HMA, also showed good results. In the presence of Cr-MCM-41 and HP or O₂, 99% and 86% of reagent conversion and 93% and 97% selectivity to KA Oil (mainly OI) were achieved, respectively [28]. In the case of *t*-BuOOH there was mainly the formation of cyclohexanone; selectivity to KA Oil was 95%, with conversion 92% [29]. Cr-HMA with HP oxidant gave 100% of selectivity with 94% cyclohexane conversion [30]. In all these cases, acetic acid was used as the solvent, and peroxy acetic acid also had a role in increasing the reaction rate.

3.2.2. Oxidation of KA oil

3.2.2.1. Oxygen as the oxidant

The second step of the KA Oil process is carried out using nitric acid as the oxidant, in the presence of homogeneous catalysts based on cupric nitrate and ammonium metavanadate. Because of the environmental and economic problems of this passage, numerous studies have been performed involving the use of oxygen or air as oxidants.

An important example is the technology of Asahi, which developed a process that uses a catalyst based on manganese acetate and cobalt, with oxygen at atmospheric pressure or air diluted with nitrogen, at a pressure of 12 atm, with water and acetic acid 80% as solvent, at a temperature of 70°C. With pure oxygen, selectivity to AA was 77% with total conversion of cyclohexanone, that allows a considerable reduction of costs by eliminating the step of recycling. The demonstration plant includes three in-series high-pressure, continuous-stirred, tank reactors which allow to obtain complete conversion. The process includes different steps for the purification of AA, because the selectivity is lower compared to that of the nitric acid process, and for the recovery of the solvent and of

catalyst. In the case of oxygen as the oxidant, there is no need of systems for the reduction of NO_x and N_2O . But this pathway has also disadvantages, such as the corrosiveness of acetic acid, the lower yields of the industrial process and the higher costs of purification of the product, aspects that make this process not so much favored from the economical point of view [31].

Another well studied process is the oxidation with air or oxygen of cyclohexanone with Keggin-type polyoxometalates catalysts. Cyclohexanone conversion shown was 99%, with 50% selectivity to AA [32], but also in this case the solvent was acetic acid. In other cases, when a mixture of acetonitrile and methanol was used as the solvent, the ester of AA was obtained (98% of conversion with selectivity of 54%) [33]. The latter had to be transformed back to AA, that implies additional costs.

There are also other studies using different catalytic systems, always with the use of oxygen, but all yields and selectivities reported are much lower than those achieved in the described processes.

3.2.2.2. Hydrogen peroxide as the oxidant

The oxidation of KA Oil has also been investigated using aqueous hydrogen peroxide (HP) as the oxidant, in the presence of catalysts (either homogeneous or heterogeneous). For example:

- a. Under homogeneous conditions oxidation of cyclohexanone with HP using acetic acid or *t*-butanol solvent gave about 50% AA yield [34];
- b. In the presence of H_2WO_4 , after 20 hours reaction time the cyclohexanone gave 91% yield to AA, whereas cyclohexanol showed 87% yield. The reaction was carried out without any solvent, and 30% aqueous solution of HP was used as the oxidant [35].

3.2.3. Direct oxidation of cyclohexane to AA

The direct oxidation of cyclohexane to AA with oxygen/air might lower the total investment costs because of:

- ✓ removal of one oxidation step;
- ✓ removal of HNO_3 production, treatment, recovery, cleaning and recycle units;
- ✓ simplification of the abatement system of the air by removal of nitrous oxide and NO_x emissions;
- ✓ simplification of the wastewater handling by removal of nitrates.

There are several studies involving either the use of homogeneous catalysts based on complexes of Co, Cu, Mn or Fe (the same catalyst type also used for the oxidation of cyclohexane to KA Oil), and heterogeneous catalysts.

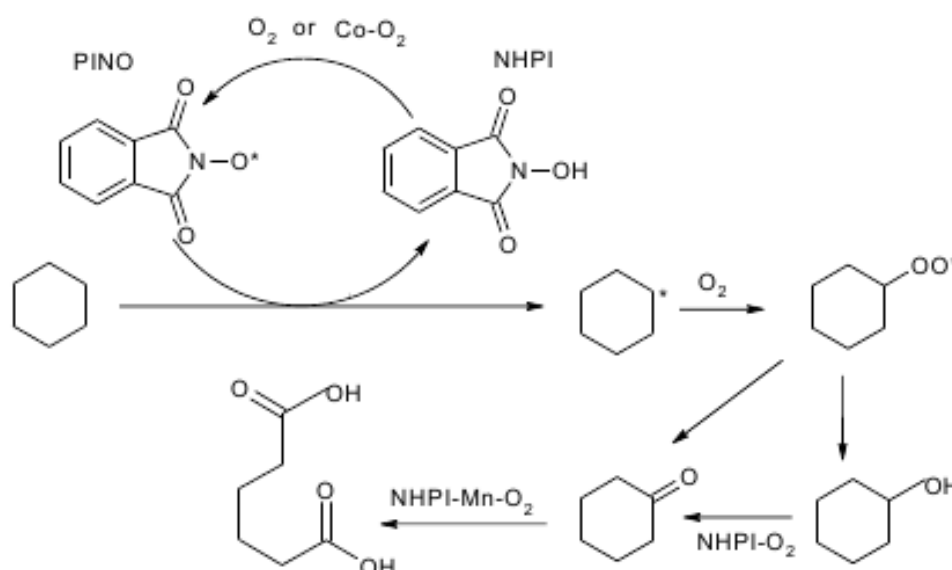
In 1940s Asahi developed a commercial process that involves the use of Co acetate with acetic acid as the solvent, under 30 atm of oxygen pressure and at the temperature of 90-100°C. The best selectivity to AA was 75%, with the conversion of cyclohexane ranging from 50 to 75%; the main by-product was glutaric acid. The good results were obtained

because of a relatively high concentration of catalyst combined with acetaldehyde or cyclohexanone, which worked as promoters [36, 37, 38].

Various companies studied the process in order to obtain higher selectivity to AA by optimizing the reaction conditions and catalyst composition. For example, Gulf performed the reaction at the same temperature as Asahi, using acetic acid as the solvent, but with higher concentration of catalyst. Conversion of cyclohexane was 80-85% with selectivity to AA 70-75% [39, 40]. In the Amoco process, 98% cyclohexane conversion was achieved, with 88% AA yield. The reaction was performed at 95°C, with 70 atm air pressure ; this patent describes the addition of controlled amounts of water during the induction period, which is a key parameter because it depletes the concentration of free radicals [41].

The process, however, was later abandoned due to problems regarding the corrosion of the materials by acetic acid, the safety issues associated to the use of high pressure oxygen in the presence of cyclohexane (high risk of flammability), and because the AA yield was less than that achieved in the DuPont process.

A remarkable result was obtained by Daicel Chemical Industry in collaboration with Kansai University, which developed a process that involves the use of N-hydroxyphthalimide (NHPI) as the catalyst for the direct oxidation of cyclohexane with air. NHPI is a cheap, nontoxic catalyst, that can be easily prepared by the reaction of phthalic anhydride and hydroxylamine (Scheme 5). A pilot plant producing 30 ton/year of AA with yields higher than 80% (selectivity 76%) and conversion of cyclohexane of 90% after 6 h of reaction at 100°C, under 10 atm air pressure was built up in Japan. The use of NHPI increased the reaction rate but did not increase the selectivity. The reaction required a co-catalyst such as acetate of Co or Mn, and was conducted in acetic acid or acetonitrile as a solvent due to the limited solubility of NHPI in non-polar solvents. The process so far has not been brought to industrial level because it requires large amounts of catalyst due to the decomposition of NHPI to phthalimide, which cannot be easily recycled and transformed back to NHPI [42, 43].



Scheme 5. Oxidation of cyclohexane with NHPI catalyst [2]

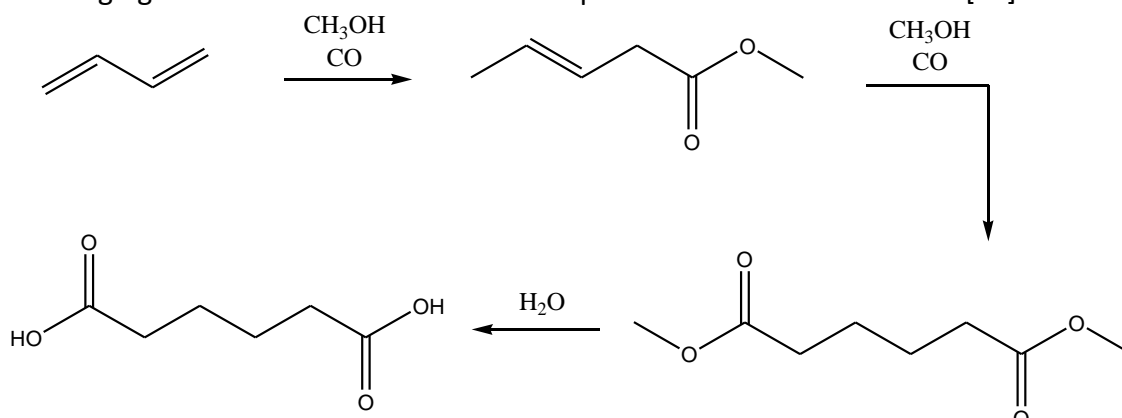
Numerous heterogeneous catalysts have been proposed for the direct oxidation of cyclohexane, but most of them give cyclohexanol and cyclohexanone as the main products, while AA remains a minor product. Catalyst that can be used include metal oxide or cations, and complexes incorporated in inorganic matrices (activated carbon, zeolites, alumina, silica or alluminophosphates). The activity of these systems is highly influenced by the type of solvent, from which the polarity of the mixture depends, that is also important since the hydrophobicity of the support allows a rapid expulsion of the oxidized products. One negative aspect common to all systems studied is the leaching of the catalyst, which does not allow to have a completely heterogeneous catalysis, and related problems in the subsequent purification steps.

3.2.4. Alternative starting materials

3.2.4.1. Butadiene

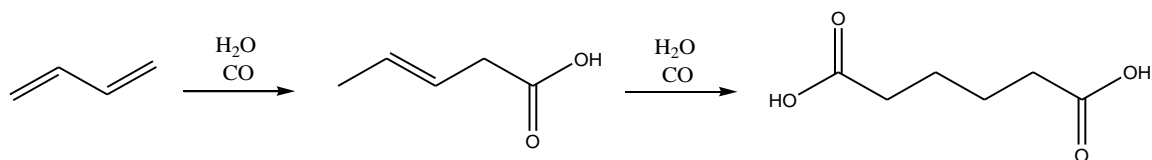
The synthesis of AA can be performed by methoxycarbonylation of butadiene according to the process developed by BASF [44]. The process consists of three steps: the addition of CO and methanol in two steps and a final stage of hydrolysis of dimethyl adipate to obtain AA (Scheme 6).

Catalyst based on Co in homogeneous phase is used in the presence of pyridine, which is necessary to avoid oligomerization reactions. The total yield of AA is 72% referred to butadiene, with product purity of 99.9%; the main by-products are methyl valerate and dimethyl esters of dicarboxylic acids with four carbon atoms, which could find uses in other applications. BASF has not continued the development of this process on an industrial scale for economic and technical reasons, such as, for example, the cost to operate under pressure ranging from 150 atm for the second step to 300 atm for the first one [45].



Scheme 6. Methoxycarbonylation of butadiene to AA.

A variant designed by DuPont and DSM consists in hydroxycarbonylation of butadiene with CO and water at 100°C and 80 atm; this process is more economical from the point of view of raw materials cost. However, it shows higher catalyst cost and difficulties in catalyst recovery (Scheme 7) [46].

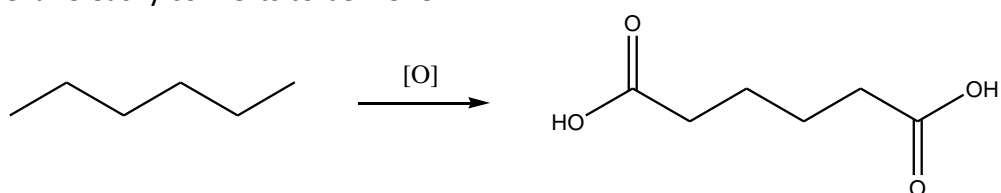


Scheme 7. Hydroxycarbonylation of butadiene to AA.

Other variations of methoxycarbonylation have been studied by Rhone Poulenc [47] and Shell Chemicals [48, 49], which developed a new catalyst able to convert butadiene into AA with CO and water. Because with this catalyst the mono-olefins are not carboxylated, the use of crude C4 fractions as starting material is allowed. This new process, however, was stopped at the level of bench-scale: the main limit for the industrialization is the use of a complex as homogeneous catalyst, composed of precious metals and phosphine ligands, which are expensive chemicals.

3.2.4.2. *n*-Hexane

The oxidation of terminal carbons of linear alkanes is an important challenge of today catalysis; in particular, the direct oxidation of *n*-hexane at C1 and C6 atoms would lead directly to AA (Scheme 8). However, with regard to this synthetic route, it also has the problem of poor availability of the reagent itself, that derives mainly from cracking plants in which hexane easily converts to benzene.



Scheme 8. One-step synthesis of AA from *n*-hexane.

To perform this reaction it is possible to use enzymes fitted with iron active centers; *n*-hexane reacts with air giving AA with high selectivity (close to 100%). The attempt to replicate these properties in non-biological systems for use in industrial plants gave poor results. Tests were made with chemical systems which involve the use of Mn-porphyrins, Co and Mn alluminophosphates or supported on zeolites, but AA yields higher than 35% have been never reached, main by-products being hexanol, hexanal and methyl-butyl ketone.

3.2.4.3. Cyclohexene

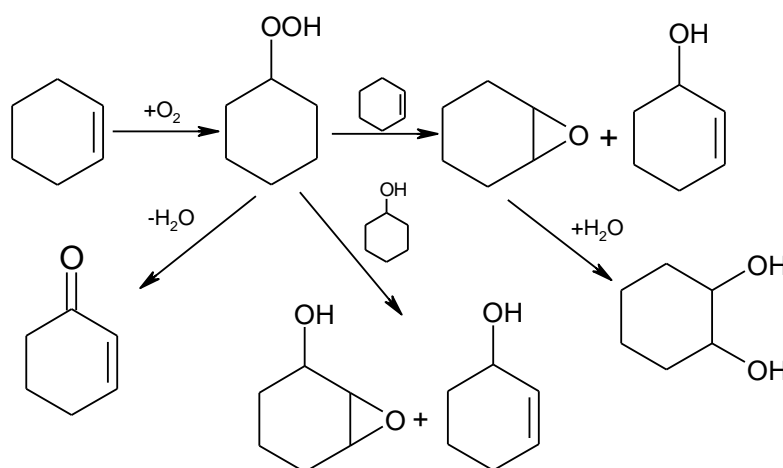
Cyclohexene can be obtained by partial hydrogenation of benzene, dehydrohalogenation of cyclohexyl halides or partial cyclohexane dehydrogenation. Asahi studied the process for the hydrogenation of benzene; this process gives good cyclohexene selectivity, but the problem is catalyst deactivation. The method of dehydrohalogenation of cyclohexyl halides would have a potential advantage of recycling hazardous halogenate

compounds. Hydrogen treatment of cyclohexyl chloride using silica supported nickel catalyst gave 97% cyclohexene selectivity at temperatures between 200 and 300°C [50].

Oxidants studied for cyclohexene oxidation are oxygen, hydrogen peroxide and tert-butyl hydroperoxide.

3.2.4.3.1. Oxidation of cyclohexene with oxygen

Prevailing product in the case of cyclohexene oxidation with oxygen in the absence of a co-reduction reagent is 2-cyclohexen-1-one [51, 52, 53], that may be further hydrogenated to the cyclohexanone. The reaction follows the autoxidation-type mechanism forming first cyclohexene hydroperoxide. If the reaction is carried out in the presence of a co-reducing agent (for example, isobutyraldehyde), high selectivity to the epoxide is obtained (88-94% with complete conversion of substrate) [54]. Asahi has proposed the oxidation of cyclohexene with O₂ using isopolyoxomolybdates. The primary products were cyclohexene oxide, CHD and 2-cyclohexene-1-ol (Scheme 9); the two former compounds are intermediates in AA synthesis. After 24 hours at 50°C and 1 atm of oxygen, 37% cyclohexene conversion was obtained with 90% selectivity to the three primary products [55].



Scheme 9. Oxidation of cyclohexene with O₂ [2]

When the system based on Pd (II) and P/Mo/V heteropoly-compound is used, the reaction follows a Wacker-type mechanism that is different from the radical-type autoxidation. The primary product in this case is cyclohexanone, which can be further oxidized with oxygen to AA. Many systems belonging to this class of catalysts were investigated. The best results were achieved with Pd(NO₃)₂/CuSO₄/H₃PMo₁₂O₄₀ in aqueous solution of acetonitrile at 80°C and 10 atm of oxygen: cyclohexene conversion was 49% with 97% selectivity to cyclohexanone [56]. More recently, at 80°C and 50 atm of air, using the same catalyst, >>99% selectivity to cyclohexanone with 80% cyclohexene conversion were reported [57].

3.2.4.3.2. Oxidation of cyclohexene with HP or *t*-BuOOH

3.2.4.3.2.1. Three-step oxidation of cyclohexene to AA

Cyclohexene can be oxidized to cyclohexene oxide using HP or alkyl hydroperoxides in the presence of either homogenous or heterogeneous catalysts. Catalysts that are active and selective in this type of reaction could be divided into two groups: (i) microporous and mesoporous materials, which contain isolated metal ions either incorporated in the structure of inorganic matrices or grafted to their surface, for example Ti (Ti-HMS, Ti-MCM-41, Ti-MCM-48), titanium silicalite [58, 59, 60], and (ii) transition metal-exchanged polyoxometalates [61, 62, 63]. $\text{TBA}_3\{\text{PO}_4[\text{WO}(\text{O}_2)_2]_4\}$, a polyoxometalate catalyst, is very active; at 70°C in 5 h reaction time, using acetonitrile as a solvent with aqueous HP, it gave almost total cyclohexene conversion with 81% epoxide yield, 10% CHD and less than 5% cyclohexenol and cyclohexenone [62].

The epoxide can be hydrolyzed to CHD or oxidized without C-C bond cleavage giving cyclohexanedione. The last step on the way to AA is the oxidative ring opening of the diketone.

3.2.4.3.2.2. Two-step oxidation of cyclohexene to AA

The two-step oxidation of cyclohexene can be done via CHD. This reaction can be performed in the presence of metal oxide (KMnO_4 , OsO_4) and with TBHP or HP as oxidants. Osmium-catalyzed dihydroxylation involves Os(VI)/Os(VIII), a substrate-selective redox system [64, 65, 66, 67]. N-methylmorpholine N-oxide (NMMO) can be used as the reoxidizing compound for Os (VI) to Os (VIII).

For the first step of the reaction, transition metal complexes, H_2WO_4 , heteropolyacids, CH_3ReO , zeolites, and hydrotalcites can be used as catalysts, but there is a problem of low selectivity due to the formation of by-products formed by C-C bond cleavage [68, 69, 70, 71, 72, 73, 74, 75].

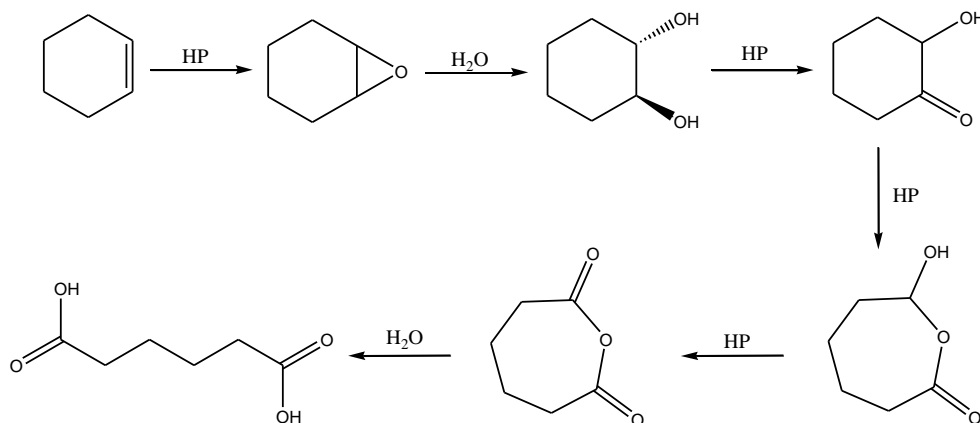
The second step of this process is the oxidative cleavage of CHD that can be performed with molecular oxygen or with hydroperoxide oxidants. Many studies were reported with oxygen, such as the oxidation of the diol with aqueous hydrogen peroxide in the presence of tungstate ions catalysts [76, 77].

In the oxidation of CHD with Ti-containing Y zeolites with hydrogen peroxide, 50% conversion with 80% selectivity to AA was achieved [78]. The main intermediate in this reaction was 2-hydroxycyclohexanone, that can be oxidized to AA. AA further reacts with HP yielding glutaric and succinic acids.

3.2.4.3.2.3. Single-step oxidation of cyclohexene to AA

Noyori has reported the oxidation of cyclohexene with 30% solution of HP in the presence of small amounts of Na_2WO_4 as the catalyst and $\text{CH}_3(\text{n-C}_8\text{H}_{17})_3\text{HSO}_4$ as a phase-transfer catalyst (PTC). The reaction proceeds at 75-90°C in the absence of solvent.

Cyclohexene was oxidized directly to crystalline AA with almost 100% selectivity; the residual aqueous phase of the mixture could be reused. PTC is needed because cyclohexene is not soluble in the aqueous phase where the tungstate reacts with HP forming the anionic peroxy species, the true oxidizing species. The reaction mechanism is shown in Scheme 10 [79, 80].



Scheme 10. Direct oxidation of cyclohexene to AA with HP

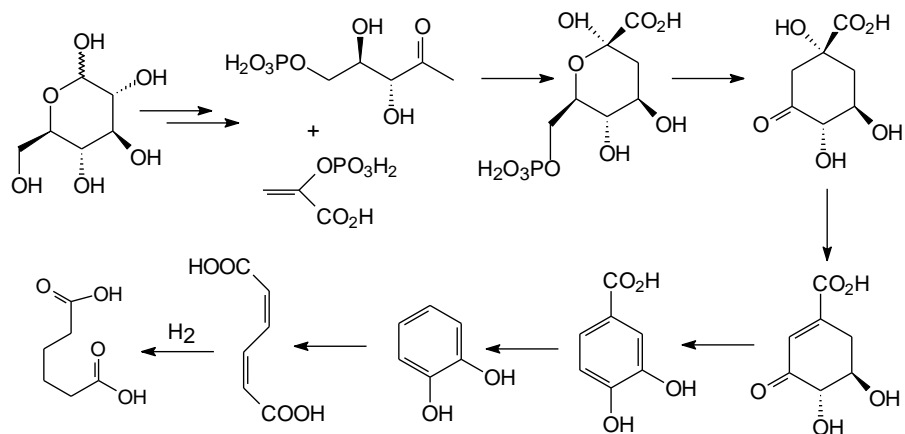
The results can be improved when an organic acid is used instead of the PTC. Almost 97% selectivity to AA with total conversion of cyclohexene was achieved with oxalic acid after 24h reaction time, using an HP:cyclohexene molar ratio of 4.4:1 [81].

Heterogeneous catalysts also have been investigated for the direct oxidation of cyclohexene to AA with HP. For example, tetrahedral tungstate units incorporated in SBA-15 or titanium framework-substituted aluminophosphate, TAPO-5. But these systems give 46% and 30% AA selectivity only, respectively, with complete conversion of the reagent [82, 83]. In case of SBA-15 with incorporated Al and grafted Ti, 80% AA yield was obtained after 24h at 80°C, with *t*-BuOOH as the oxidant. The main by-products of this reaction were CHD, 2-hydroxycyclohexanone, glutaric and succinic acids [84, 85].

The oxidation with HP allowed to use milder reaction conditions (temperature and pressure), but the main problem concerns the cost of HP (4 equivalents of HP are necessary for cyclohexene oxidation). In fact, the value of AA is lower than the cost of the HP needed for this oxidation reaction.

3.2.4.4. D-glucose as a starting compound to produce AA

Draths and Frost proposed a two-step synthesis of AA starting from D-glucose [86, 87]. The first step is the conversion of sugar to *cis,cis*-muconic acid by genetically modified *Escherichia coli*. Then muconic acid can be hydrogenated to AA with a catalyst based on Pt supported on activated carbon, operating at room temperature and 35 bar H₂, or with nanoparticles of Pt-Ru supported on silica at 80°C and 30 bar.



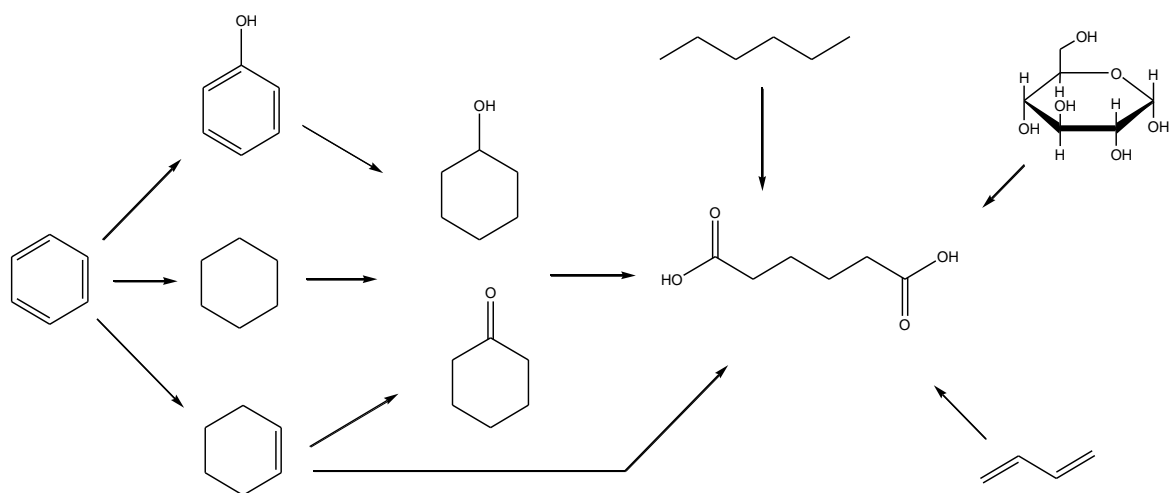
Scheme 11. Two-step transformation of D-glucose to AA[88]

The yield of muconic acid for the first step is 25%, that is a good result for a biotechnological process. In the second step, yield is 95% (with any of reported catalysts).

This route from glucose presents environmental and economic advantages, since it uses a renewable source that can be obtained even from lignocellulosic biomass, starting from a low-cost raw material and at the same time providing added value to a waste compound. The main problem of this route is represented by the cost of the final product, that is not yet competitive with that of the traditional process. Moreover, process improvements are needed to make the large-scale production competitive with that one of the traditional process.

3.3. Conclusions concerning possible synthetic routes to AA

Possible synthetic routes (both conventional and alternative) to AA are summarized in Scheme 12. There are numerous studies on new processes for AA production, some of them are "green", but only a few examples are really sustainable in terms of both environmental and economic viewpoints.



Scheme 12. Summary of the various pathways for AA synthesis [2]

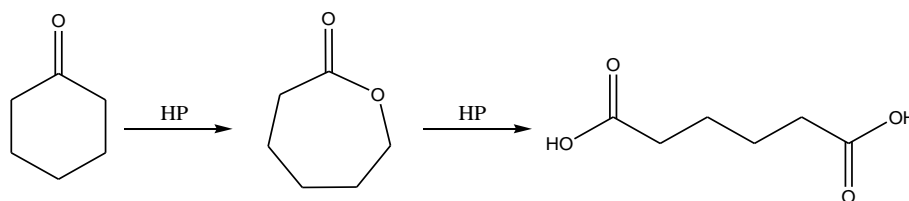
The main limiting factor is economics. The synthesis from glucose is "green", but the cost of the final product is still too high. Even the direct synthesis of AA from cyclohexene perfectly adheres the Green Chemistry principles, but the use of large amounts of HP makes the process economically uncompetitive. The main obstacle to the other proposed alternative processes relates to the use of acetic acid as the solvent, that requires additional costs for handling and special materials.

The more sustainable path would be the one that is able to employ a starting material of low cost, possibly coming from renewable sources, with air or oxygen as the oxidizing agent and using water as a solvent, or eventually using no solvent at all.

The search for an alternative process that is sustainable from all these standpoints is a very active field of research, aimed at both the improvement of the already explored ways, and the investigation of new synthetic approaches.

Baeyer-Villiger reaction: Oxidation of cyclohexanone with hydrogen peroxide

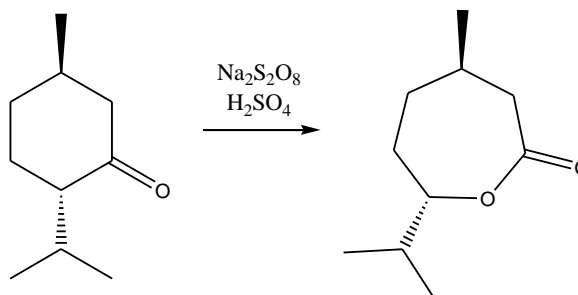
The aim of this part of my research work was to investigate the Baeyer-Villiger oxidation of cyclohexanone to ϵ -caprolactone (CL) with hydrogen peroxide; the latter can be oxidized further to AA (Scheme 13).



Scheme 13. Reaction scheme of cyclohexanone oxidation to AA

4. Baeyer-Villiger reaction

The Baeyer-Villiger (BV) oxidation is one of the most widely used reactions in organic synthesis. The reaction was discovered in 1899 when Adolf von Baeyer and Victor Villiger were studying the oxidation of menthone with sodium persulfate and sulfuric acid (Caro's acid) in the absence of solvent, generating the corresponding lactone [89] (Scheme 14).



Scheme 14. Oxidation of menthone studied by Baeyer and Villiger

Then this reaction achieved tremendous success thanks to its versatility, that allows to synthesize a variety of molecules ranging from pharmaceuticals, such as antibiotics, steroids, pheromones, to fine chemicals and intermediates for the chemical industry.

The basic reaction is the oxidation of a carbonyl group by a peracid with insertion of oxygen; various substrates can be used for this reaction:

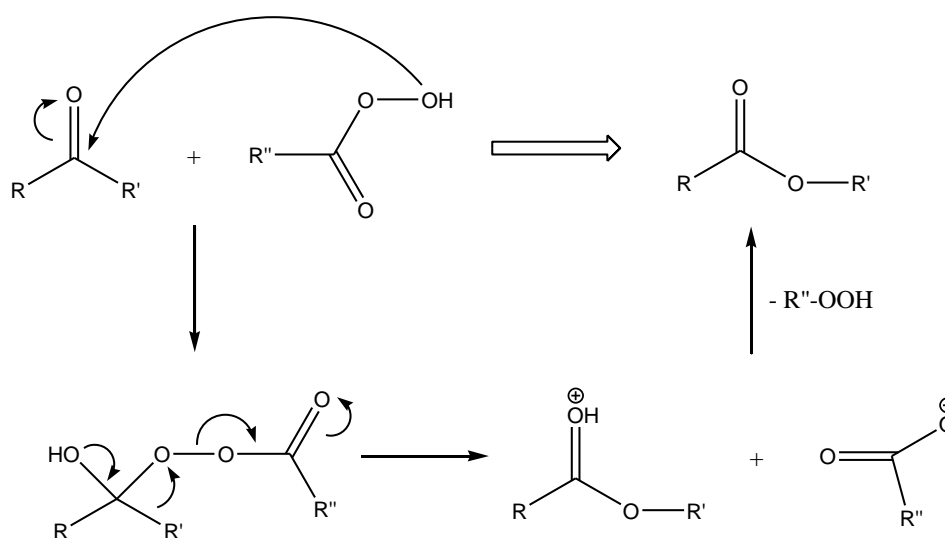
- ketones can be converted into esters,
- cyclic ketones are oxidized to lactones,
- benzaldehydes are transformed into phenols,
- carboxylic acids or anhydrides are used to synthesize diketones.

The Baeyer-Villiger reaction is compatible with a large number of functional groups in the substrate, it is highly regioselective due to easy prediction of the attitude of the

migration groups; generally it is also stereoselective: the configuration of migration groups is saved. Different oxidants are used in this reaction such as *m*-chloroperoxybenzoic acid, peroxytrifluoroacetic acid, peroxybenzoic acid and peroxyacetic acid, hydrogen peroxide, *tert*-butyl hydroperoxide [90].

The reaction mechanism was shown for the first time by Criegee in the 40s: the first step is a nucleophilic attack at the carbonyl carbon by the peroxy acid with formation of the so-called Criegee intermediate; then the migration of one of the two alkyl groups on the peroxygen occurs, with concomitant release of the carboxylate anion. The second step determines the overall speed of the reaction (Scheme 15).

The use of organic peracids as the oxidants involves various problems: first, formation of the corresponding carboxylic acid or its salt in the reaction mixture, which has to be recovered or eliminated (this means increasing the costs of the process); secondly, these oxidants are generally expensive and hazardous because of their intrinsic instability.



Scheme 15. Mechanism of the Baeyer-Villiger oxidation

One solution is to generate in-situ the peracid by reaction of the corresponding aldehyde with oxygen, or carboxylic acid and HP, a procedure which, however, is subject to different constraints from the industrial point of view.

An alternative way is to use a more green oxidant, such as HP in the presence of a catalyst, which would bring several advantages:

- it is the cheaper and safer than organic peroxyacids traditionally used;
- the active oxygen content is higher;
- the only co-product it generates is water, that implies a simplification of the subsequent purification steps.

Despite this, HP also has some disadvantages:

- the presence of water in the reaction mixture as a co-solvent or co-product can lead to the hydrolysis of the ester products;

- HP is a weak oxidant and it needs a catalyst in order to be activated, but different catalysts show a low selectivity in respect to its activation, and cause the formation of hydroxy radicals and hydroperoxides;

- the decomposition of HP may develop pure oxygen causing an increase of pressure that generates problems of safety in the presence of flammable organic species.

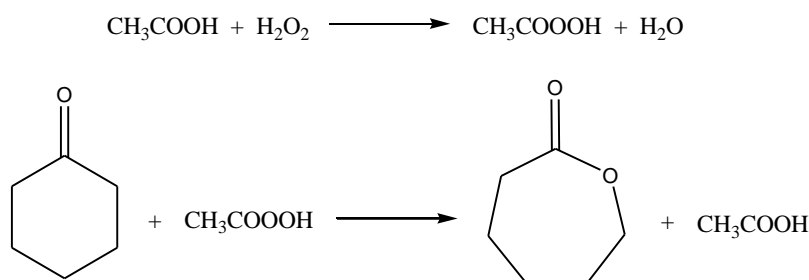
For this reason, when HP is used it is important to avoid the accumulation of oxygen, by working under a stream of nitrogen; the reaction environment should not be contaminated, and a low concentration of the peroxy compounds should be maintained [91].

5. ϵ -Caprolactone

ϵ -Caprolactone (CL) is a colorless to yellow liquid with a perceptible odor. It is soluble in water and miscible with most organic solvents [92].

CL is used for the production of polycaprolactone, a biodegradable polyester with a low melting point, and as an intermediate for the production of adhesives, paints and additive for resins and polymers.

Currently CL is produced industrially via the Baeyer-Villiger oxidation of cyclohexanone with *m*-chloroperbenzoic acid and peracetic acid [93] (Scheme 16).



Scheme 16. Current industrial processes for CL production

Within this context, many studies have been published in recent years dealing with synthetic procedures for CL that do not involve the use of an organic peracid, but of an oxidant with lower environmental impact such as oxygen or HP, in the presence of an heterogeneous catalyst.

Heterogeneous catalysts that are active in cycloalkanones oxidation with HP can be divided into four groups:

1. Brønsted-type acid catalysts (zeolites H- β and USY) [94], alumina [95] and polyoxometalates [96];
2. Lewis-type acid catalysts based on Sn(IV) [97, 98], Sb(V) [99] or supported complexes of Pt [100];
3. basic oxides [101];
4. Catalysts based on elements able to promote the formation of Me-OOH species, such as Ti(IV) [102, 103].

The aim of my work was to investigate the mechanism of cyclohexanone hydroperoxidation, which is the first step in the formation of CL. CL can then be converted into AA, a reaction which involves the hydrolysis into 6-hydroxyhexanoic acid, and the oxidation of the latter into AA. These last steps have not been investigated during my PhD work.

6. Experimental Part

Our study of cyclohexanone hydroperoxidation can be divided into three parts:

- kinetic experiments: the effect of the presence of catalyst on cyclohexanone conversion;
- identification of the reaction products;
- study on the mechanism of cyclohexanone oxidation with HP.

6.1. Catalysts

The catalysts, with some characteristics, used for reactivity experiments are shown in Table 1. These catalysts were kindly provided by Prof. Oxana Kholdeeva (Ti-MMM and SBA-16 materials), Boreskov Institute of Catalysis, Novosibirsk, and Prof. Paolo Pescarmona (TUD-materials and Ga₂O₃), University of Leuven, Belgium. They were used either because some of the elements (Me) incorporated in the structure are known to activate HP and produce a Me-OOH (hydroperoxo) species, such as in the case of Ti⁴⁺, or because they show Lewis acid properties, which is an important feature in hydroperoxidation of ketones. In fact, the carbonyl is activated by interaction with the Lewis acid; this is the case, for instance, of Sn⁴⁺ and Zr⁴⁺. The Table also reports literature references where the preparation and characterization of catalysts is described.

Table 2. Catalysts used for the BV oxidation of cyclohexanone and their characteristics

Catalyst	Type of support/ framework	Si/Me; Content of Me, %	Surface area, BET (m ² /g)	Lewis/Brønsted acidity	Ref.
20MB (Ti-MMM)	Mesoporous Ti-silicate with hexagonal structure	2.7%	1200	Lewis acid	104
16MB (Ti-MMM)	»	1.6%	1147	Lewis acid	105, 106, 107
MK143(1) (Ti-MMM)	»	1.0%	-	Lewis acid	104
MK143(3) (Ti-MMM)	»	1.8%	1119	Lewis acid	107
SBA-16 (Ti)	Mesoporous silica, cubic structure	0.7%	992	Lewis acid	
Zr-TUD-1	Three-dimensional sponge-like mesoporous silica	51	651	Lewis acid	108
Hf-TUD-1	»	53	715	Lewis acid	108

Sn-TUD-1	»	54	729	Lewis acid	108
Ga ₂ O ₃ nanorods	-	0	155	Lewis acid	109, 110
Zeolite HY		15		Brønsted acid	
TS-1	MFI structure (Ti-silicalite)	2.0%		Lewis acid	111

6.2. Catalytic measurements of cyclohexanone hydroperoxidation

Typical conditions used for the reaction were: in a 10 ml pyrex reactor with screw stopper, a mixture of 0,1 ml H₂O, 3 mmol 30% H₂O₂ and 1 mmol cyclohexanone was dropped in; the mixture was then stirred at 50°C for the required time. In the case of catalyzed reactions, the procedure was the same, but 15mg of the catalyst was added (except with Ga₂O₃ and Zeolite HY).

6.3. Treatment of the reaction mixture

The treatment of the reaction mixture varies according to the type of analysis to be performed.

If the sample was to be injected into HPLC instrument, the reaction mixture was transferred to a centrifuge tube, to which the solution obtained by washing the reactor with 2 ml of the eluent mixture was added; then the mixture was centrifuged. The supernatant was then transferred to a 10 ml volumetric flask, and a second washing of the reactor with additional 2 ml of the eluent mixture was carried out. The mixture was centrifuged again after transferring the liquid in the first centrifuge tube. After joining the supernatant fraction in the volumetric flask, a washing of the catalyst with 2 ml of eluent mixture was carried out. This final solution was joined to the previously centrifuged liquids in the volumetric flask and made up to volume always with the eluent mixture.

If, however, the mixture had be analyzed with ESI-MS, we added CH₃OH to dilute it up to a total volume of 2 ml; then the solution was transferred into a centrifuge tube, and centrifugation was performed in order to separate the catalyst.

To analyze the mixture by means of NMR, immediately at the end of the reaction a fraction of the aqueous mixture was extracted with CDCl₃, and the chloroform extracts were separated with the aid of a membrane filter and analyzed by means of NMR.

6.4. Analysis of the products

The quantitative analysis of the components of the reaction mixture was carried out by means of HPLC, while the qualitative analysis was performed with ESI-MS and NMR spectroscopy.

6.4.1. HPLC

The instrument used is an HPLC Agilent 1260 Infinity Quaternary LC Series. The column used is a Poroshell 120 EC-C18 (2.7 μm , 4.6 x 50 mm), thermostated at 25°C. The injection was done with the calibrated loop 20 μl . The elution was carried out under isocratic conditions with a mixture of 0.01 M H_3PO_4 : CH_3CN =95:5, by volume, eluent flow of 0.5 ml/min. The detector is a DAD (Diode Array Detector), which can record multiple wavelengths simultaneously.

6.4.2. ESI-MS

The ESI-MS technique is a mass spectroscopy that allows the analysis of ions without fragmentation of the molecules. The sample is injected into the instrument with a syringe whose needle is held at a potential difference of a few KV due to an electrode, after which the solution passes through a capillary where solvent evaporation and gradual concentration of the charges present in drops occur, up to a limit point in which the repulsion of the charged particles causes the explosion into smaller droplets. The same mechanism is repeated several times until obtaining a spray of charged molecules that go to bind with the ions already present in the initial solution, a combination that allows the analysis in a quadrupole mass spectrometer. After the analysis a spectrum with the signals of the masses and their relative intensity is recorded.

By means of this method, it is possible to reduce the fragmentation of large and thermally labile molecules. To facilitate the evaporation, often volatile organic solvents such as acetonitrile or ethyl ether are added to aqueous solutions. In order to decrease the initial size of the droplets, it is possible to add compounds which increase the conductivity, for example, acetic acid, which also acts as a source of protons facilitating the processes of ionization. The analysis can be scanned in positive ions or negative ions. In the first case it is possible to see the signals of the masses plus 1, 23 or 39 mass units corresponding to addition of a hydrogen, sodium or potassium ion, while for negative ions the increase of 35 units is due to chlorine ions, or the decrease of 1 unit due to elimination of hydrogen ion. The instrument used is a Waters - Micromass ZQ 4000.

6.4.3. NMR

Where not otherwise specified, ^1H and ^{13}C NMR spectra were recorded at 25°C on a Varian Inova 300, at 300 MHz and 75 MHz or Varian Inova 600, at 600 MHz and 150 MHz respectively. Chemical shifts (δ) for ^1H and ^{13}C are given in ppm relative to residual signals of the solvents. The following abbreviations are used to indicate the multiplicity: s, singlet; d, doublet; t, triplet; q, quartet; m, multiplet; bs, broad signal. CDCl_3 was passed over a short pad of alumina before use. Coupling constants are given in Hz.

Reactions were performed also in NMR tube. To allow spectroscopical measurements, NMR tube reactions were run in deuterium oxide at a concentration 20 times lower than

batch reactions, all other parameters being unchanged. In both cases stoichiometric ratio between the reactants was 3 molar equivalents of HP compared to cyclohexanone and the temperature was kept at 50°C. The only effect of this concentration change we observed was a slower reaction in NMR tube. NMR profiles are the same both for NMR tube and batch reactions.

6.5. Computational investigations

The computational investigation has been carried out in order to recognize the reaction course leading from cyclohexanone to the final products.

All of the simulations have been carried out with the Gaussian09 Software [112].

Preliminary calculations have been performed using Density Functional Theory (DFT). Reactants, intermediates, transition structures and products have been initially optimized adopting the B3LYP [113, 114] functional and the standard 6-31G(d,p) basis set in the gas phase. To confirm the nature of the stationary points, vibrational frequencies (in the harmonic approximation) were calculated for all of the optimized structures at the same level of theory as geometry optimizations and it was verified that local minima had only real frequencies, while transition states (TS) were identified by the presence of a single imaginary frequency corresponding to the expected motion along the reaction coordinate.

Unscaled results from the frequency calculation have been used to compute zero-point energies and their thermal corrections, enabling for the calculation of the Gibbs free energy of the system considered.

As for TSs, intrinsic reaction coordinate (IRC) calculations were performed in both directions (for 100 steps) at the same level of theory in order to investigate the process in detail. The starting and final structures were then optimized in order to connect the TSs to complexed reagents and products.

For each reacting situation considered, several conformations (e.g. differing for the displacement of one or more O-H bonds) have been optimized, and the parameters of the most stable among these have been used as the starting point for a refinement by adopting a higher level of theory, viz. using the composite method CBS-QB3 [115] in the gas phase.

The CBS-QB3 is part of the so-called "Complete Basis Set" (CBS) methods of Petersson and coworkers for computing very accurate energies and involves the following steps: optimization and frequency calculations performed at the B3LYP/CBSB7 level; single point calculations performed at CCSD(T)/6-31+G(d') and MP4SDQ/CBSB4 levels. The total energy is then extrapolated to the infinite-basis-set limit using pairs of natural-orbital energies at the MP2/CBSB3 level and an additive correction to the CCSD(T) level.

With both levels of theory (DFT and CBS-QB3), Gibbs free energies (G) obtained in vacuo have been corrected in order to take into account the solvent (water) effects by adding the ΔG of solvation, in turn calculated as recommended by the G09 software. In particular, this value has been calculated at the B3LYP/6-31G(d,p) level of theory by using the SMD model by Thrular and co-workers [116]. This is the recommended choice for

computing ΔG of solvation, obtained by performing single-point gas phase and SMD calculations for the system of interest and taking the difference of the resulting energies.

Thermochemical data have been calculated adopting the default options, *viz.* temperature: 298.150 K and pressure: 1.00000 atm. The conversion factor between Hartree and kcal mol⁻¹ has been: 1 Hartree = 627.509 kcal mol⁻¹. The computed enthalpy, entropy and Gibbs free energy were converted from the 1 atm standard state into the standard state of molar concentration (ideal mixture at 1 mol L⁻¹ and 1 atm) in order to allow a direct comparison with the experimental results in water solution. In particular, for conversions from 1 atm standard state to 1 mol/L standard state, the following contribution needs to be added to Gibbs free energy: $RT \ln R'T$, where R' is the value of R in L · atm · K⁻¹ · mol⁻¹ [117]. This contribution always cancels out unless a process where a molecularity change (Δn) between reagents and products occurs. Accordingly, this contribution should be written as: $\Delta n RT \ln R'T$. As an example, in the reaction: $A + B \rightarrow C$, $\Delta n = -1$ and the contribution will be $-RT \ln R'T$ (-1.90 kcal mol⁻¹ at 298.150 K).

As mentioned, the DFT level of theory has been only adopted for preliminary and screening purposes, thus all the Gibbs free energies data reported in the text do refer to the CBS-QB3 level of theory, also including the solvent effect (hereafter named "SMD- CBS-QB3").

7. Results and discussion

During our study we checked the reactivity at 50°C of all catalysts shown in Table 2; we measured cyclohexanone conversion and we determined the reaction products. We also investigated the uncatalyzed cyclohexanone oxidation with HP.

7.1. Kinetic experiments

Figure 5 shows the result obtained with some of the catalysts listed in Table 2. For comparison, the behavior shown in the absence of catalyst is also reported.

These catalysts are made of silica-based structures with incorporated Ti. The most active catalysts from this group were 20MB, 16MB and MK143(3), all belonging to the Ti-MMM class. The catalyst with the lowest content of Ti, SBA-16, showed the lowest activity in the reaction. The results show that there is a rough proportionality between the Ti content in catalysts and the conversion of cyclohexanone. The only exception was TS-1, which however has a microporous structure, with smaller pores compared to the mesoporous structure of MMM catalysts. This might affect diffusion of reactants and hence decrease the reaction rate.

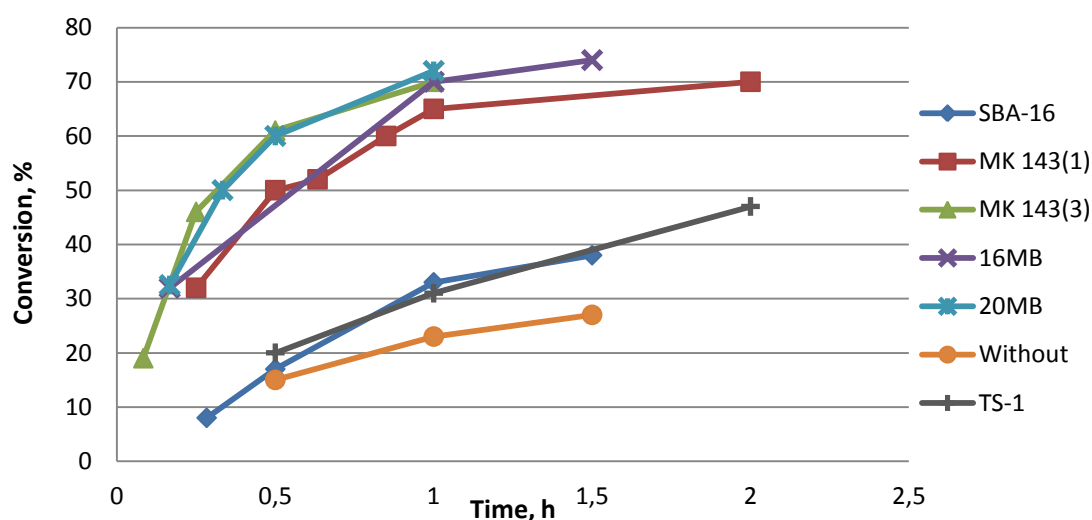


Figure 5. Oxidation of cyclohexanone with HP in the presence of different catalyst and the uncatalyzed reaction. Conditions: 1mmol cyclohexanone, 3 mmol H₂O₂ (30% solution), 1ml H₂O, 50°C, m(catalyst) = 15mg

Results of the reactions carried out with catalysts containing elements other than Ti are shown in Figure 6. Some samples are made of the so-called TUD silicate structure, which can host various types of elements [108]. Moreover, the reactivity of gallium oxide with a nano-rod morphology, and of a H-Y zeolite (a Brønsted-type acid catalyst) are also reported. The most active catalyst was gallium oxide. In the presence of Ga₂O₃ cyclohexanone conversion was 80% already after 1 hour of reaction (the amount of gallium oxide used was 7mg, instead of 15mg employed for other catalysts). It is necessary to take into account that the distribution of the metal in the TUD silicate structure, either

homogeneous inside the solid or concentrated at its surface, can greatly affect the reactivity. The large difference in reactivity of Ga₂O₃ and Me-TUD catalysts can be explained by the fact that gallium oxide catalyst is in the form of bulk nanorods, thus presenting a high ratio between the surface area and its volume; moreover, Ga³⁺ active sites are not diluted inside an inert matrix. It is possible that in the case of Me-TUD systems diffusional phenomena limit the reactivity, while in the case of gallium oxide active centers are directly accessible to the reactants. From the literature, it is possible to derive the following scale of Lewis acidity for the investigated catalysts shown in Figure 6: Zr⁴⁺ < Hf⁴⁺ < Sn⁴⁺ < Ga³⁺ [108, 118]. According to this scale, the activity of the catalysts increase with increasing the Lewis acidity and the most active catalyst is the strongest Lewis acid – Ga³⁺.

Also Zeolite H-Y showed high activity (the kinetic experiments were carried out with 7 mg of this catalyst). The activity of this catalyst, showing only Brønsted-type acidity, might be due to the fact that the protonation of H₂O₂ leads to the formation of a strongly electrophilic species, showing enhanced reactivity in carbonyl hydroperoxidation.

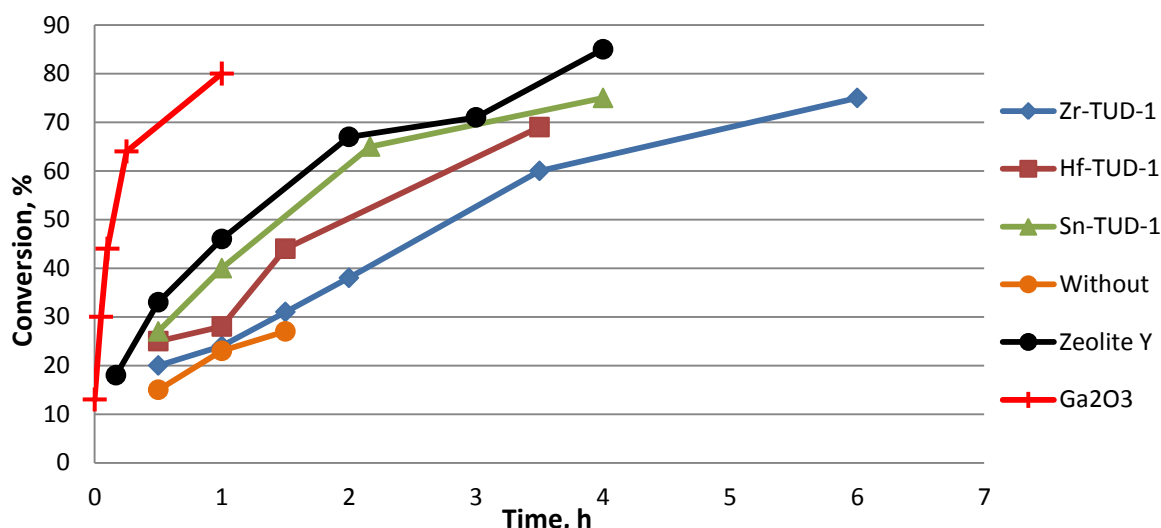


Figure 6. Oxidation of cyclohexanone with HP in the presence of different catalyst compared with the uncatalyzed reaction. Conditions: 1mmol cyclohexanone, 3 mmol H₂O₂ (30% solution), 1ml H₂O, 50°C, m(catalyst) = 15mg (for Ga₂O₃ and Zeolite Y m(catalyst) = 7 mg)

Under these reaction conditions, the formation of ε-caprolactone has never been detected. Probably, the reason lies in the low temperature of the reaction, which limits the consecutive transformation of the hydroperoxides formed (see below). It is worth noting however, that in aqueous medium the CL, if formed, would probably be readily hydrolyzed to produce the 6-hydroxyhexanoic acid. The analysis of the mixtures and identification of the reaction products is described in the next chapter.

7.2. Identification of the reaction products

Reaction mixtures were first analyzed by means of HPLC. The analysis showed the presence of only one reaction product, which was then found to correspond to the

overlapping of several products which could not be separated. Therefore, we used ESI-MS and NMR spectroscopy for the identification of these compounds.

The ESI-MS and NMR spectra of the mixture obtained with the uncatalyzed reaction are given in the Figures 7 and 9, respectively.

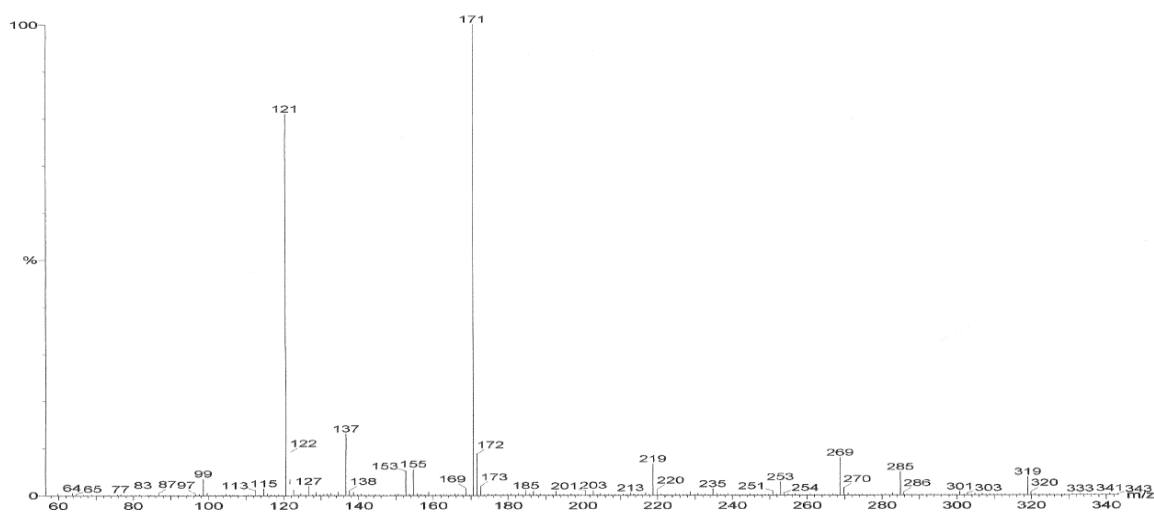


Figure 7. ESI MS spectrum of the uncatalyzed reaction mixture. Conditions of the reaction: 1mmol cyclohexanone, 3 mmol H₂O₂ (30% solution), 1ml H₂O, 50°C, 2 hours

The main peaks identified were those related to cyclohexanone (MW=98 peak at $m/z=121=98+23$) while peaks at $m/z=155$ and $m/z=171$ could correspond to one compound with MW=132 ($155=132+23$, $171=132+39$). Moreover, a peak of small intensity having $m/z=137$ was shown, which could match a substance of molecular weight equal to 114 (+Na⁺); the most probable hypothesis is that the signal corresponds to ϵ -caprolactone (having MW=114), but the latter was not detected by HPLC, probably because of its low concentration.

To confirm the possible presence of ϵ -caprolactone and to understand what the compound with MW=132 is, ¹³C-NMR analysis was carried out on the same mixture, after extraction with deuterated chloroform (CDCl₃).

¹³C NMR clearly shows a quaternary peak around 110 ppm with all other relevant peaks exactly matching those reported in [119] for the Criegee intermediate, 1-hydroperoxycyclohexan-1-ol (Figure 8). The molecular weight of this compound is 132.

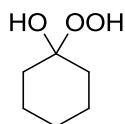


Figure 8. 1-Hydroperoxycyclohexan-1-ol (Criegee intermediate)

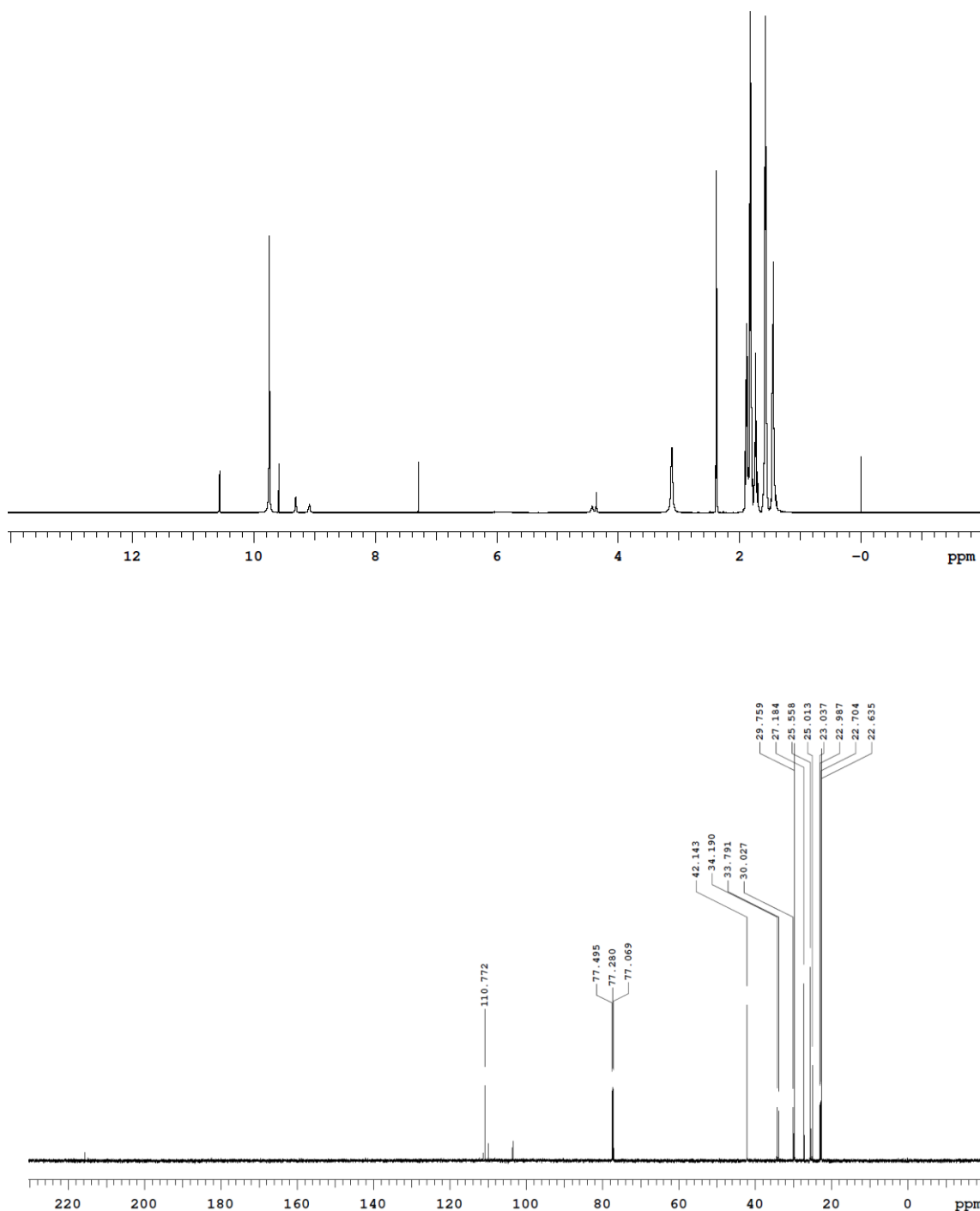


Figure 9. ^1H and ^{13}C NMR spectra of the uncatalyzed reaction mixture extracted with CDCl_3 . Conditions of the reaction: 1mmol cyclohexanone, 3 mmol H_2O_2 (30% solution), 1ml H_2O , 50°C , 2 hours

The signal of the C sp^2 of CL, which should be located at 177 ppm, was absent in the NMR spectrum; the question arises why this compound is identified by means of ESI-MS. One hypothesis that could explain this fact is that the CL is formed starting from the Criegee intermediate during the injection in ESI-MS instrument.

Next step was the identification of the products of the reactions that were performed in the presence of catalysts. We managed to isolate the crystals of one of the

products from the reaction mixture in the presence of the Zeolite H-Y. This solid was characterized by means of XRD, NMR and ESI-MS techniques (Figures 10, 11, 12).

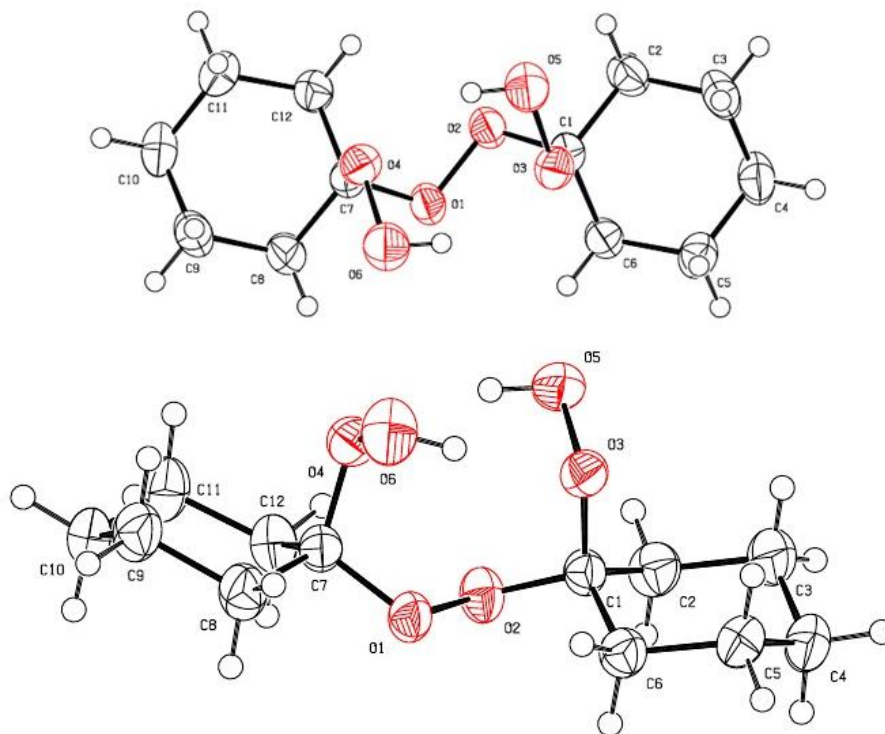


Figure 10. Structure of the crystals that were obtained from the reaction mixture in the presence of Zeolite H-Y obtained by means of XRD.

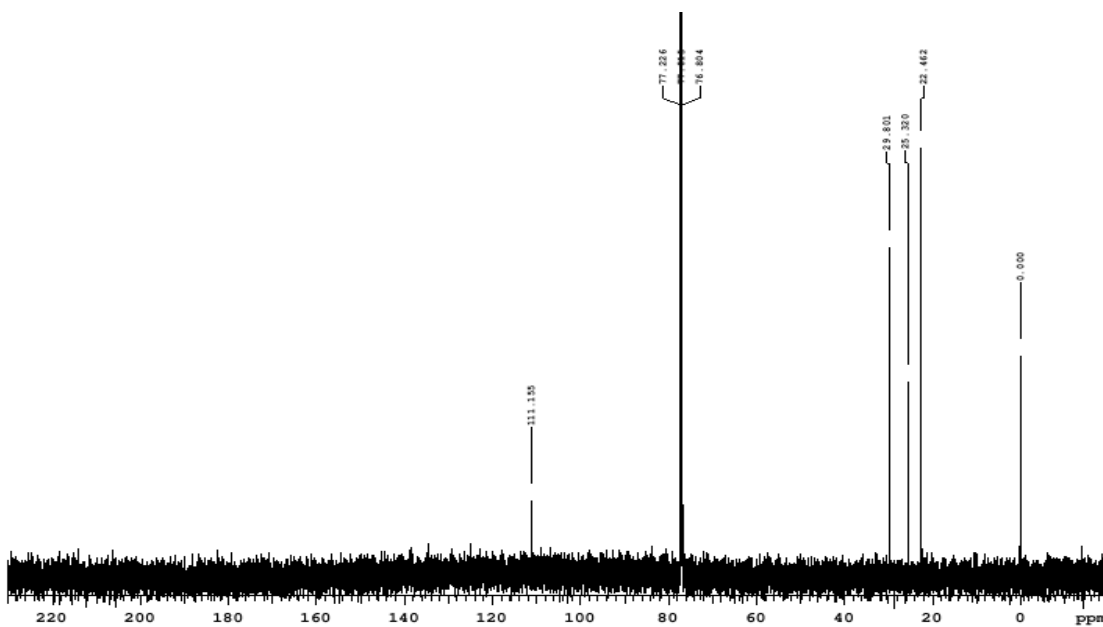


Figure 11. ^{13}C NMR spectrum of the crystals that were obtained from the reaction mixture in the presence of Zeolite H-Y, dissolved in CDCl_3

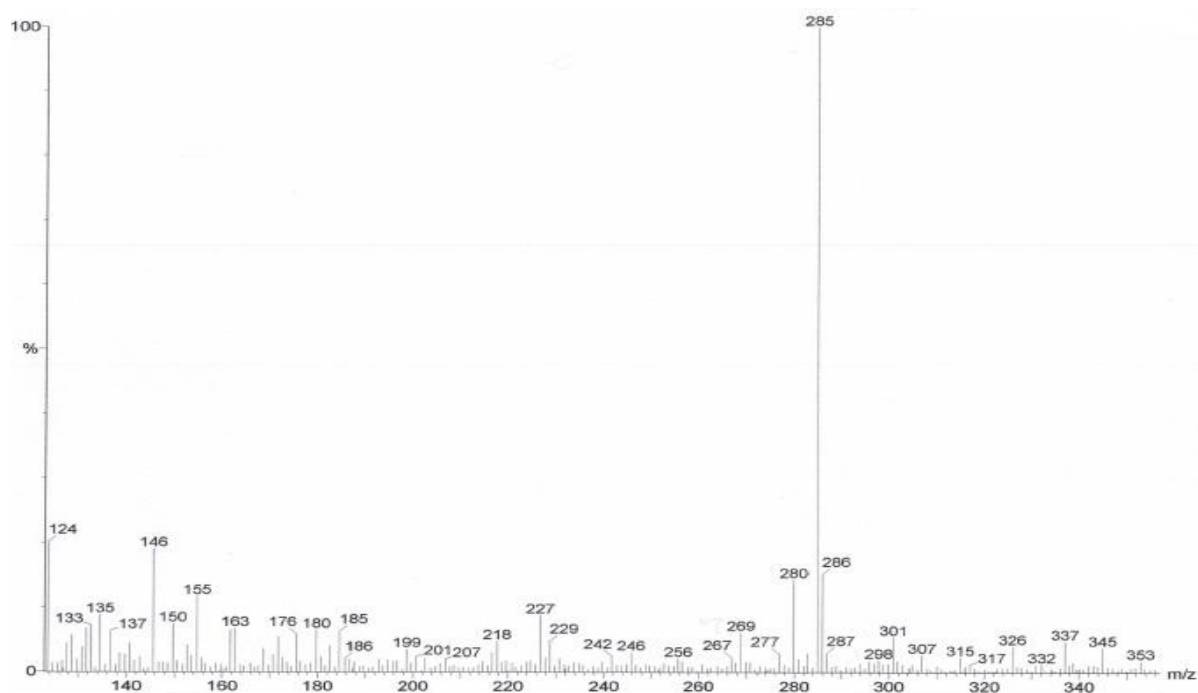


Figure 12. ESI-MS spectrum of the crystals that were obtained from the reaction mixture in the presence of Zeolite H-Y, dissolved in CH₃OH

By means of these techniques it was possible to identify the compound. The name of this compound is 1-[(1-hydroperoxycyclohexyl)hydroperoxy]cyclohexanol, Its molecular structure is given in Figure 13; it has MW=262 (ESI-MS: peak at m/z=285=262+23).

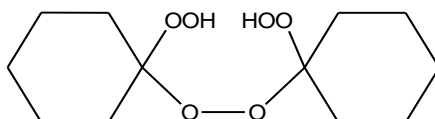
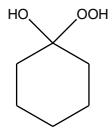
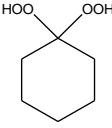
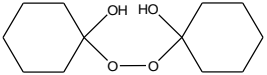
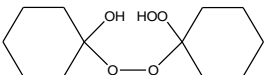
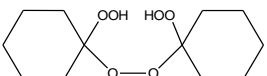
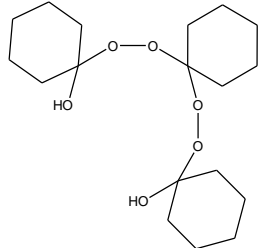
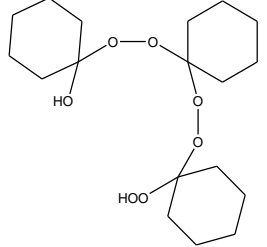
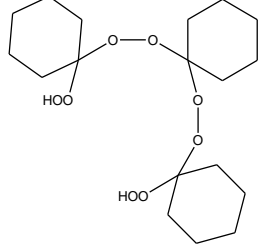


Figure 13. 1-[(1-hydroperoxycyclohexyl)hydroperoxy]cyclohexane. Crystals that were obtained from the reaction mixture in the presence of Zeolite H-Y

Further, by means of ESI-MS we could identify other products of the catalyzed reactions. The list of products is given in Table 3.

Table 3. Products of catalyzed reactions

Product	Name of the product	MW (g/mol)	Letter
	1-Hydroperoxycyclohexan-1-ol (Criegee intermediate)	132	a
	1,1- Dihydroperoxycyclohexane	148	b
	1-[(1-hydroxycyclohexyl) peroxy]- cyclohexanol	230	c
	1-[(1-hydroperoxycyclohexyl) peroxy]-cyclohexanol	246	d
	1-[(1-hydroperoxycyclohexyl) hydroperoxy]-cyclohexane	262	E
	1-[[1-[(1-hydroxycyclohexyl) dioxy] cyclohexyl]dioxy]-cyclohexanol	344	F
	1-[[1-[(1-hydroperoxycyclohexyl) dioxy]cyclohexyl]dioxy]- cyclohexanol	360	G
	1-[[1-[(1- hydroperoxycyclohexyl) dioxy]cyclohexyl]dioxy]- hydroperoxycyclohexane	376	H

Identification of the products and their distribution were performed for the reactions catalyzed with Zr-TUD-1, Hf-TUD-1, Sn-TUD-1, Ga₂O₃, TS-1 and MK-143(1). Since it is not

possible to make a quantitative analysis of these compounds by means of HPLC, because the relevant standards are not available and also because most of these molecules cannot be separated in the chromatographic column, we proceeded with a semi-quantitative analysis by means of ESI-MS.

The evaluation was carried out taking as reference the peak of tetrahydrofuran (THF), added as internal standard in a precise amount, and relating the intensity of the other identified peaks to that one of the standard. To the most intense peaks we attributed three pluses (+++), and then two or one according to the ratio between the intensities. A "-" sign has been assigned when a compound is not present in the mixture.

The results of this semi-quantitative analysis are given in Table 4.

Table 4. Results of the semi-quantitative analysis carried out by ESI-MS.
+++ high concentration; ++ medium concentration; + low concentration; - product is absent

Catalyst	X _{CHN} (%)	Identified compounds							
		a	b	c	d	E	F	g	H
Zr-TUD-1	24	++	++	+++	+++	+	++	+	+
	41	+	+	+	++	+++	+	+	++
Hf-TUD-1	25	++	++	+++	+++	+	++	+	+
	42	+	+	-	++	+++	+	+	++
Sn-TUD-1	33	++	+++	++	+++	++	++	-	-
	75	+	++	-	+	+++	+	+	++
Ga ₂ O ₃	34	+	+++	-	+	++	+	-	+
	81	-	+	-	+	+++	-	-	+++
MK-143(1)	25	++	++	+	++	+	+	+	+
	70	+	+	-	+	++	-	+	++
TS-1	25	++	++	++	+++	-	+	-	-
	50	+	++	+	+++	-	+	+	-

For some catalysts we also calculated the ratios between the peak intensity of the product and the intensity of the internal standard THF. Catalysts Zr-TUD-1 and Ga₂O₃ were studied more in detail, because in the scale of Lewis acidity the former holds the lowest acidity and the latter the highest Lewis acidity. The results are shown in Table 5.

Table 5. Results of the semi-quantitative analysis carried out by ESI-MS. The numbers are the ratios between areas of the peaks of the product and THF.

Catalyst	X _{CHN} (%)	Identified compounds							
		a	b	c	d	e	F	g	h
Zr-TUD-1	20	0.7	4.4	2.3	4.6	1	0.8	0	0
	24	0.5	5.3	1.1	7.1	2.2	1.1	0.3	0.3
	41	0.2	3.6	0.2	4.6	3.4	0.6	0.4	1.2
Hf-TUD-1	25	0.9	4.8	2.1	7.6	1.5	1	0.3	0
	42	0.1	2.2	0	3.3	3.5	0.2	0.6	1.7
Sn-TUD-1	33	1	7.4	2.3	8.7	2.5	0.9	0	0
	75	0.2	2.2	0	1.9	3.9	0.1	0.3	1.3
Ga ₂ O ₃	10	0.2	3.7	0	0.6	0.7	0.2	0	0.3
	30	0.1	5.1	0	0.9	2.2	0.3	0	0.6
	44	0.1	4.5	0	1.1	3.5	0.3	0	1.2
	64	0	1.4	0	0.2	2	0.1	0	1.2
	80	0	0.9	0	0.1	3.5	0	0	1.8

The following considerations can be done based on these semi-quantitative data:

- The compound **a** (Criegee intermediate) was present in all reaction mixture in low or medium concentrations;
- The formation of product **b** seemed slow in the presence of Zr and Hf-based and MK-143(1) catalysts, while it was faster in the case of Sn and Ga, but the concentration of **b** decreased at high cyclohexanone conversion, an event which is typical of a product that is initially formed and then takes part in subsequent reactions;
- The product **c** formed quickly in large amount with Zr and Hf-based catalysts, and with TS-1, and only in a small amount in the case of Sn-TUD-1; **c** was not detected in the reaction with Ga₂O₃. At high cyclohexanone conversion the amount of **c** in the reaction mixture decreased, which means that the product is involved in a consecutive reaction after its formation;
- A similar trend was also shown in the case of compound **d**, since it remained in low concentration when cyclohexanone conversion was high;
- Product **e** was a secondary product for Zr-TUD-1, Hf-TUD-1 and MK-143(1), while its formation was faster in the case of Sn-TUD-1 and Ga₂O₃; **e** did not form in the presence of TS-1;
- Product **f** was present in the final mixtures of Zr, Hf and Sn-TUD-1 catalysts and TS-1, but is not detected in the case of Ga₂O₃ and MK-143(1) at high CHN conversions;
- Product **g** formed in small quantities in all cases, with the exception of gallium oxide;

- Product **h** showed the typical behavior of a secondary product; it formed in a significant amount in the case of the Ga-based catalyst, and did not form at all in the case of TS-1.

- Concluding, the Lewis acidity of catalysts affected the product formation. More acid catalysts, such as Sn-TUD-1 and Ga₂O₃, formed a greater amount of the bis-hydroperoxide and less of the Criegee, and showed the higher rates of transformation of this molecule into heavier condensed products, which are also bis-hydroperoxides.

7.3. Study of the mechanism of BV oxidation of cyclohexanone with hydrogen peroxide

In the analysis of the reaction mixture of cyclohexanone (CHN) oxidation with aqueous solution of HP by means of NMR spectroscopy, we detected the formation of the Criegee intermediate (chapter 7.2).

In order to understand the mechanism of formation of this compound from cyclohexanone, we carried out in-situ NMR-experiments. For these experiments we used cyclohexanone labeled with ^{13}C in the carbonyl group, in order to obtain a stronger signal for this atom.

The first experiment was performed by means of the following procedure: the mixture contained 25 mg of ^{13}C -CHN and 0.75 mL of deuterated water (D_2O) was loaded in the NMR tube. The ^{13}C -NMR analysis of ^{13}C -cyclohexanone was done, and then we added 80 μL of 30% HP and let the reaction proceed until 55 hours, at 50°C . The same operating conditions and amounts of reagents were used in all subsequent in-situ NMR experiments. The concentrations used for these tests were about $1/20^{\text{th}}$ of those used in similar reactions followed by ESI-MS and HPLC. The spectra were acquired every hour from the time $t=0$ (time when we added HP) to 55 hours.

The spectrum recorded before the the addition of hydrogen peroxide is shown in Figure 14; it clearly shows a ^{13}C peak at 220 ppm, indicating the presence of the ketone only.

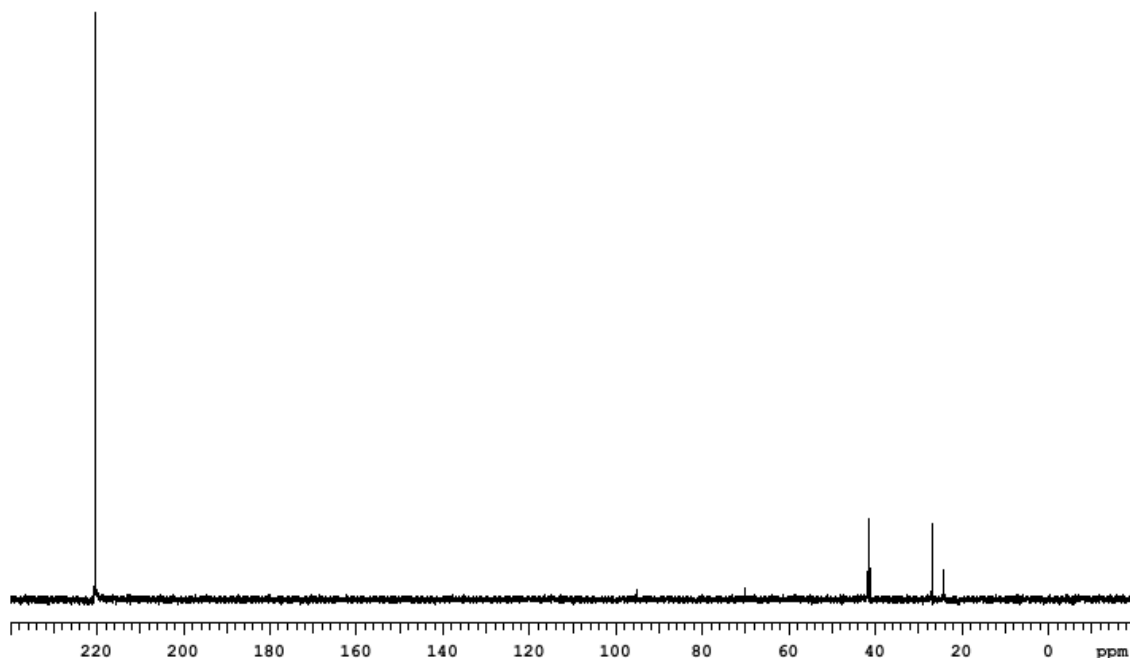


Figure 14. ^{13}C -NMR spectrum of ^{13}C -cyclohexanone

At this point the NMR tube was removed from the NMR instrument, and immediately HP was added. The tube was placed again in the NMR instrument and a new spectrum was recorded after a minimum shimming of the instrument. The whole

operation took no more than 5 minutes. The spectrum recorded just after HP addition is reported in Figure 15.

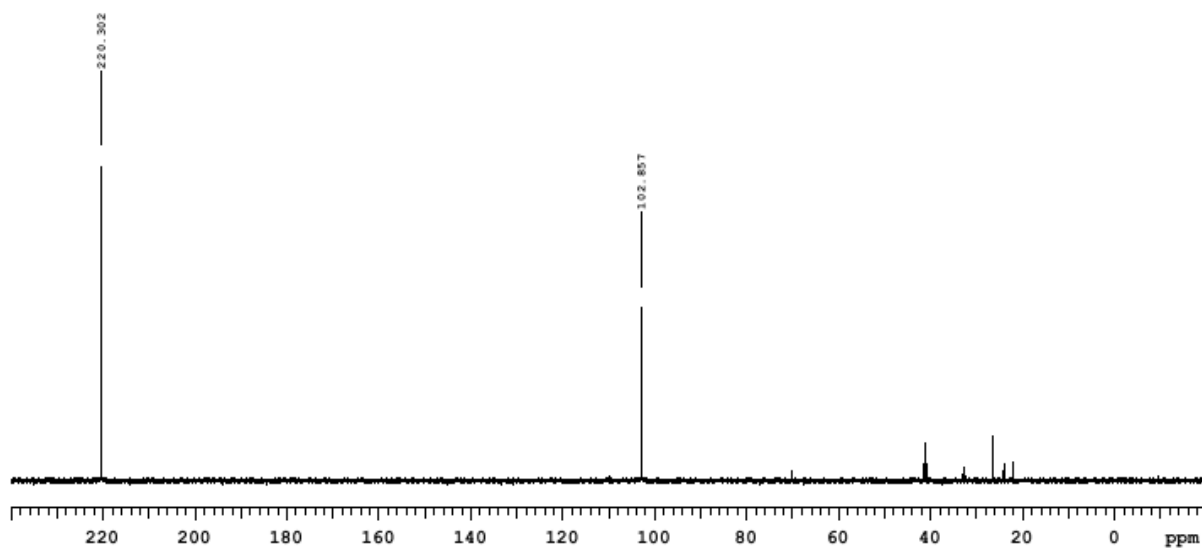


Figure 15. ^{13}C -NMR spectrum of the reaction mixture at the time $t=0$. Temperature 50°C

The NMR spectrum recorded at time $t = 0$ shows, besides the peak of the carbonyl carbon in the reagent, a new peak at $\delta = 103$ ppm with an intensity equal to that of the ^{13}C -CHN.

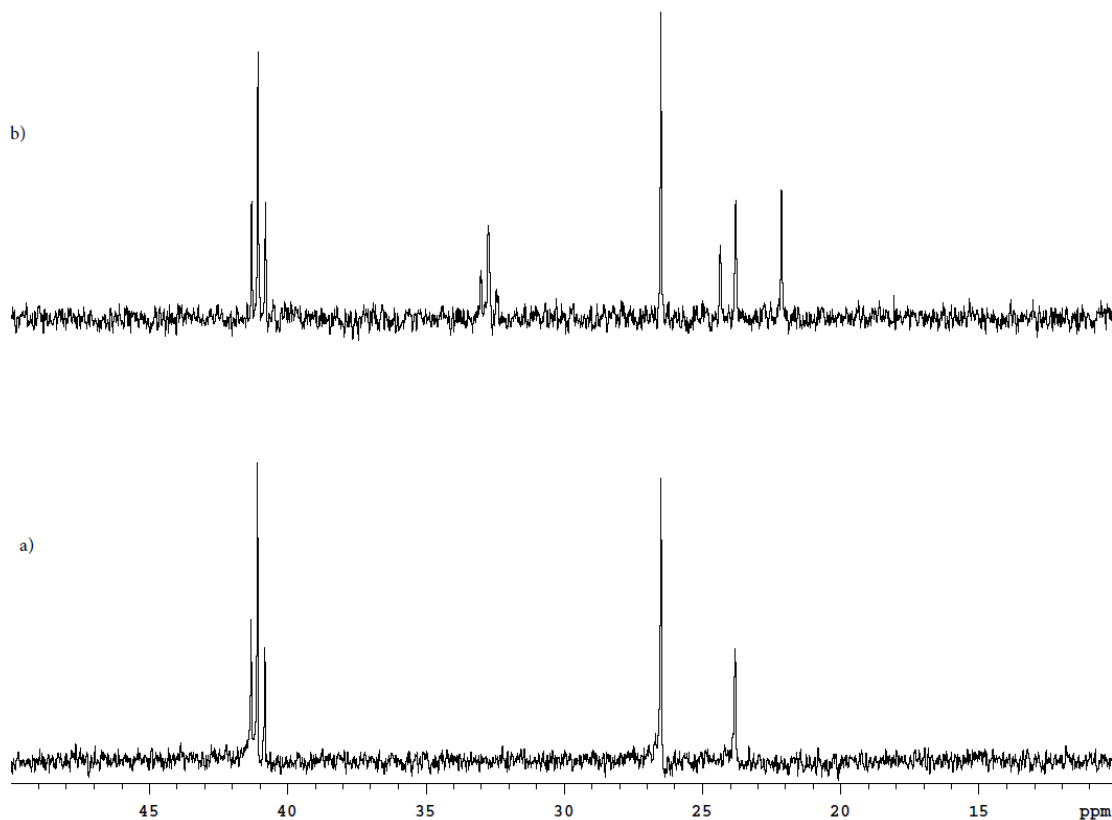


Figure 16. Comparison between the aliphatic portions of the spectra reported in Figures 14 and 15

Analysis of the aliphatic portions (Figure 16) of the two ^{13}C NMR spectra reported in Figures 14 and 15 highlights that the unknown compound is symmetrical, like cyclohexanone. In fact, the aliphatic portion of the ^{13}C NMR spectrum prior to the addition of H_2O_2 (Figure 16a) clearly showed three different signals: one downfield signal for the two symmetrical C2 and C6 carbons, one signal for the two symmetrical C3 and C5 carbons and one signal for the C4 carbon. After the addition of HP (Figure 16b) three new signals appeared in the aliphatic portion of the ^{13}C NMR spectrum, indicating that the symmetry of the starting cyclohexanone was retained in the unknown compound. Moreover, the C2 and C6 signals of the unknown compound were shifted upfield indicating that they were less deshielded, meaning that they were now bonded to a C1 carbon, less electrophilic than the starting carbonyl group.

After HP addition, ^{13}C NMR spectra were recorded at regular intervals over 55h. An array of NMR spectra was obtained (Figure 17). The analysis of this array shows that after initial fast formation of the unknown with ^{13}C peak at 103 ppm, a new compound with a typical ^{13}C shift of 110 ppm slowly started to form and its formation steadily increased over time. On the basis of both the results obtained from the batch reaction and the fact that the NMR peak at 110 ppm matches that one obtained by the batch reaction, we can assign this signal to the Criegee intermediate.

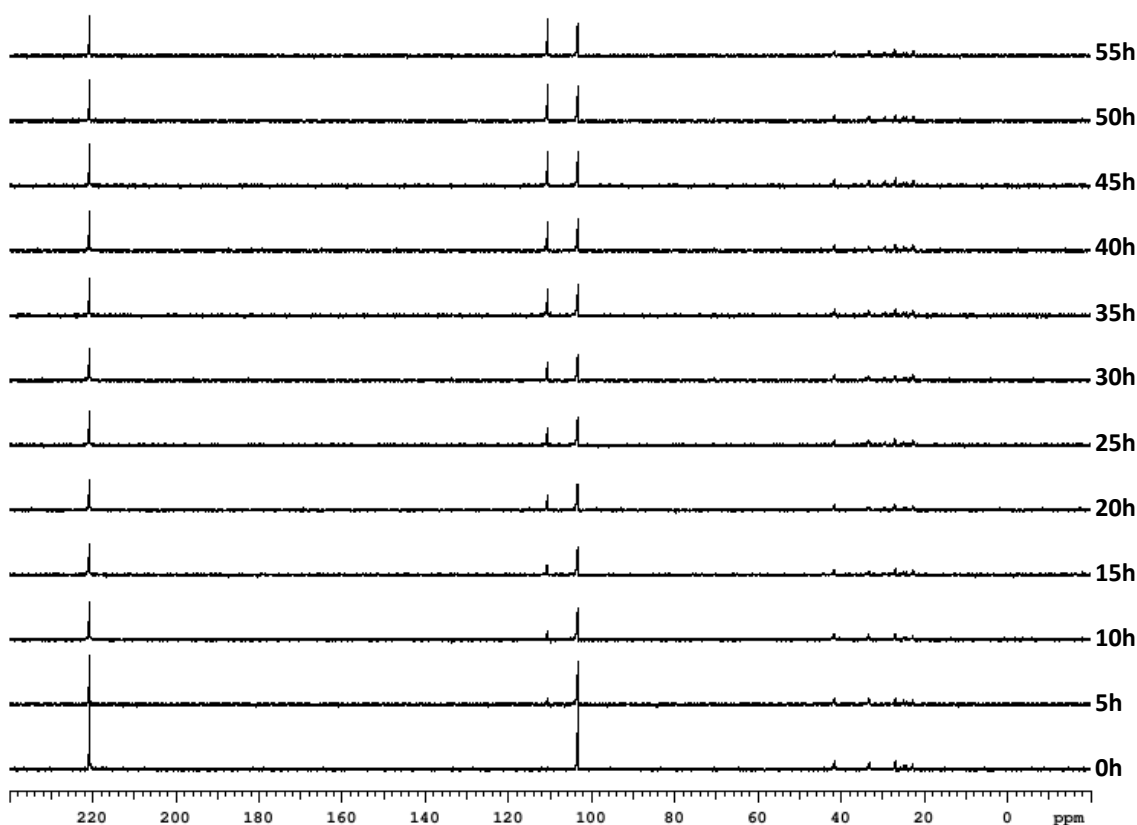


Figure 17. Array of the ^{13}C NMR spectra for the reaction of ^{13}C -cyclohexanone with H_2O_2 , taken at regular intervals over 55h

To try to get more insight on the kinetics of the reaction, any single spectrum of the array above was analyzed, and the peaks at 220, 103 and 110 ppm were integrated separately. Integration of ^{13}C NMR signals is not an easy and reliable operation, however in this case integration was performed on signals derived from a carbon atom not in natural abundance, but on an atom with 99% isotopic abundance and might be useful to qualitatively spot trends.

The analysis is reported in Figure 18, where are reported the relative intensities of the starting cyclohexanone (CHN) the unknown (DIOX) and the Criegee. The graph seems to indicate that cyclohexanone and the unknown were in a ratio about 1:1 and that this ratio was maintained throughout the course of the reaction. They both steadily decreased over time while there was a steady and linear increase in the amount of Criegee.

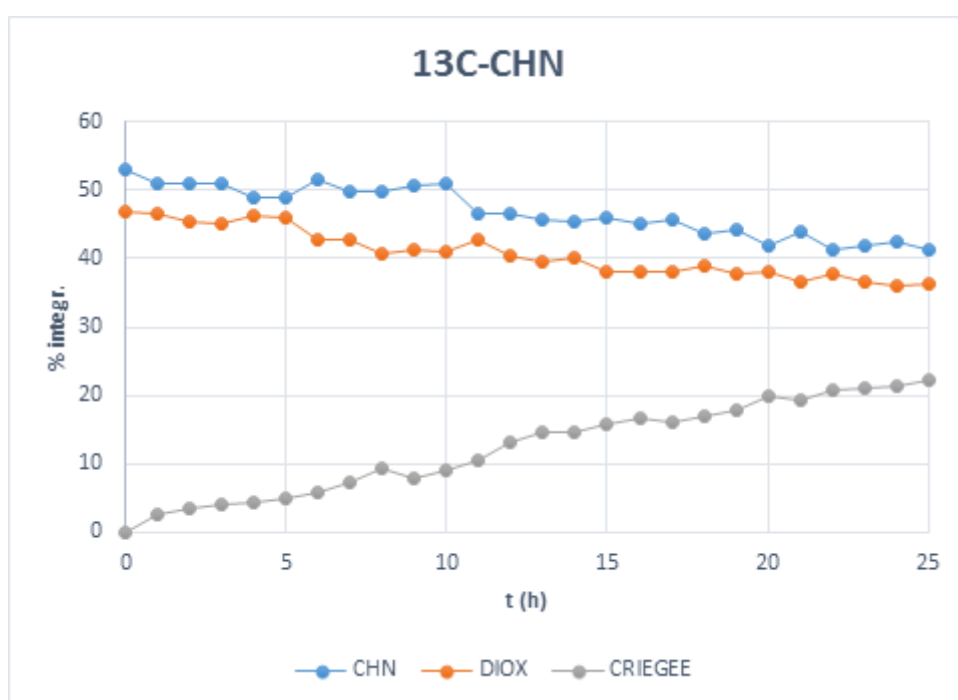


Figure 18. Relative amounts of the starting cyclohexanone, unknown and Criegee as determined from integration of the corresponding ^{13}C signals.

^{13}C NMR analysis showed that the unknown compound retains the symmetry of the starting cyclohexanone and has a characteristic ^{13}C NMR peak at 103 ppm. This information can be paired to that obtained from ESI-MS measurements, that show an unknown peak at $m/z=115$, that we supposed to be CL.

Based on these observations, the structure of the unknown compound can be tentatively assigned to the cyclohexylidene dioxirane (Figure 19). In fact, this compound retains the starting cyclohexanone symmetry, its C1 is less electrophilic than that of cyclohexanone, and its mass (114) is in accordance with ESI-MS data.

Moreover, the low temperature ^{13}C NMR spectrum of this dioxirane is reported in the literature [120] and the chemical shift reported there $\delta = 104.3$ ppm is very close to what we observed.

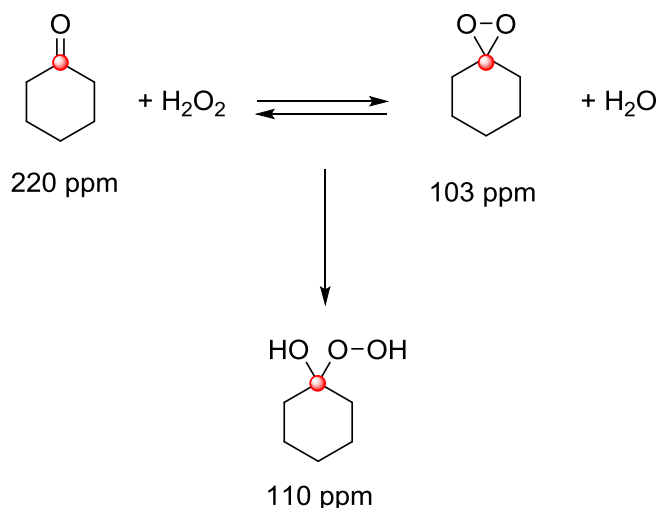
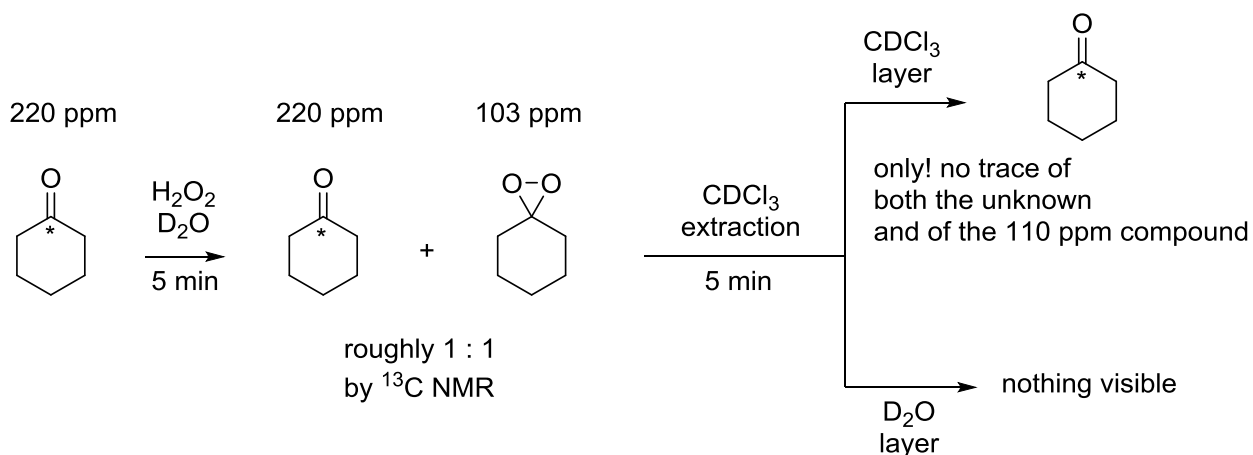


Figure 19. Different species observed by ^{13}C NMR during the reaction between ^{13}C -cyclohexanone and H_2O_2 .

The only doubts that were left at this point were the fact that in the JACS paper [120] it was reported that the dioxirane cannot survive longer than few minutes in CDCl_3 at room temperature. Moreover, we were wondering whether the different solvents used for the various NMR analyses in the literature and ours solvents (dioxane, CDCl_3 , D_2O) might be responsible for a dramatic resonance shift, thus altering considerably that basis of our structure assignment. We therefore did another NMR experiment (Scheme 17). ^{13}C -cyclohexanone was mixed with D_2O as usual and then HP was added. As usual- the unknown compound at 103 ppm immediately formed as a 1 : 1 peak compared to starting ^{13}C -cyclohexanone. Immediately after (5 min) recording this NMR, the same sample was extracted with CDCl_3 and ^{13}C NMR spectra were recorded for both the CDCl_3 layer and the D_2O layer. The CDCl_3 layer only contained starting ^{13}C -cyclohexanone: no peak was visible in the region 80-120 ppm. The D_2O layer showed no visible peak (Figure 20).



Scheme 17. Scheme of the NMR experiment with the aim to check the stability of unknown compound in organic solvent

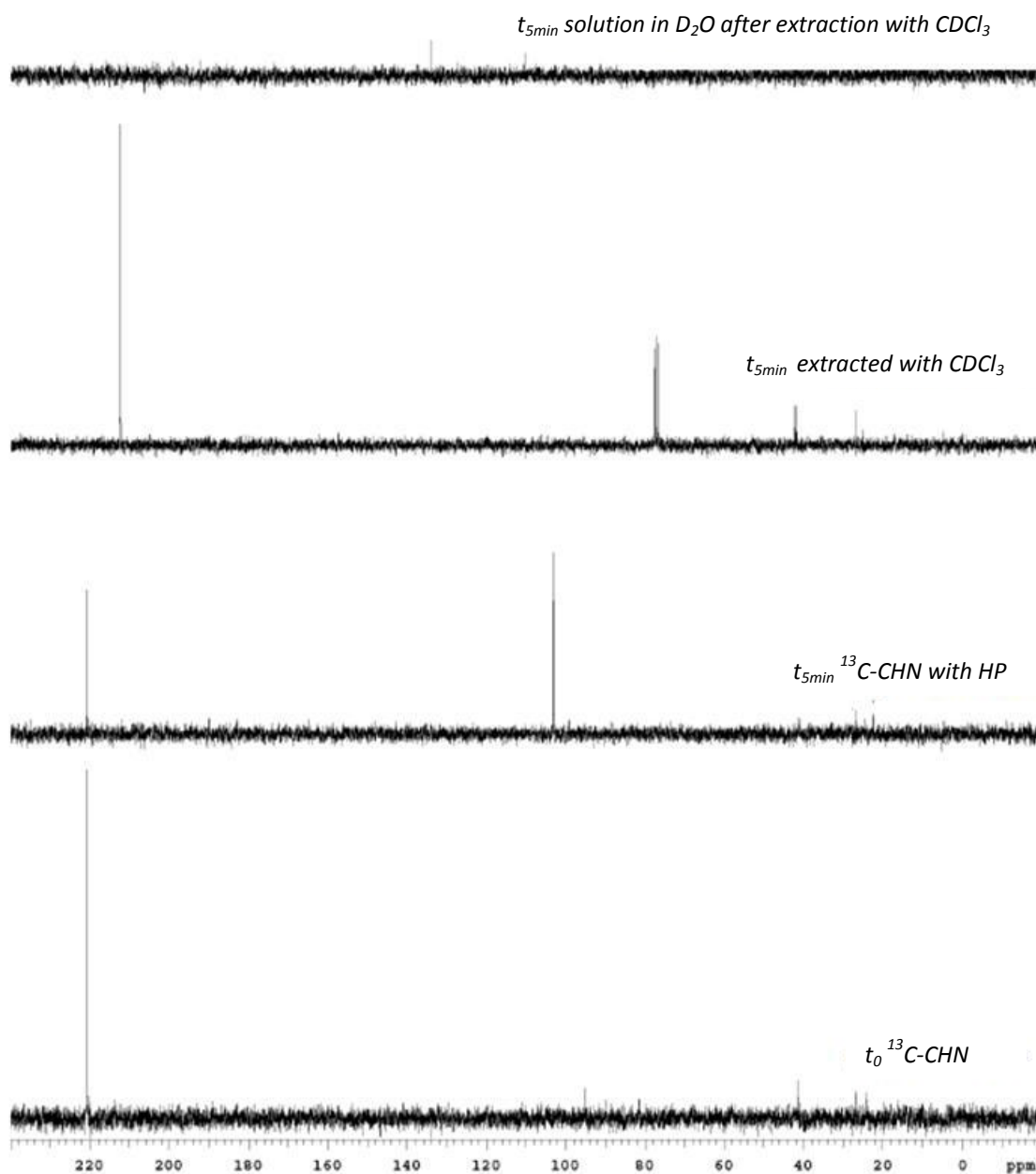


Figure 20. ^{13}C -NMR spectra of the mixture after 5 min of reaction, extracted solution and solution in deuterated water after the extraction with CDCl_3

In our view, this means that:

- the unknown at 103 ppm cannot be the Criegee, since we know from the batch reaction that the Criegee can be extracted into CDCl_3 and it can survive those conditions;
- in CDCl_3 the unknown at 103 ppm either reverts back to the starting ^{13}C -CHN or is destroyed;

- the unknown at 103 ppm must be in some way stabilized by the water environment, since during the NMR studies we performed in D₂O, it remained present for as long as a whole weekend;
- the unknown compound is the dioxirane of cyclohexanone.

Further investigations were carried out with the aim to understand the mechanism leading from cyclohexanone to the dioxirane intermediate and further to the final products.

To determine whether the hydrogen atoms in α position to the carbonyl-group of cyclohexanone took part in the reaction, we carried out more experiments to verify the presence of a kinetic isotope effect using both cyclohexanone (CHN) and cyclohexanone labelled with four deuterium atoms in the α -positions to the carbonyl (D₄-CHN). If the H atoms in α position were involved in the reaction mechanism, we should note:

- 1) a decrease in the rate of oxidation of D₄-CHN compared to CHN;
- 2) in the ESI-MS spectra we should see that the deuterium atoms have been exchanged with hydrogen.

The reactions were conducted using the 30% aqueous solution of HP (CHN:HP = 1:3) and H₂O as the solvent (CHN:H₂O = 1:20), at a temperature of 50°C. ESI-MS spectra were recorded at time t = 0 h and after 2 hours of reaction. Spectra are given in Figures 21 and 22.

In the ESI-MS spectrum of the reaction mixture at time t=0 (Figure 21) there were only peaks that corresponds to the D₄-CHN (MW=102): m/z = 103 = 102+1 and m/z = 205 = 102*2 + 1.

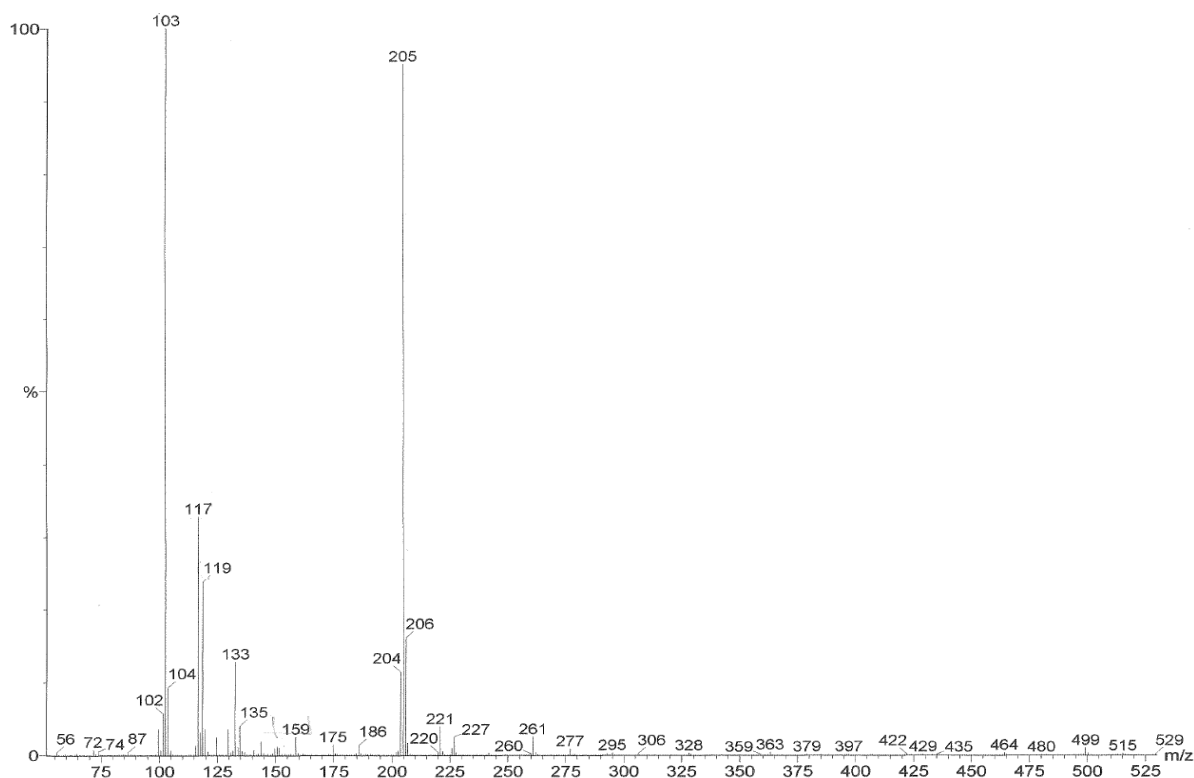


Figure 21. ESI-MS spectrum of the reaction mixture at time t=0, starting compound – D₄-CHN

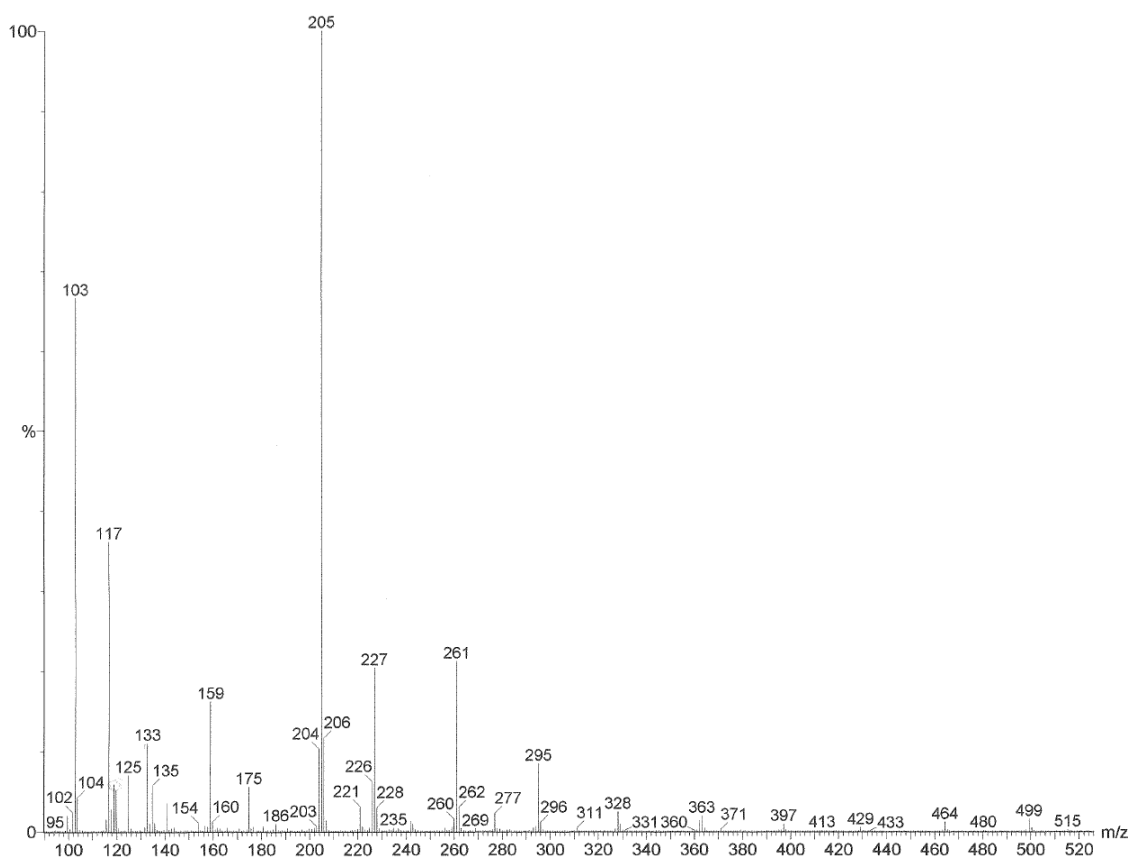


Figure 22. ESI-MS spectrum of the reaction mixture after 2 hours of reaction, starting compound – D_4 -CHN

In the ESI-MS spectrum recorded after 2 hours of reaction, there are the peaks of the D_4 -Criegee intermediate (MW = 136, m/z = 159 = 136 + 23), the dioxirane of D_4 -CHN (MW = 118, m/z = 119 = 118 + 1) and D_4 -CHN (MW = 104, m/z = 103 = 102 + 1; dimer MW = 204, m/z = 205 = 204 + 1). As can be noted, there are only signals related to species having all 4 deuterium atoms (in α -positions) in the spectrum; this means that the C-D bonds are not involved in the reaction mechanism.

In order to check whether the rates of oxidation of D_4 -CHN and CHN were different, we performed another set of experiments. First, we compared their reactivity at 50°C and 30°C, and calculated the kinetic constants of the reaction. Conditions of reaction were:

- 0.1 mL of CHN/ D_4 -CHN;
- 0.1 mL of H_2O ;
- 0.34 mL of H_2O_2 ;
- 50/30°C.

Comparison of the conversion achieved with D_4 -CHN and CHN is shown in Tables 6 and 8, and in Figures 23 and 24.

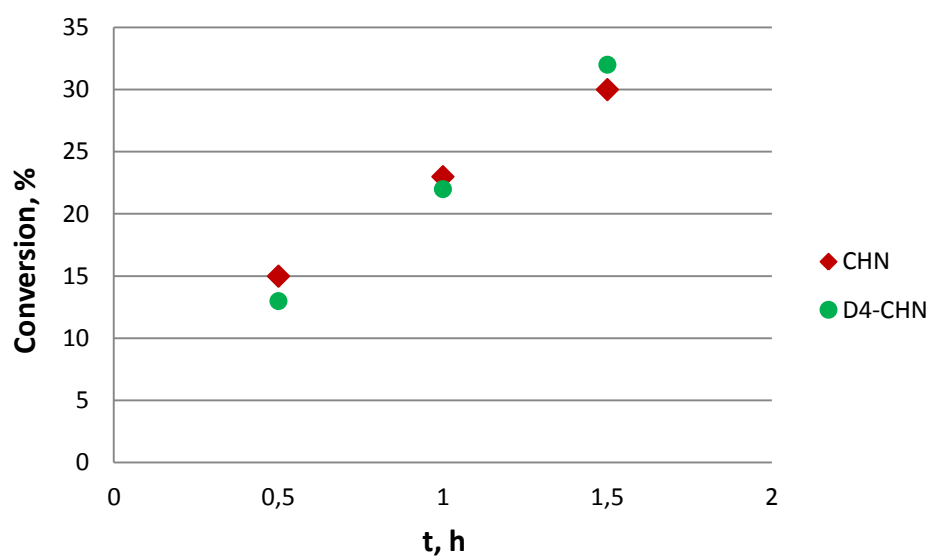
The kinetic constants of the reactions are reported in Table 7 and 9.

Table 6. Reactivity of the CHN and D₄-CHN at 50°C

Time, hours	X (CHN), %	X (D ₄ -CHN), %
0.5	15	13
1	23	22
1.5	30	32

Table 7. The kinetic constants of the cyclohexanone oxidation at 50°C

Reagent	k, sec ⁻¹
CHN	$5.6 \cdot 10^{-5}$
D ₄ -CHN	$6.7 \cdot 10^{-5}$

**Figure 23.** Conversion of the CHN and D₄-CHN at 50°C**Table 8.** Reactivity of the CHN and D₄-CHN at 30°C

Time, hours	X (CHN), %	X (D ₄ -CHN), %
0.5	9	-
1	14	9
1.5	24	-
3	-	16
4	-	21

Table 9. The kinetic constants of the cyclohexanone oxidation at 30°C

Reagent	k, sec ⁻¹
CHN	$4.9 \cdot 10^{-5}$
D ₄ -CHN	$1.4 \cdot 10^{-5}$

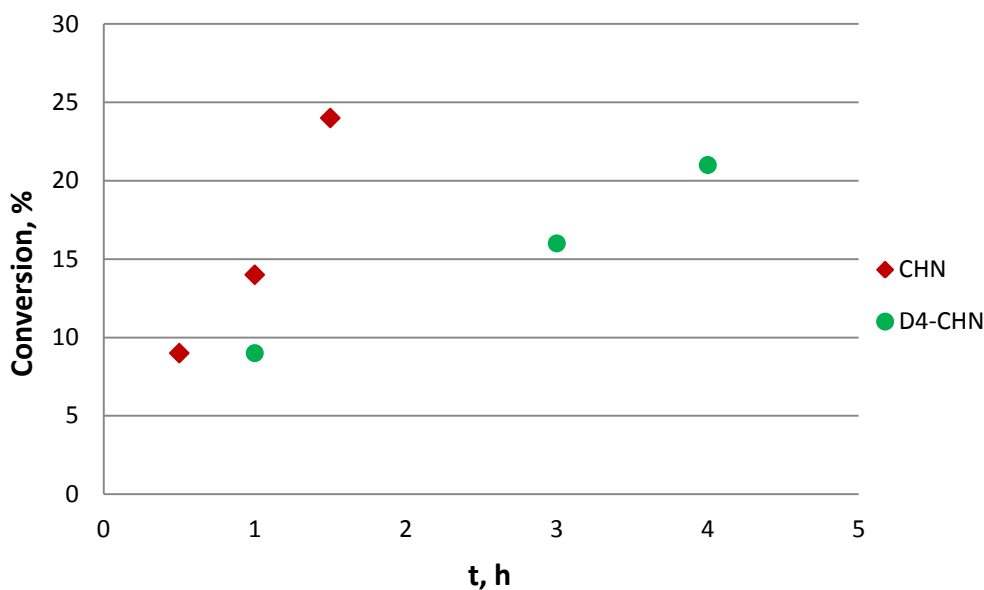


Figure 24. Conversion of the CHN and D₄-CHN at 30°C

The conversion rate for D₄-CHN and CHN at 50°C were the same. The values of the kinetic constants were also very similar. This confirms that there is no kinetic isotopic effect, and that the α -carbon and hydrogen atoms are not involved in the reaction mechanism. However, at 30°C the conversion rate for the D₄-CHN was slower than for the CHN. Probably, in this case we have some inhibition effect due to the steric hindrance of deuterium atoms.

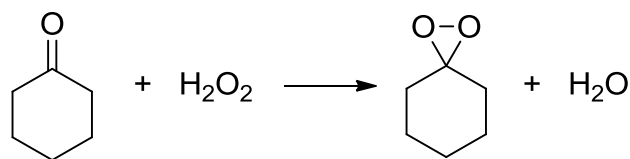
Another experiment was carried out in order to confirm the absence of the isotopic effect: we carried out the reaction of an equimolar mixture of D₄-CHN and CHN, at 50°C with HP, and measured reactants conversion by means of GC-MS. Conditions of reaction were the same, except that in this experiment we used a mixture containing 0.05 mL of D₄-CHN and 0.05 mL CHN. After reaction, we carried out the usual treatment of the reaction mixture, and finally carried out an extraction of 2 mL of the mixture with CH₂Cl₂. We also conducted the same treatment with the starting mixture in order to have a reference analysis, comparing the GC-MS spectra of the two extracts. We then calculated the ratio between the two compounds, and we found it to be equal to 1 in both the fresh and used solutions. In other words, the two compounds reacted exactly with the same rate, which confirms that the α -atoms are not involved in the reaction mechanism.

Next step was the computational study of the uncatalyzed cyclohexanone oxidation into dioxirane and other products. The calculations were done in the collaboration with Dr. Davide Ravelli, University of Pavia.

The study is presented in different sections, the first one focusing on the formation of the dioxirane, and further two rationalizing the formation of the final products.

Dioxirane formation

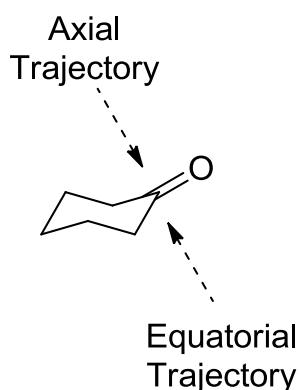
As for dioxirane formation from cyclohexanone, the theoretical simulations predict a slightly endergonic process, as indicated in Scheme 18.



$$\text{SMD-CBS-QB3 } \Delta G = + 1.64 \text{ kcal mol}^{-1}$$

Scheme 18. The process considered for the formation of dioxirane intermediate and the predicted Gibbs free-energy change associated with it (solvent effect included)

The mechanism involved in the dioxirane formation was next considered through a detailed computational simulation. First of all, it must be pointed out that the peculiar "chair-like" conformation of cyclohexanone offers two non-equivalent faces of the carbonyl group, thus two distinct trajectories have been considered, one equatorial (hereafter tagged as "EQ") and one axial (hereafter tagged as "AX"; see Scheme 19).



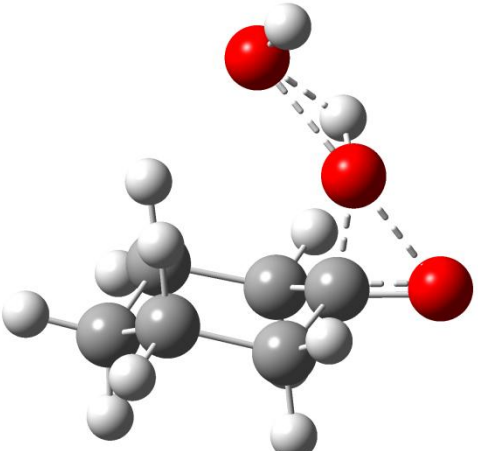
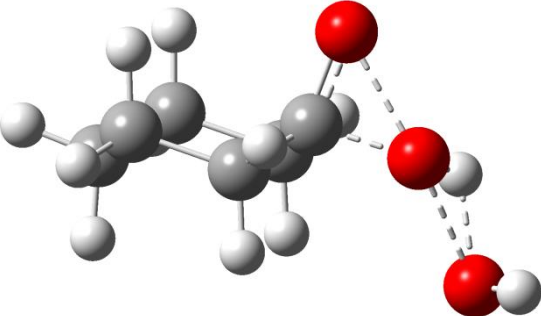
Scheme 19. The different modes of approach to the cyclohexanone molecule considered in the present study

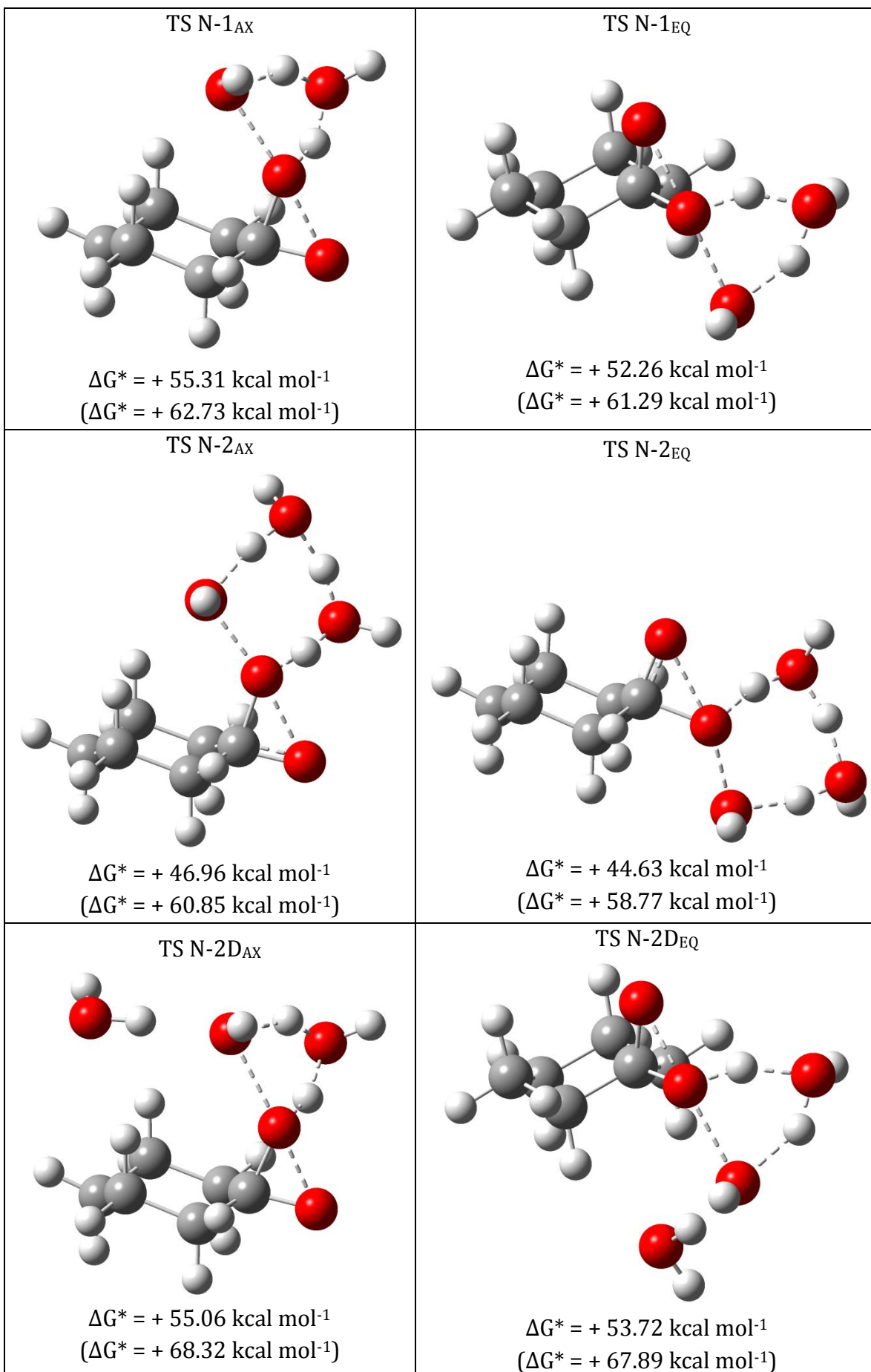
The reaction involves a rearrangement of the hydrogen peroxide molecule to give a water molecule with the concomitant release of an O atom to the carbonyl group. Several possible pathways were considered based on the role of solvent molecules as proton relays, i.e. accepting and releasing a proton at the same time, finally resulting in the reaction above. A different number of water molecules (from 0 to 2) was explicitly incorporated in the optimization of the structure and then the continuum solvent effect was included via single point calculations (see Computational part for details).

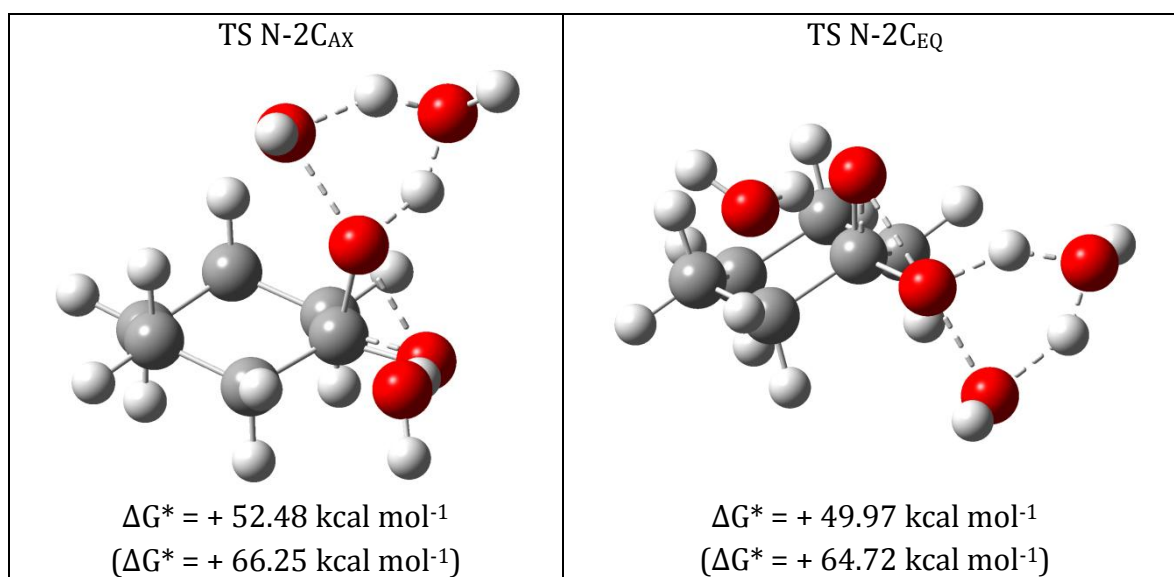
The first situation examined (hereafter named as "N-0", where N stands for Neutral - indicating that no charged species is involved - and the number specifies how many water molecules have been included into the optimization; see Table 10 for details) refers to the involvement of a single hydrogen peroxide molecule, where the final water molecule

incorporates the distal oxygen and a H from the adjacent oxygen atom. This process occurs with an activation Gibbs free energy (ΔG^*) of more than 50 kcal mol⁻¹, independently from the trajectory adopted by the approaching hydrogen peroxide molecule. Next, we introduced a water molecule acting as a relay system in the optimization (pathway dubbed as "N-1"), accepting a H from proximal oxygen and releasing another H to the distal one, in a cyclic TS. Very similar activation energies as those obtained above for N-0 were found ($\Delta G^* > 50$ kcal mol⁻¹). The incorporation of a further molecule of water in the cyclic transition state in such a way as to obtain a larger ring ("N-2" pathway) resulted in slightly lower activation energies, in this case around 45 kcal mol⁻¹ (*ca.* 5-10 kcal mol⁻¹ lower than above). We further examined the situation including two molecules of water by considering different arrangements of the reacting cluster. Thus, we took the TSs from N-1 pathway as the starting structures and added the second H₂O molecule coordinated via hydrogen bonding to either the distal oxygen (N-2D pathway) or to the carbonyl oxygen (N-2C pathway). Activation energies consistently around 50 kcal mol⁻¹ were again observed.

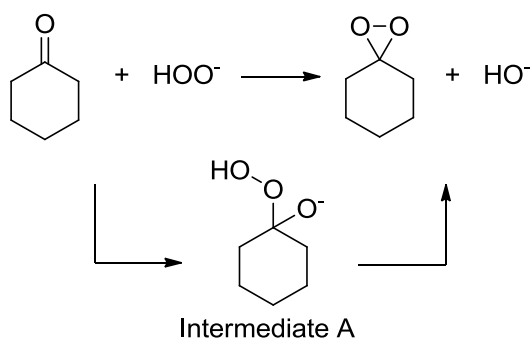
Table 10. Optimized transition structures for the formation of dioxirane from cyclohexanone under neutral conditions, involving from 0 up to 2 molecules of water as catalysts. ΔG^* at the SMD-CBS-QB3 level of theory have been reported, taking the difference between the TSs and the complexed reagents; the values in parentheses refer to the ΔG^* when considering the sum of Gibbs free energies of cyclohexanone and hydrogen peroxide.

AXIAL Trajectory	EQUATORIAL Trajectory
<p style="text-align: center;">TS N-0_{AX}</p>  <p style="text-align: center;">$\Delta G^* = + 53.00$ kcal mol⁻¹ ($\Delta G^* = + 56.02$ kcal mol⁻¹)</p>	<p style="text-align: center;">TS N-0_{EQ}</p>  <p style="text-align: center;">$\Delta G^* = + 52.83$ kcal mol⁻¹ ($\Delta G^* = + 54.73$ kcal mol⁻¹)</p>





Since hydrogen peroxide is slightly more acidic than water, it is expected to be partially dissociated in the reaction mixture and a non-negligible amount of the hydroperoxide anion is expected to be present in solution. Thus, we evaluated the possible role of this anion by modeling the reaction of cyclohexanone and HOO^- to give the dioxirane and the hydroxide anion (HO^-), hereafter tagged as "anionic pathway" (these paths were dubbed with the letter "A"). First, we examined whether this reaction occurred either via a two-step mechanism, involving the initial nucleophilic addition of the anion to the carbonyl to give a tetrahedral intermediate finally evolving into the product, or in a single step, as reported in Scheme 20.

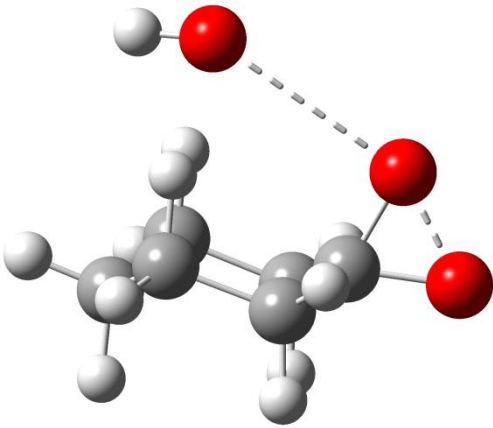
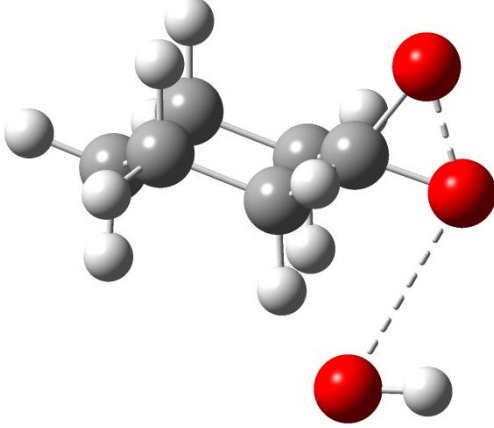
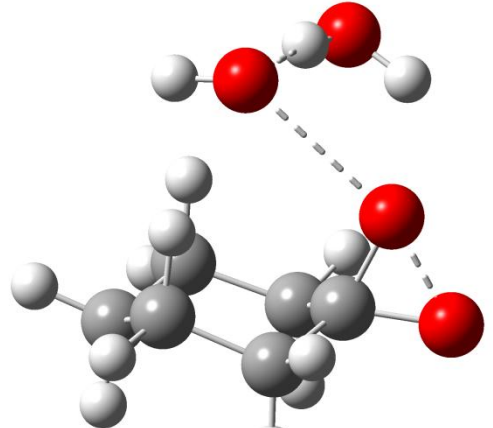
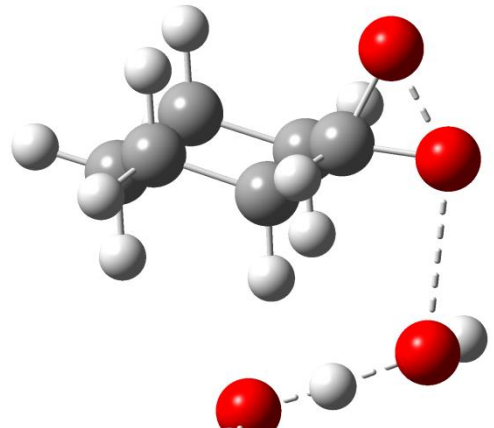


Scheme 20. Possible anionic pathways for the formation of the dioxirane intermediate

Indeed, any attempt to locate "Intermediate A" using the DFT approach failed, since it was not possible to optimize a structure as that reported in Scheme 20 but only a sort of complex, where a hydroperoxide anion was interacting with the carbonyl (by the way, the energy of this complex was very similar to the sum of the energies of cyclohexanone and hydroperoxide anion alone; data not shown). This is a strong indication that the anionic pathway should follow a single-step mechanism. Adopting the same approach as above, we devised several situations, where molecules of water have been included in the optimization to check their role in the reaction. Indeed, it was found that the uncatalyzed process (tagged "A-0"; no water molecule included) occurred with a markedly lower

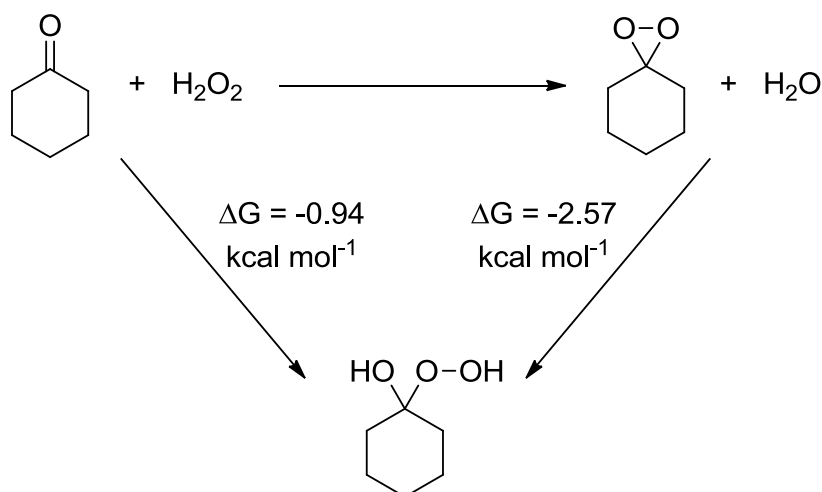
activation energy with respect to the neutral path described above. Indeed, the axial trajectory showed an activation energy around 20 kcal mol^{-1} , while the equatorial one was less favorable, around 25 kcal mol^{-1} . Again, the effect of introducing a molecule of water in the role of the catalyst was likewise evaluated. In particular, since no cyclic transition state could be modeled here, we decided to check the effect of coordination of the distal oxygen, where the most important structural changes were occurring (pathway dubbed as "A-1"). This had a further beneficial effect, since a marked decrease of ΔG^* was observed, with both reaction pathways showing a value around 14 kcal mol^{-1} .

Table 11. Optimized transition structures for the formation of dioxirane from cyclohexanone under anionic conditions, involving from 0 to 1 molecules of water as catalysts. ΔG^* at the SMD-CBS-QB3 level of theory have been reported, taking the difference between the TSs and the complexed reagents; the values in parentheses do refer to the ΔG^* when considering the sum of the Gibbs free energies of cyclohexanone and the hydroperoxide anion

AXIAL Trajectory	EQUATORIAL Trajectory
<p data-bbox="475 842 587 869">TS A-0_{AX}</p>  <p data-bbox="363 1328 699 1406">$\Delta G^* = + 19.33 \text{ kcal mol}^{-1}$ ($\Delta G^* = + 34.32 \text{ kcal mol}^{-1}$)</p>	<p data-bbox="1066 842 1177 869">TS A-0_{EQ}</p>  <p data-bbox="954 1328 1289 1406">$\Delta G^* = + 25.48 \text{ kcal mol}^{-1}$ ($\Delta G^* = + 35.21 \text{ kcal mol}^{-1}$)</p>
<p data-bbox="475 1429 587 1456">TS A-1_{AX}</p>  <p data-bbox="363 1955 699 2033">$\Delta G^* = + 14.02 \text{ kcal mol}^{-1}$ ($\Delta G^* = + 33.32 \text{ kcal mol}^{-1}$)</p>	<p data-bbox="1066 1429 1177 1456">TS A-1_{EQ}</p>  <p data-bbox="954 1955 1289 2033">$\Delta G^* = + 13.43 \text{ kcal mol}^{-1}$ ($\Delta G^* = + 29.82 \text{ kcal mol}^{-1}$)</p>

Criegee intermediate formation

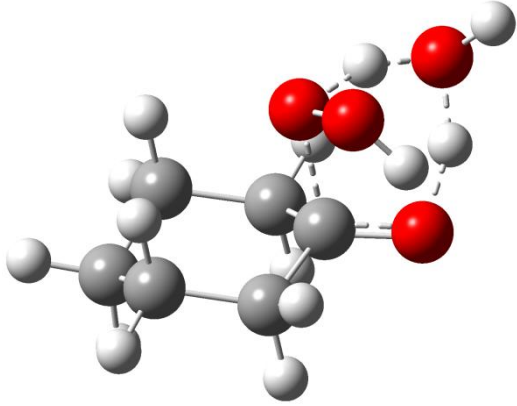
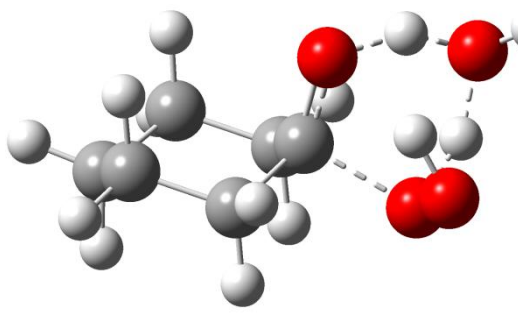
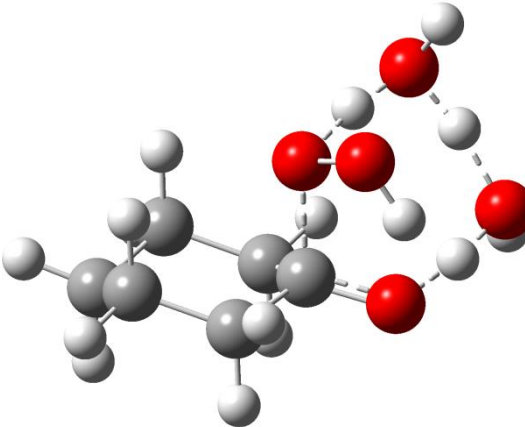
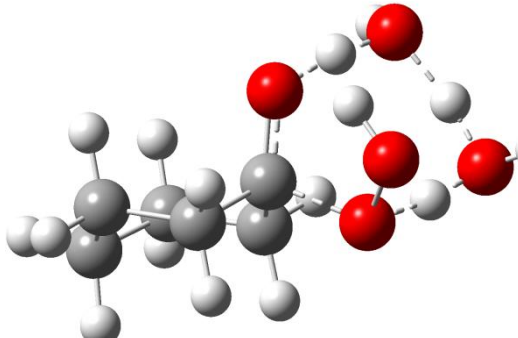
Next, we shifted our attention on the formation of the Criegee intermediate. This may be formed either from the starting ketone or from the dioxirane intermediate. The thermodynamics of both reactions is reported in Scheme 21 and highlights the slightly exergonic character of both processes.



Scheme 21. The processes considered for the formation of the Criegee adduct and the predicted Gibbs free-energy change associated with them (solvent effect included)

Thus, we explored in details both reaction pathways, adopting the same approach as above, by inclusion of molecules of water as catalysts in the role of facilitating the structural rearrangement. As for the formation of the Criegee adduct from cyclohexanone (hereafter dubbed as pathway "K"), this can be described as the formal addition of a molecule of hydrogen peroxide to the carbonyl moiety. Indeed, no uncatalyzed pathway was found (no "K-0" path), while the inclusion of one (K-1) or two (K-2) molecules of water resulted in the location of the desired cyclic transition states, showing activation energies around 29 and 23 kcal mol^{-1} , respectively (see Table 12). The corresponding anionic pathway was not investigated, since this would involve the same Intermediate A reported in Scheme 20 (not observed; see above for details).

Table 12. Optimized transition structures for the formation of the Criegee adduct from cyclohexanone under neutral conditions, involving from 1 to 2 molecules of water as catalysts. ΔG^* at the SMD-CBS-QB3 level of theory have been reported, taking the difference between the TSs and the complexed reagents; the values in parentheses do refer to the ΔG^* when considering the sum of the Gibbs free energies of cyclohexanone and hydrogen peroxide.

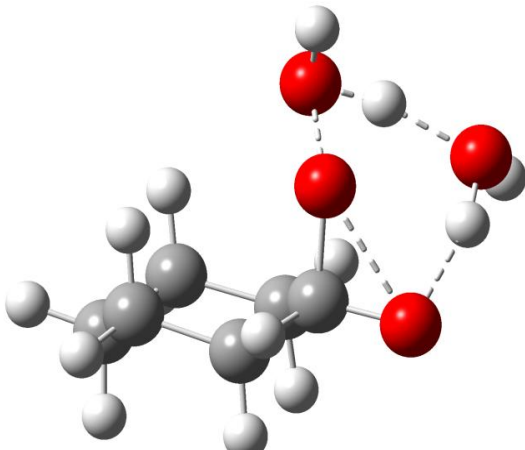
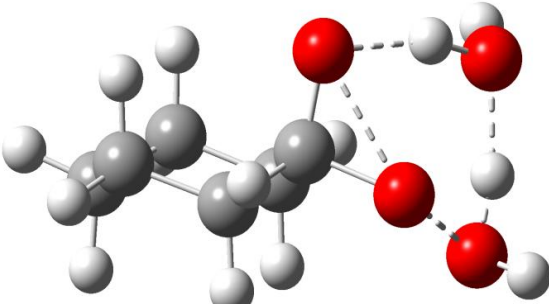
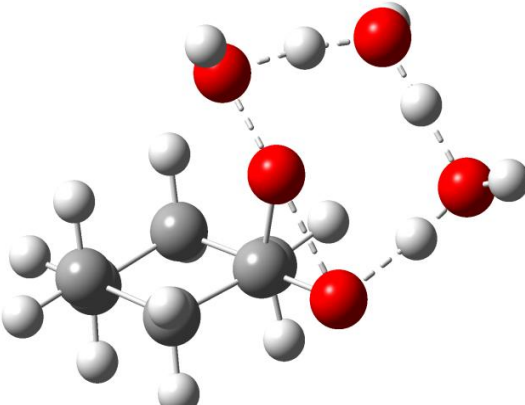
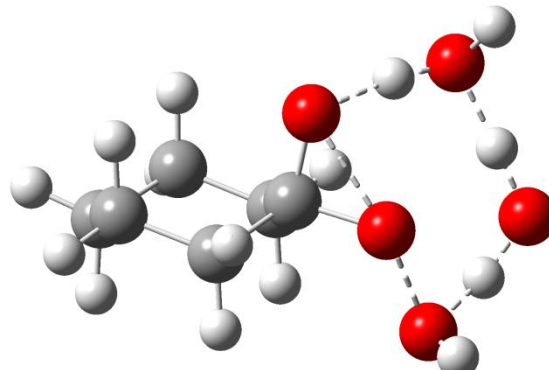
AXIAL Trajectory	EQUATORIAL Trajectory
<p data-bbox="475 448 587 481">TS K-1_{AX}</p>  <p data-bbox="359 907 702 996">$\Delta G^* = + 29.43 \text{ kcal mol}^{-1}$ ($\Delta G^* = + 36.87 \text{ kcal mol}^{-1}$)</p>	<p data-bbox="1066 448 1177 481">TS K-1_{EQ}</p>  <p data-bbox="949 907 1292 996">$\Delta G^* = + 28.69 \text{ kcal mol}^{-1}$ ($\Delta G^* = + 36.96 \text{ kcal mol}^{-1}$)</p>
<p data-bbox="475 1014 587 1048">TS K-2_{AX}</p>  <p data-bbox="359 1500 702 1590">$\Delta G^* = + 23.44 \text{ kcal mol}^{-1}$ ($\Delta G^* = + 36.37 \text{ kcal mol}^{-1}$)</p>	<p data-bbox="1066 1014 1177 1048">TS K-2_{EQ}</p>  <p data-bbox="949 1500 1292 1590">$\Delta G^* = + 23.48 \text{ kcal mol}^{-1}$ ($\Delta G^* = + 35.61 \text{ kcal mol}^{-1}$)</p>

Analogously, we evaluated the reaction course from dioxirane to the Criegee adduct. We initially reasoned that this process involves a simple hydrolysis of the three-membered ring. In turn, this could occur via breaking of either the O-O or one of the two C-O bonds. As in the case of cyclohexanone, also here two different approaching modes can be envisaged; indeed, we named the pathways as axial or equatorial according to the molecule side involved in the formation of the new O-O bond (see Scheme 19 above).

As for the O-O breaking pathway, we found several TSs (the corresponding pathways have been named as "D"), but none of them pertained to the uncatalyzed process (no TS D-0 structure found), while the corresponding situations including 1 or 2 molecules of water,

acting as proton relays, gave activation energies around 48 and 34 kcal mol⁻¹, respectively, supporting the role of water in facilitating this rearrangement (Table 13).

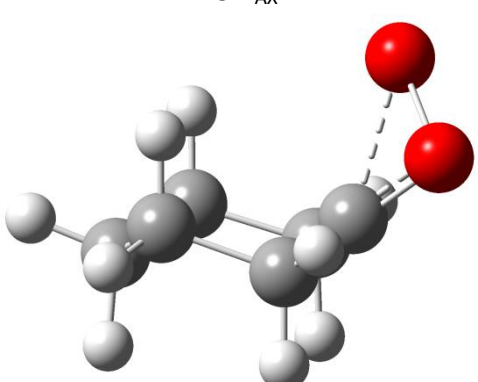
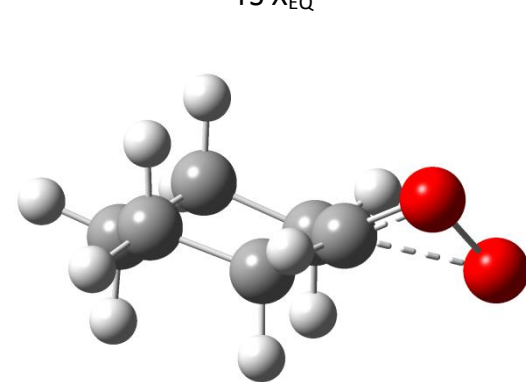
Table 13. Optimized transition structures for the formation of the Criegee adduct from the dioxirane under neutral conditions, involving from 1 to 2 molecules of water as catalysts. ΔG^* at the SMD-CBS-QB3 level of theory have been reported, taking the difference between the TSs and the complexed reagents; the values in parentheses refer to the ΔG^* when considering the sum of the Gibbs free energies of dioxirane and water

AXIAL Trajectory	EQUATORIAL Trajectory
<p>TS D-1_{AX}</p>  <p>$\Delta G^* = + 47.89 \text{ kcal mol}^{-1}$ ($\Delta G^* = + 59.94 \text{ kcal mol}^{-1}$)</p>	<p>TS D-1_{EQ}</p>  <p>$\Delta G^* = + 48.50 \text{ kcal mol}^{-1}$ ($\Delta G^* = + 59.55 \text{ kcal mol}^{-1}$)</p>
<p>TSD-2_{AX}</p>  <p>$\Delta G^* = + 35.23 \text{ kcal mol}^{-1}$ ($\Delta G^* = + 52.91 \text{ kcal mol}^{-1}$)</p>	<p>TSD-2_{EQ}</p>  <p>$\Delta G^* = + 33.48 \text{ kcal mol}^{-1}$ ($\Delta G^* = + 50.44 \text{ kcal mol}^{-1}$)</p>

In contrast, all the attempts to identify a similar process involving the cleavage of either of the C-O bonds failed, since the system evolved to the formation of a carbonyl oxide intermediate (pathway hereafter tagged as "X"; Table 14), independently from the number of water molecules included in the simulation. Also in this case, the usual axial/equatorial dichotomy has been observed. Once formed, the carbonyl oxide, which is a valence isomer

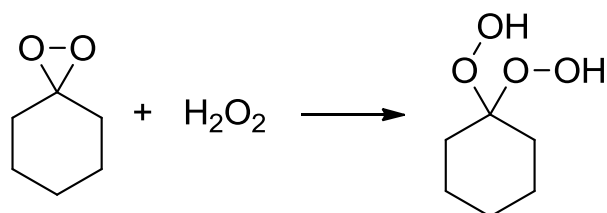
of the original dioxirane, can undergo a hydration reaction to give the Criegee adduct. Indeed, this process occurs with very low activation energies, in the 10-15 kcal mol⁻¹ range (data not reported).

Table 14. Optimized transition structures for the isomerization of dioxirane to carbonyl oxide. ΔG^* at the SMD-CBS-QB3 level of theory have been reported, taking the difference between the TSs and the starting dioxirane

AXIAL Trajectory	EQUATORIAL Trajectory
<p>TS X_{AX}</p>  <p>$\Delta G^* = + 36.87 \text{ kcal mol}^{-1}$</p>	<p>TS X_{EQ}</p>  <p>$\Delta G^* = + 36.62 \text{ kcal mol}^{-1}$</p>

Bis-hydroperoxide formation

Finally, some hypotheses on the formation of the α,α -bis-hydroperoxide have been considered. Thermodynamic considerations supported that this product would not arise from the original ketone, since this would involve two hydrogen peroxide molecules at the same time, an unlikely process. A more palatable hypothesis was that the bis-hydroperoxide arose from the dioxirane, via a further step involving a single molecule of H₂O₂, a process calculated to be exoergonic, with a ΔG near -10 kcal mol⁻¹.



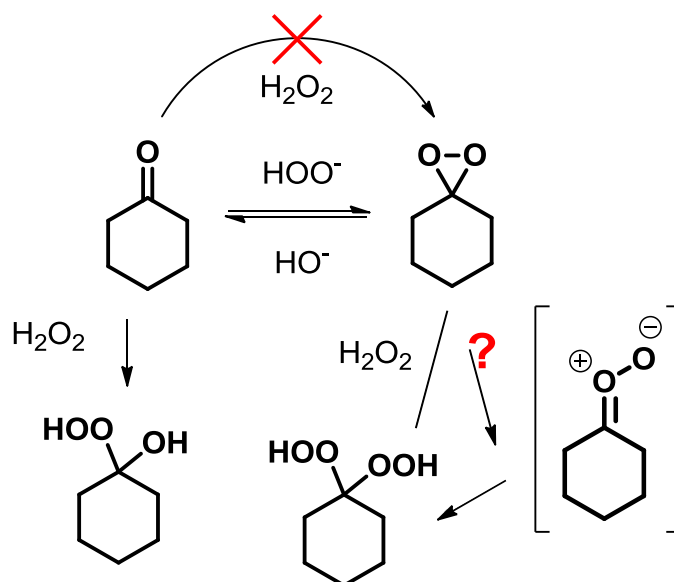
SMD-CBS-QB3 $\Delta G = - 8.54 \text{ kcal mol}^{-1}$

Scheme 22. Possible pathway for the formation of the bis-peroxide

We undertook the same investigation as above in order to describe the opening of the three-membered ring, but any attempt to describe either the O-O and the C-O bonds breaking in the presence of hydrogen peroxide and a variable amounts (from 0 to 2) of water molecules failed. Indeed, we propose a similar behavior as that observed above for the

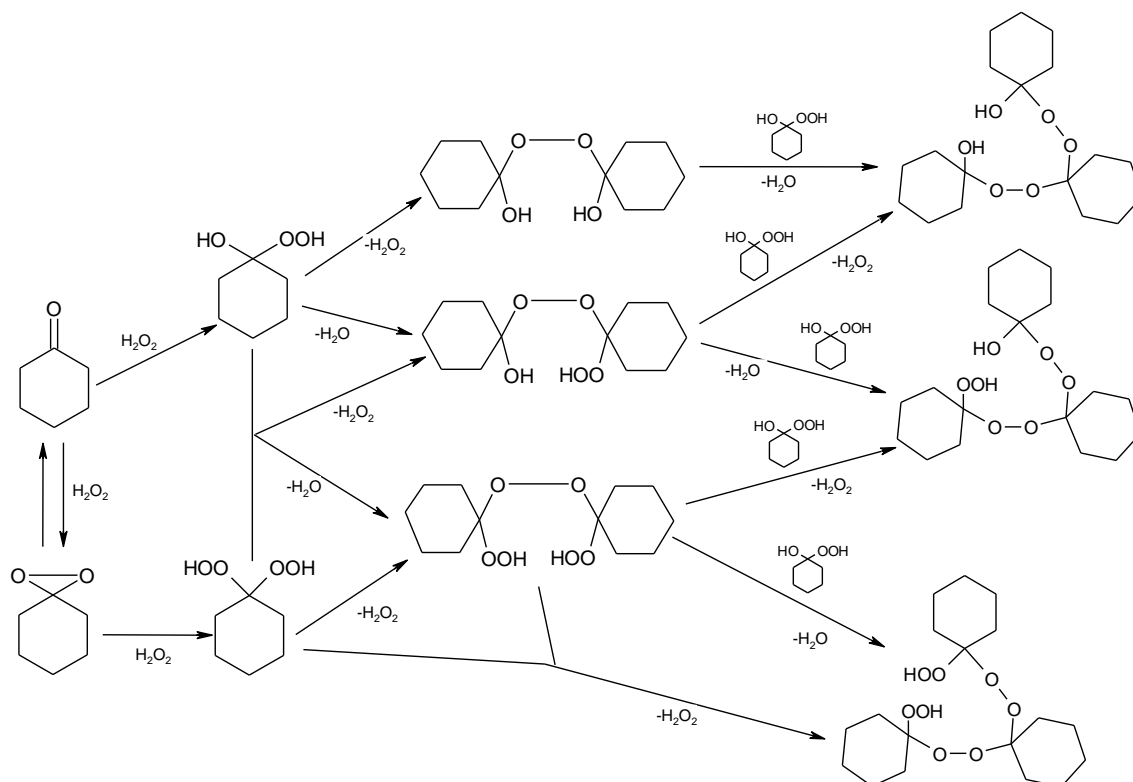
Criegee adduct, claiming the involvement of a carbonyl oxide intermediate, that further undergoes addition of a hydrogen peroxide molecule to give the final bis-hydroperoxide.

To conclude the computational part, a plausible reaction mechanism supported by both theoretical simulations and experimental data is reported below (see Scheme 23). The dioxirane results from a sort of nucleophilic addition to the carbonyl by the hydroperoxide anion. The huge activation energies observed for the corresponding neutral pathway militates against the intervention by a (neutral) hydrogen peroxide molecule. Experiments suggest that the dioxirane and the starting ketone are in fast equilibrium with each other, and both of them may be responsible for the formation of the Criegee adduct. Indeed, theoretical calculations suggest that addition of hydrogen peroxide to the ketone is more favored than hydrolysis of the dioxirane intermediate (compare the activation energies of the pathways "K" and "D"). If operating, the latter path may involve a further intermediate, viz. the carbonyl oxide. Formation of the bis-hydroperoxide, presumably involves again the dioxirane, likewise via the carbonyl oxide.



Scheme 23. Proposed reaction mechanism of the uncatalyzed oxidation of cyclohexanone

In case, when the reaction is carried out in the presence of the catalyst, the Criegee intermediate and bis-hydroperoxide are further transformed into heavier compounds (Scheme 24).



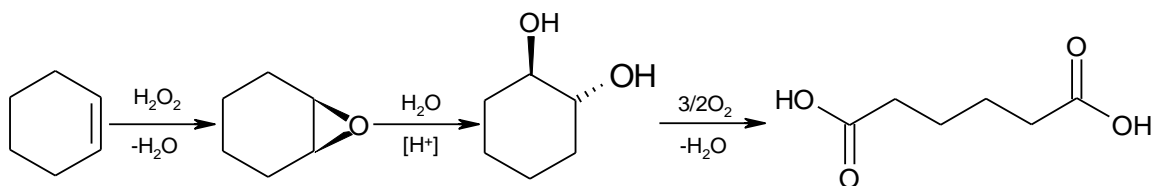
Scheme 24. Reactions that take place in the BV oxidation of cyclohexanone in the presence of catalyst.

Concluding, some important considerations can be argued based on the reaction mechanism hypothesized and the role of Lewis-acid catalysts in cyclohexanone hydroperoxidation:

1. Cyclohexanone reacts to yield either the dioxirane compound, or the Criegee intermediate. Indeed, the former species is in equilibrium with the cyclohexanone, and the equilibrium is established very rapidly.
2. The dioxirane species may evolve towards the formation of the bis-hydroperoxide compound. Both the latter and the Criegee intermediate undergo successive condensation reactions, leading to different types of heavier compounds.
3. The Lewis acidity of the catalyst seems to play an important role in addressing the transformation of cyclohexanone either to the Criegee or to the dioxirane. Probably the interaction of the ketone with the Lewis site stabilizes the dioxirane, shifting the equilibrium towards an enhanced quantity of this compound.

The two-step oxidation cyclohexene to adipic acid via 1,2-cyclohexanediol

This part of my research dealt with the two-step process for the production of AA, where first cyclohexene (CH-ene) is oxidized to *trans*-1,2-cyclohexanediol (CHD) with hydrogen peroxide (HP), and then the latter is transformed to AA with molecular oxygen (Scheme 25). The research was carried out in collaboration with Radici Chimica Spa and was patented [121].



Scheme 25. Two-step approach to produce AA starting from cyclohexene

8. The first step: cyclohexene dihydroxylation

The dihydroxylation of olefins can be performed in the presence of KMnO_4 , OsO_4 or alkylhydroperoxides via the formation of epoxide that is further hydrolyzed into the cis-diol [122, 123, 124]. Due to the low efficiency of these oxidants, numerous studies have been carried out in order to find active systems for the transformation of olefins into diols using HP as the oxidant. Hydrogen peroxide is a strong and “green” oxidant, because the only by-product it gives is water. The dihydroxylation of olefins with HP can be catalyzed by complexes of transition metals, for example, polyoxometalates [125], CH_3ReO_3 [126], H_2WO_4 [127, 128], and by various heterogeneous catalysts. The use of heterogeneous systems, such as zeolites, Ti- β [129], Nb-MCM-41 [130], Ti-MMM and Ce-SBA [131], Ti- β [132] etc., was investigated, even in the absence of organic solvents. These systems showed low selectivity to the formation of the diol (<60%) due to the formation of the by-products epoxides, alcohols, and ketones. It has been reported that it is possible to increase the yield of the diol until 98% by using a resin-supported sulfonic acid with 30% aqueous HP at 70°C, without solvent [133]. Cyclohexene epoxide can be formed by two routes: epoxidation by cyclohexenyl hydroperoxide or by HP [134].

The systems based on tungstate anions are the most studied catalysts to produce the epoxide, because are more prone to give oxygen transfer rather than disproportionation [135, 136, 137, 79, 138]. In the dihydroxylation of cyclohexene to CHD, Venturello and Gambaro achieved 87% yield to the diol; the reaction was performed at 70°C with both cyclohexene and catalyst dissolved in benzene and an aqueous solution of HP [70].

In our investigation we used homogeneous tungstic/phosphoric acid catalytic system and HP as the oxidant.

8.1. Experimental part

8.1.1. Synthesis of the catalyst

The catalyst for the first step of the process was prepared by the following method: in the aqueous HP with the required concentration we dissolved tungstic and phosphoric acids. We investigated the effect of the amount of each component on the selectivity to CHD.

8.1.2. Catalytic measurements

Catalytic experiments were performed in a three-neck flask of 250 mL volume equipped with a condenser, magnetic stirrer and thermometer. The solution containing the catalytic system, HP and Aliquat 336 (a quaternary ammonium salt of octyl and decyl chains), which was used as a phase transfer agent (PTA), were loaded in the flask and heated up to 50°C, then left stirring at this temperature for 15-30 minutes. Next, cyclohexene was added to the mixture dropwise (5g/min); the temperature of the mixture was controlled by the heating bath to keep the temperature at 70°C. When the temperature was stabilized, the reaction was conducted for the required reaction time.

We also carried out an experiment using optimal conditions, but changing the sequence of reactants addition. The results were the same as those obtained with the standard procedure.

8.1.3. Treatment of the reaction mixture

When the reaction was finished, the reaction mixture was filtered and then divided into two parts.

The first part was analyzed by means of ionic chromatography in order to determine the amount of carboxylic acids, and by titration with KMnO_4 in order to determine the amount of residual HP.

The second part of the solution was loaded into the rotating evaporator to eliminate water. The resulting solid was weighed and then dissolved in methanol and analyzed by means of gas chromatography, in order to determine the amount of CHD and of other non-acid reaction products, such as 2-cyclohexene-1-ol and 2-cyclohexene-1-one.

8.1.4. Analysis of the reaction products

As it was already mentioned before, the mixtures were analyzed by means of ionic and gas chromatography.

8.1.4.1. Ionic chromatography

The analysis was done with an ionic chromatograph Dionex 2000isp with IonPac ICE AS1e column and suppressor AMMS ICE. As an eluent, we used the 2.5% solution of octanesolphonic acid in isopropanol.

8.1.4.2. Gas chromatography

For the GC analysis we used a chromatograph Agilent 6850 GC, equipped with FID detector, PTV injector, and a HP-INNOWax Polyethylene Glycol capillary column, using a temperature ramp from 50°C to 230°C.

8.2. Results and discussion

The experiments were carried out with tungstate acid as the catalyst, phosphoric acid as co-catalyst and Aliquat 336 as phase-transfer agent.

First of all, we studied the role of both PTA and H_3PO_4 by varying the molar ratio of these compounds. The results of these experiments are summarized in Table 15.

Table 15. Effect of the H_3PO_4 and PTA on the cyclohexene conversion and selectivity to CHD. Reaction conditions: $T=70^\circ\text{C}$, HP concentration 7.5 wt.%

Entry	H_2WO_4	$\text{H}_3\text{PO}_4/\text{H}_2\text{WO}_4$	PTA/ H_2WO_4	CH-ene/ H_2WO_4	HP/ H_2WO_4	t, h	X (CH-ene), %	Y (CHD), %
1	1	0	0.48	100.4	112.6	3.3	82.9	78.1
2	1	0.27	0.74	100	113.1	3.0	100	97.4
3	1	0.5	0	100.4	111.5	3.4	7.6	-
4	1	0.5	0.25	100.3	110.2	2.6	100	90.3
5	1	0.5	0.32	99.5	110.6	2.7	100	96
6	1	0.5	0.5	100.5	110.1	2.7	100	97.2

It can be seen that in the absence of PTA (entry 3) or phosphoric acid (entry 1) the cyclohexene converted less than using both of these compounds; however, the effect of PTA was greater than that of H_3PO_4 . Using an equimolar amount of H_3PO_4 and PTA we could achieve 97.2% yield of CHD with complete conversion of cyclohexene; the residual amount of unconverted HP in this case was very low (0.4%). By-products of cyclohexene oxidation with HP were 6-hydroxyhexanoic, 6-oxohexanoic acids and dicarboxylic acids. We also performed the experiment with the ratio of the components that corresponds to the Venturello system stoichiometry (entry 2) [70] and we obtained 97.4% CHD yield with complete conversion of the reagent.

When the amount of PTA was decreased, the yield to CHD also decreased and more carboxylic acid formed; the reaction stopped in the absence of PTA (entry 3). Thus, the roles of PTA were:

- transferring the activated form of the catalyst from the aqueous phase containing HP to the organic phase to oxidize cyclohexene;
- keeping the CHD in the organic phase, stopping its further oxidation.

From the obtained results it follows that phosphoric acid shows no effect on selectivity to CHD, but it accelerates the cyclohexene oxidation.

We could achieve almost 100% selectivity to CHD using the molar ration between HP and cyclohexene equal to 1.1, which is typically used for epoxidation. In literature, a 98-100% selectivity to the epoxide using 1 eq of HP and the selective formation of AA with 4

moles of hydrogen peroxide per mol of cyclohexene [139, 140] were reported; the formation of the CHD was not observed.

To determine the effect of HP, we performed the experiments using different ratios between HP and cyclohexene and changing the concentration of the HP solution. The resulted are given in Table 16.

Table 16. Effect of HP concentration on cyclohexene conversion and selectivity to CHD. T=70°C

Entry	H ₂ WO ₄	H ₃ PO ₄ / H ₂ WO ₄	PTA/ H ₂ WO ₄	CH-ene/ H ₂ WO ₄	HP/ H ₂ WO ₄	HP conc., wt. %	t, h	X (CH-ene), %	Y (CHD), %
6	1	0.5	0.5	100.5	110.1	7.5	2.7	100	97.2
7	1	0.5	0.5	100.1	110.3	15.2	2.5	100	96.3
8	1	0.5	0.5	100.3	110.6	19.9	2.6	100	94.5
9	1	0.5	0.5	100.9	218.8	7.7	2.8	100	94.9
10	1	0.5	0.5	99.8	327.2	7.8	2.7	100	92.7
11	1	0.5	0.5	100.7	220.9	15.1	2.8	100	86.6
12	1	0.5	0.5	100.5	329.2	20	2.7	100	83.1

We observed a small decrease in the selectivity to CHD when HP concentration was higher than 7.5% (entry 6-8). In the case of a large excess of HP, but with low concentration (entry 9-10), there was the same insignificant effect on the selectivity to CHD; the difference was that a great fraction of HP remained unconverted (39 and 62%). However, when a large excess of HP with high concentration was used, we observed a significant effect on the selectivity to CHD, with greater formation of by-products (entry 11-12).

It was not possible to investigate the effect of the temperature due to the fact that 75°C is the reflux temperature of the mixture.

We carried out some experiments in order to determine the effect of phosphoric acid and PTA on the hydrolysis of cyclohexene epoxide (CEP). The conditions and results of these experiments are summarized in Table 17.

Table 17. Experiments starting from cyclohexene epoxide. T=70°C, 3 hours

Entry	H ₂ WO ₄	H ₃ PO ₄ / H ₂ WO ₄	PTA/ H ₂ WO ₄	CEP / H ₂ WO ₄	HP/ H ₂ WO ₄	HP conc., wt. %	X (CEP), %	Y (CHD), %
13	1	0.6	0.5	100.7	109.6	7.7	99.8	82.4
14	1	0	0.5	100.1	111.9	7.6	100	84.6
15	1	0.5	0	99.9	111.2	7.5	100	80.2

From these results we can conclude that the epoxide hydrolysis is very fast; after 3 hours it was completely converted, and CHD was stable under reaction conditions. In all the experiments, most of HP remained unconverted (the amount of residual HP was 70-80%).

The effect of phosphoric acid or PTA on the hydrolysis of the epoxide was insignificant, with only small difference of CHD selectivity in the experiments carried out in the absence of either PTA (entry 15) or phosphoric acid (entry 14) (to be compared to the experiment carried out in the presence of both compounds (entry 13)). The main by-products were dicarboxylic acids: AA, which was the prevailing one, glutaric acid and traces of succinic acid (for example, in experiment 13 yield to AA was 7%, with 3.9% of glutaric acid).

As it was already mentioned, CHD is stable under reaction conditions. But, probably, this is due to the low temperature of reaction. In order to prove this hypothesis, we conducted experiments starting from 1,2-cyclohexanediol and varying reaction conditions (temperature, concentration of HP and its amount). The results are given in Table 18.

Table 18. Experiments with CHD as the starting reagent. DA – dicarboxylic acids

Entry	H ₂ WO ₄	H ₃ PO ₄ / H ₂ WO ₄	PTA/ H ₂ WO ₄	CHD/ H ₂ WO ₄	HP/ H ₂ WO ₄	HP, wt. %	t, h	T, °C	X(CHD), %	Y(DA), %	Y(others), %
16	1	0.5	0.5	101.1	111.1	7.6	3.2	70	23.1	6.4	16.7
17	1	0.5	0	100.8	111.5	7.6	3.1	70	19.5	3.5	16
18	1	0.5	0.5	101.4	333.6	7.6	2.9	70	17.2	2.8	14.4
19	1	0.5	0.5	99.7	337	31.1	3	70	26.4	14	12.4
20	1	0.5	0.5	99.9	332.1	31.1	3.1	90	97.4	91.8	5.6
21	1	0.5	0.5	100.5	333.7	31.1	6	90	97.4	93.3	4.1
22	1	0.5	0	100.5	333.8	31.1	6.2	90	98.1	93.9	4.2

Under the conditions used for cyclohexene oxidation, CHD was less reactive. Main products were 2-hydroxycyclohexanone, monocarboxylic acids and some amount of dicarboxylic acids. At higher temperature (90°C), dicarboxylic acids were the prevailing products.

The presence of the phase-transfer agent had almost no effect on CHD conversion (entries 16 and 17 at 70°C and 21 and 22 at 90°C).

Increase of the HP amount at 70°C had no significant effect on CHD conversion (entries 17, 18). However, when we increased the concentration of HP, while keeping the ratio CHD:HP=1:3 as in experiment 18, CHD conversion increased and a greater formation of dicarboxylic acids was shown (entry 19).

At 90°C, with molar ratio CHD:HP=1:3 and high concentration of HP in the solution, we observed almost complete conversion of CHD with high selectivity to dicarboxylic acids (entries 20, 21). Under the same conditions, but without PTA (entry 22), results did not change; this means that PTA had no effect on CHD oxidation. In all the experiments AA was the prevailing product; for instance in experiment 22 AA yield was 92.1%, glutaric acid yield 1.6%, succinic acid 0.2%.

From the results obtained we can conclude that temperature is the main parameter responsible for the oxidation of CHD into dicarboxylic acids. PTA is important only in the step of cyclohexene oxidation into the epoxide and has no effect on the epoxide hydrolysis or CHD oxidation.

In summary, the reaction of cyclohexene dihydroxylation into CHD, carried out in the absence of organic solvent with a catalytic system based on tungstate and phosphoric acids, and using aqueous solution of hydrogen peroxide as an oxidant and a phase transfer agent, gave 97.2% selectivity to the diol with complete conversion of cyclohexene. The only drawback of this process is related to the recovery of both the PTA and the catalytic system, which is a very difficult operation to do.

9. The second step: 1,2-cyclohexanediol oxidation

The oxidation of CHD with molecular oxygen was investigated using heterogeneous and homogeneous catalysts. For this purpose we chose heterogeneous Ru and Au-based catalysts, and homogeneous Keggin-type P/Mo/V heteropolyacids.

9.1. Ru-based catalysts

Ru-based catalysts are widely used for alcohols oxidation to aldehydes or ketones [141]. For example, catalysts used include supported Ru, such as Ru-Al-Mg hydrotalcites [142], Ru-grafted hydrotalcites [143], Ru-Co-hydroxyapatite [144] Ru(OH)_x as a bulk catalyst [145] and supported on alumina [146, 147, 148], on magnetite [149], on cerium dioxide [150] or on titania [151].

Felthouse reported that ruthenium pyrochlore oxides are active catalysts for the oxidative cleavage of vicinal diols to produce dicarboxylic acids [152]. In the literature there are numerous studies concerning the oxidation of alcohols to acids using VIII group metals of [153, 154, 155].

We chose ruthenium hydroxide supported on alumina $\text{Ru(OH)}_x/\text{Al}_2\text{O}_3$ as catalyst for CHD cleavage.

9.2. Experimental part

9.2.1. Synthesis of the catalyst

Synthesis of the catalyst was done following the method described in the literature [155].

First γ - Al_2O_3 was calcined in static atmosphere at 550°C for 3h. In a beaker a solution of Ru^{3+} was prepared by dissolving $\text{RuCl}_3 \cdot x\text{H}_2\text{O}$ in 60 ml of water. The concentrations of the solution were different according to the percentage (by mass) of Ru that was to be deposited on alumina. Catalysts with 0.6, 1.3, 2.5 and 4.9% of Ru were prepared. The amounts of Ru that were necessary to obtain the desired catalysts are given in Table 19.

Table 19. The amount of Ru required for the preparation of catalysts

Content of Ru in catalyst, %	Denotation of the catalyst	Mol of Ru
4.9	Ru-4.9	$1.02 \cdot 10^{-3}$
2.5	Ru-2.5	$5.09 \cdot 10^{-4}$
1.3	Ru-1.3	$2.56 \cdot 10^{-4}$
0.6	Ru-0.6	$6.15 \cdot 10^{-5}$

After dissolution of $\text{RuCl}_3 \cdot x\text{H}_2\text{O}$, 2g of alumina were added to the solution to get a suspension; then the system was subjected to strong stirring at room temperature during 15 min. The basicity of the suspension was measured with a pH meter. The pH was adjusted to 13.2 by adding first solid NaOH and then a 1M NaOH solution when the desired pH was approached. The strongly basic environment serves to activate the surface sites of the alumina tearing the H^+ ion to form the Al-O^- species. Then the beaker was covered with a watch glass and the suspension was left under stirring for 24h. Finally, the suspension was filtered on a Buchner filter, washed with 2 liters of distilled water to remove all traces of the base and of ions (Cl^- , Na^+ and Al^{3+}) that were adsorbed on the solid. The catalyst was then dried in a stove at 120°C for one night; the dark green powder obtained was ready to use and was stored in a properly labeled glass vial.

9.2.2. Characterization of the catalyst

9.2.2.1. XRD analysis

X-ray diffraction (XRD) patterns of catalysts were recorded on a Philips X'Pert vertical diffractometer equipped with a pulse height analyzer and a secondary curved graphite-crystal monochromator, with Ni-filtered CuK_α radiation ($\lambda = 1.54178\text{\AA}$). A 2θ range from 5° to 80° was studied at a scanning speed of $70^\circ/\text{h}$.

All samples were characterized by means of XRD. No signals corresponding to either Ru metal clusters or RuO were found. Therefore, we can suggest that ruthenium species were highly dispersed on the alumina surface.

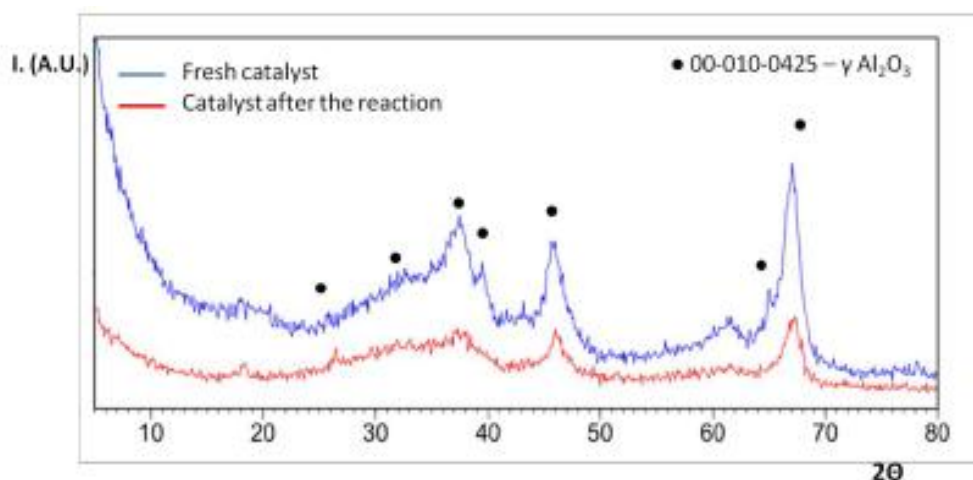


Figure 25. XRD pattern of the Ru(OH)_x/Al₂O₃ catalyst with 4.9% of Ru

The catalyst after the reaction were also characterized by means of XRD. If we compare these two patterns, it is clear that catalyst structure did not undergo any significant change during reaction. Examples of the patterns are given in Figure 25.

9.2.2.2. HR-TEM

High-Resolution transmission electron microscopy (HR-TEM) images were obtained with a Jeol 3010-UHR instrument (acceleration potential 300 kV, LaB6 filament). Samples were dry dispersed on lacey carbon Cu grids.

The images obtained by TEM are presented in Figure 26. Pictures show the presence of nanoparticles of Ru(OH)_x with the diameter of a few nanometers, and the absence of crystalline aggregates; these results are in a good agreement with the data obtained by XRD.

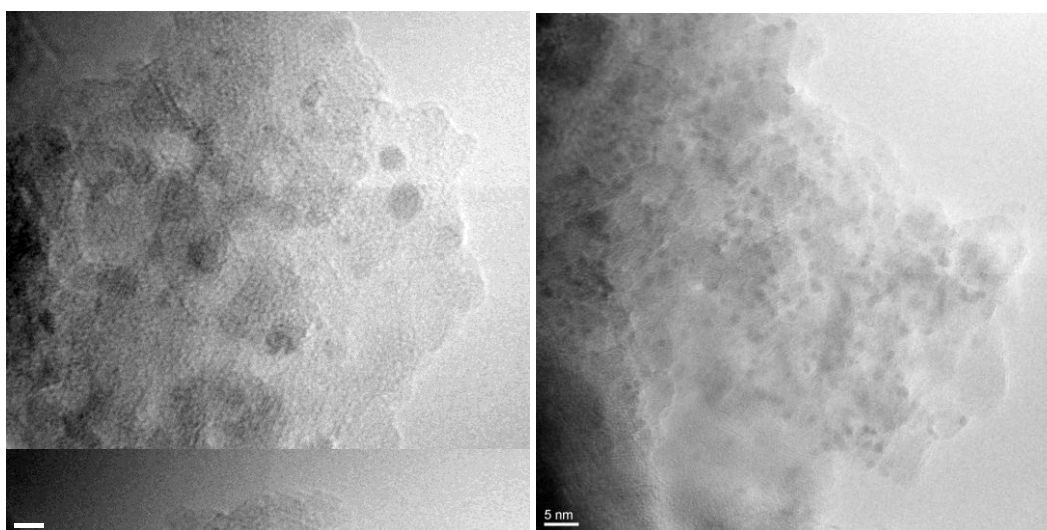


Figure 26. HR-TEM pictures of the Ru(OH)_x/Al₂O₃ catalyst (2.5% of Ru)

9.2.3. Catalytic measurements

The reaction was conducted in a semi-continuous reactor (volume 50 mL) made of glass, model Büchi Miniclave. The reactor is composed of a glass container of 100 mL volume, capable of withstanding high pressures (5 bar at 150°C or 10 bar at 100°C) with a support made of a rigid metal grid, and a cap able to guarantee the sealing, equipped with the gas lines and the systems of control and safety valves. The scheme of the reactor is shown in Figure 27.

- R1: Reactor consists of an upper cap for closing, glass vessel of 100 mL volume, the metal grid as support and protection, and the magnetic stirrer. The heating of the reactor was made with a silicone oil bath on a manually adjustable heating plate;
- V1: valve for sampling;
- V2: shut-off valve for venting of the reactor;
- V3: shut-off valve of the oxygen line;
- E1: condenser with ethylene glycol cooled to -10°C;
- RD1: rupture disk calibrated at a pressure of 7 bar, connected with a metal tube to a plastic pail of 3L volume; the latter is submerged in sand;
- PI: pressure indicator to measure the relative pressure, in bar units;

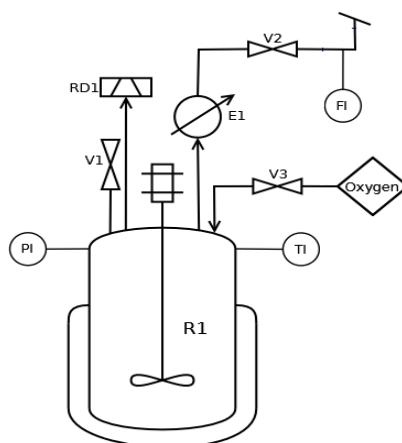


Figure 27. Scheme of the reactor

- TI: temperature indicator (a thermocouple protected with a teflon sheath) to measure values of the temperature, in °C;
- FI: indicator of gaseous flow, consisting of a bubble flowmeter.

Procedure for catalytic experiments is the following: the mixture of the reagent, catalyst, sodium hydroxide and water is loaded into the reactor; a magnetic stirrer is placed in the vessel. The reactor is then placed in a silicone oil bath that is heated with an electric plate, and agitation is started. When the temperature inside the reactor reaches the required value, we open the valve of oxygen manually; this moment is taken as the zero time of the reaction.

Typical reaction conditions were:

- 0,6 g of CHD;
- 0,2 g of the Ru(OH)_x supported on Al₂O₃ catalyst;

- 3,0 g of a solid NaOH;
- 50 ml of distilled water;
- oxygen flow 300mL/min;
- temperature 90°C.

In most experiments, sampling of the liquid phase from the reaction mixture was carried out all along the test time. This procedure involves the following steps:

- 1) closing the shut-off valve of oxygen inlet feed;
- 2) opening the valve for sampling;
- 3) sampling of about 2 mL of the reaction mixture with a glass syringe;
- 4) closing the sampling valve and opening the valve for oxygen inlet;
- 5) accurate measurement of the volume drawn with a graduated cylinder, after leaving the sample cool down to room temperature.

This technique is used when it is necessary to determine yields of the products and substrate conversion in function of time.

9.2.4. Treatment of the reaction mixture

After sampling, the separation of the catalyst from the liquid phase was done by centrifugation. The supernatant was then acidified with 85% H₃PO₄ to pH between 2 and 3 (controlled with a pH-meter), and then the mixture was diluted with distilled water to 5 mL volume in a volumetric flask. The mixture was analyzed by means of HPLC; the acidification of the liquid sample is necessary because a pH comprised between 2 and 3 lies the optimal value to obtain a good separation of the peaks in the HPLC chromatogram.

When the reaction was performed without sampling, the separation of the catalyst was done by filtration. Also in this case, acidification with H₃PO₄ is necessary.

9.2.5. Analysis of the reaction products

As it was already mentioned before, the mixtures were analyzed by means of HPLC. We also analyzed some mixture by means of ESI-MS spectroscopy, to identify unknown compounds.

Description of the analysis is given in a chapter 6.4.

9.3. Results and Discussion

9.3.1. Influence of pH value

Preliminary experiments were carried out with the aim to demonstrate the need for highly basic reaction medium. The role of pH was confirmed by experiments made at increasing pH value, in the presence of the catalyst containing 2.5 wt% Ru.

Results are shown in Figure 28. At pH=5.5 there was no formation of AA, with only 10% of CHD conversion; at pH=10 the reagent conversion reached 20%, but still there was no AA formed. Only at strongly basic pH=13.4, the CHD (conversion 55%) was oxidized into AA.

Since further experiments were carried out at a strongly basic pH, it was necessary to check the stability of $\text{Ru(OH)}_x/\text{Al}_2\text{O}_3$ catalysts under reaction conditions. Results are given in the next chapter.

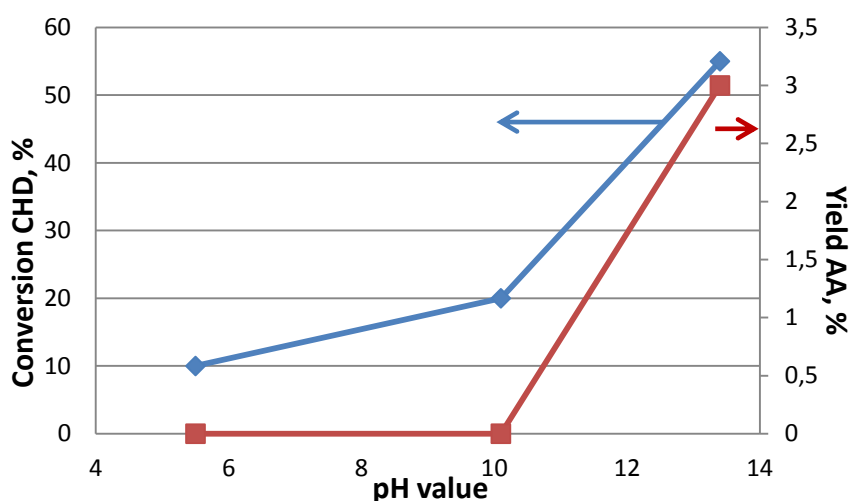


Figure 28. Effect of pH on the AA yield and CHD conversion

9.3.2. Stability of catalysts under reaction conditions

To check the stability of the catalyst under reaction conditions we carried out three different types of experiments:

- dissolution experiments: to check if the support is stable under strongly basic reaction conditions;
- leaching experiments: to check if leaching of Ru into the reaction mixture occurs;
- recyclability experiments: to check if the catalyst keeps its initial activity or deactivates during reaction.

9.3.2.1. Dissolution of the support

The alumina is an amphoteric oxide and it dissolves in strongly basic medium. Therefore, the catalyst might be unstable under reaction conditions. To check whether alumina is solubilized, we weighted the catalyst after reaction and calculated the amount that had dissolved under typical reaction conditions (5h reaction time, pH=13.4, 90°C). The results are shown in Table 20.

Table 20. Results of catalyst stability tests

Catalyst	Degree of dissolution, %
Ru-4.9	<<1
Ru-2.5	<1
Ru-1.3	16
Ru-0.6	31

The degree of dissolution was a function of the Ru content in the catalyst: with catalysts having the greater Ru loading, the dissolution of alumina during reaction decreased, and with a loading of 2.5% Ru it became negligible.

These data suggest that the $\text{Ru}(\text{OH})_x$ species are grafted to the Al_2O_3 surface and protect the latter from dissolution, but this occurs only when the Ru amount is enough to react with all Al-OH surface groups and entirely cover the alumina surface.

9.3.2.2. Leaching experiments

Leaching experiments were done using this procedure: first, the reaction was carried out during 3h, then the catalyst was filtered off. Thereafter, the mixture was again loaded into the reactor, and the reaction was continued for 3 h more in the absence of the catalyst. Results are shown in Figure 29.

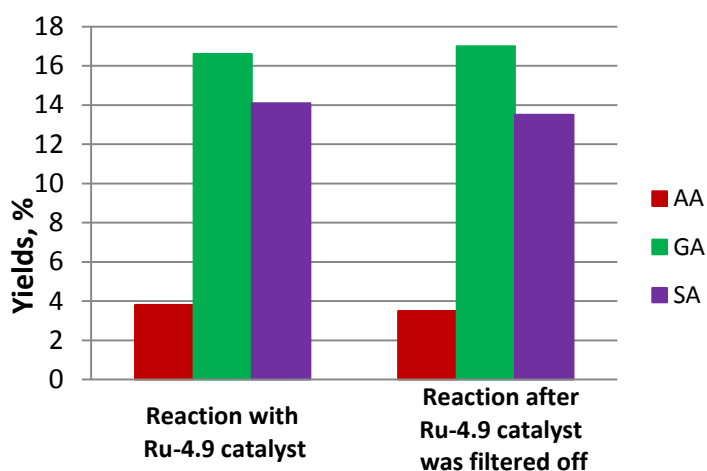


Figure 29. Results of the leaching experiments for Ru-4.9
AA - adipic acid, GA - glutaric acid, SA – succinic acid

This type of experiment was carried out with catalysts Ru-2.5 and Ru-4.9 only, because they were the only ones which did not undergo dissolution during reaction.

As we can see from Figure 29, the results did not change, and the amount of residual CHD was the same in both mixtures. For the Ru-2.5 catalyst, we also found no leaching.

9.3.2.3. Recyclability experiments

Recyclability experiments were performed only for Ru-4.9 and Ru-2.5 catalysts. The procedure was the following: first, the reaction was carried out for 3 h, then the catalyst was filtered off, washed with water and reloaded with fresh reagents for the 3h more. There was no deactivation of the catalysts; in fact, both kept the initial activity, as shown in Figure 30 for catalyst Ru-4.9.

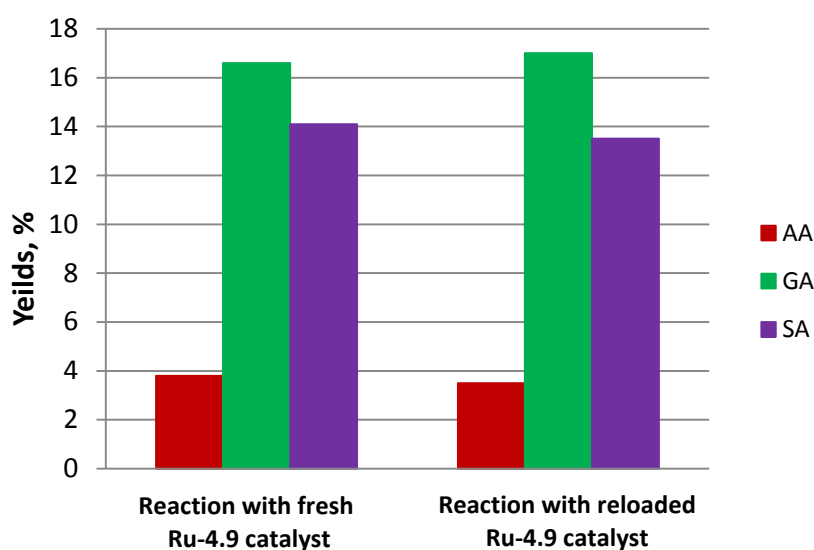
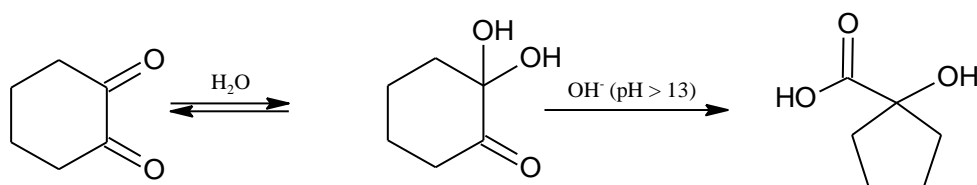


Figure 30. Results of recyclability experiments for Ru-4.9
AA - adipic acid, GA - glutaric acid, SA – succinic acid

9.3.3. Reactivity experiments

For all catalysts, we carried out the reactivity experiments and identified the main reaction products. They were: AA, glutaric acid (GA), succinic acid (SA), and 1-hydroxycyclopentanecarboxylic acid (HCPA). We also detected the formation of 1,2-cyclohexanedione (CHDO) in small amount.

Formation of HCPA was confirmed by means of ESI-MS spectroscopy and GC-MS chromatography. It is known from literature that HCPA forms from CHDO under strongly basic conditions [156] (Scheme 26).



Scheme 26. Formation of HCPA from CHDO

CHD conversion plotted in function of time for catalysts with different Ru contents are shown in Figure 31 and Table 21.

Table 21. Effect of Ru content and time on CHD conversion

t, h	Ru-4.9	Ru-2.5	Ru-1.3	Ru-0.6	Al ₂ O ₃
0	-	-	-	23	12
0,5	24	-	27	26	8
1	49	43	31	52	8
3	65	62	76	67	7
5	77	74	91	80	-

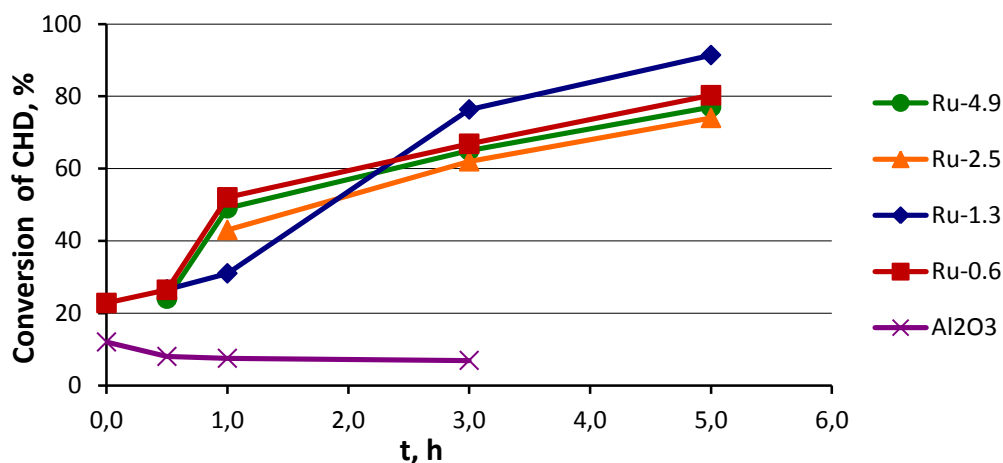
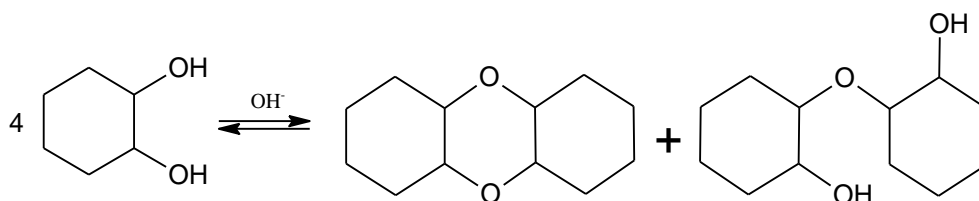


Figure 31. Effect of reaction time on CHD conversion in the presence of catalysts with different Ru contents

In all cases, except alumina, conversion of CHD increased with increasing the time of reaction. The content of Ru did not affect the conversion and already in the beginning of the reaction (0 h) a conversion of 20% was shown (with alumina 12%). By means of ESI-MS analysis we found the formation of CHD self-condensation compounds (Scheme 27).



Scheme 27. Formation of condensation compounds from CHD

Even though the content of Ru did not affect conversion so much, catalysts with 0.6% and 1.3% of Ru gave a slightly higher conversion of CHD. Probably, this was due to the dissolution of these catalysts under reaction conditions; therefore, in these cases both heterogeneous and homogeneous catalysis contributed to CHD conversion.

Yield to reaction products are given in the Tables 22-25 and in Figures 32-35.

Table 22. Effect of reaction time and Ru content in catalysts on AA yield (%)

t, h	Ru-4.9	Ru-2.5	Ru-1.3	Ru-0.6
0	-	-	0	0
0,5	2	-	3	0
1	3	2	4	1
3	4	3	5	10
5	3	3	3	5

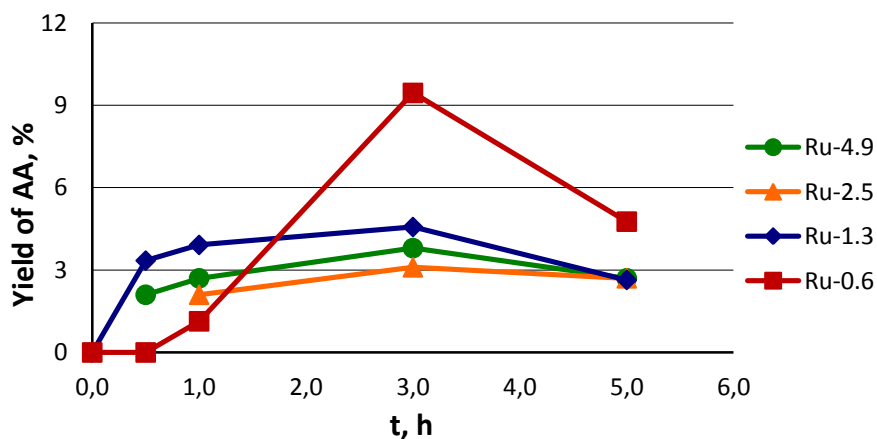


Figure 32. Effect of reaction time and Ru content in catalysts on AA yield

Table 23. Effect of reaction time and Ru content in catalysts on GA yield (%)

t, h	Ru-4.9	Ru-2.5	Ru-1.3	Ru-0.6
0	-	-	0	0
0,5	8	-	5	3
1	14	14	9	8
3	17	16	6	14
5	10	8	6	13

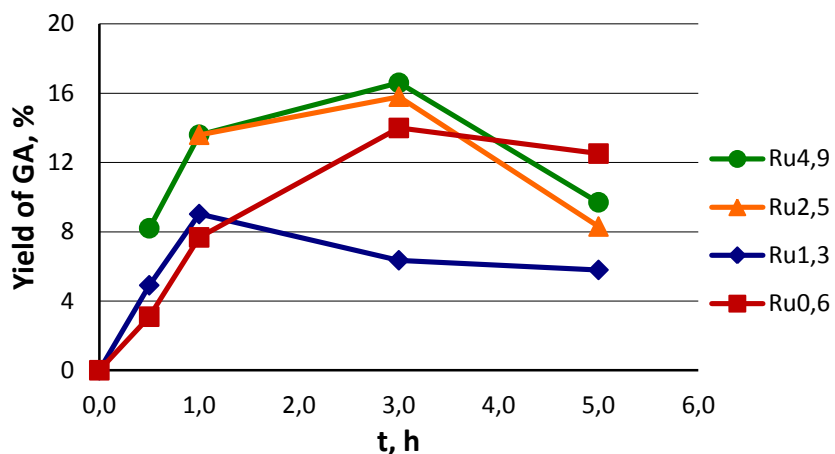


Figure 33. Effect of reaction time and Ru content in catalysts on GA yield

Table 24. Effect of reaction time and Ru content in catalysts on SA yield (%)

t, h	Ru-4.9	Ru-2.5	Ru-1.3	Ru-0.6
0	-	-	0	0
0,5	2	-	1	1
1	9	7	2	2
3	14	13	5	7
5	24	19	7	15

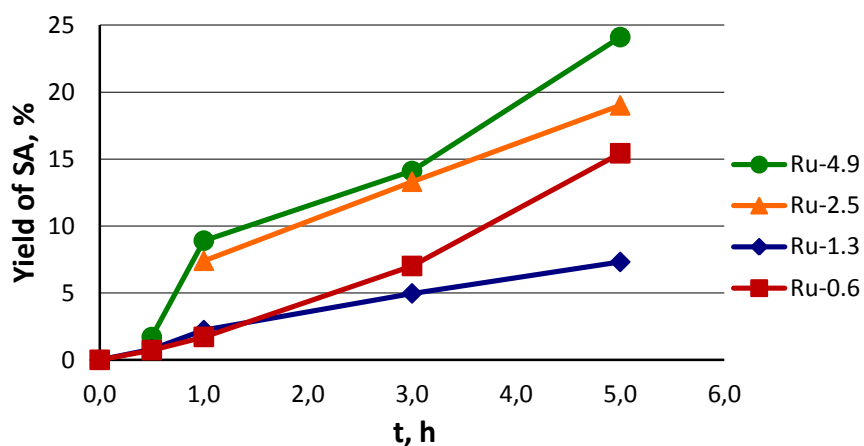


Figure 34. Effect of reaction time and Ru content in catalysts on SA yield

Table 25. Effect of reaction time and Ru content in catalysts on HPCA yield (%)

t, h	Ru-4.9	Ru-2.5	Ru-1.3	Ru-0.6
0	-	-	0	0
0,5	4	-	1	4
1	7	7	6	4
3	13	11	9	7
5	19	19	13	10

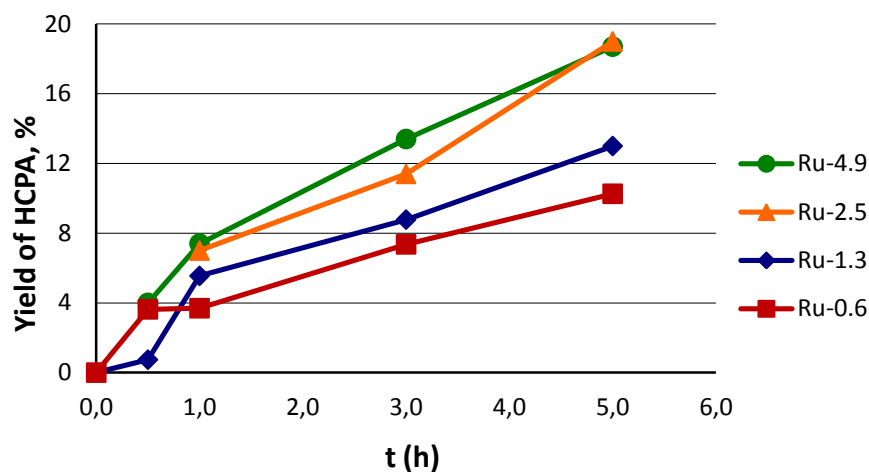


Figure 35. Effect of reaction time and Ru content in catalysts on HCPA yield

Concerning the formation of AA, there was an effect of Ru content in catalysts on AA yield. When Ru-0.6 was used, the formation of AA started only after 30 minutes of reaction, and then increased in the same way as CHD conversion did. The maximum AA yield of 10% was reached after 3h reaction time, but then the amount of AA started to decrease, and after 5h the yield was about 5%. The same AA decomposition was also observed with other catalysts.

The higher AA yield obtained with Ru-0.6 catalyst is likely the result of the dissolution of catalyst, and the leaching of Ru^{3+} . This process needs time to start, leading to the induction period experimentally observed. However, with catalyst Ru-1.3, the induction period was not shown, probably because 1.3% of Ru was enough to form AA from the beginning of CHD conversion.

HCPA, GA, and AA are primary products of the reaction, whereas SA is a secondary product. The amount of SA increased slowly and only after 3h of reaction, when the amount of AA and GA started to decrease, SA yield grew faster. Finally, SA was the prevailing product in the mixture. The yield of HCPA increased with the reaction time, but it did not decompose or transform into other products.

The yields of AA, GA, and SA were always high with Ru-0.6 catalyst; this occurred probably because of the high degree of Ru dissolution in the reaction medium. The activity of the other catalysts was a function of Ru content ($\text{Ru-4.9} > \text{Ru-2.5} > \text{Ru-1.3}$).

We also detected the formation of lighter compounds produced by decomposition of the main reaction products. Their yield increased with the increase of time. CHDO also formed, but in a very small amount (yield 0.2%) and only at short reaction time. This result indicates that CHDO could be either an intermediate compound of the reaction, that very rapidly transforms into other products, or a minor by-product. But as it was mentioned above, it is known from the literature that HCPA forms from CHDO under strongly basic conditions. We did not detect the formation of 2-hydroxycyclohexanone (HCHN), but the latter could be the precursor of CHDO formation. To understand the role of CHDO in CHD

oxidation mechanism, and whether HCHN is an intermediate compound, we carried out experiments using CHDO and HCHN as starting compounds.

9.3.4. Reactivity of the CHDO and HCHN. Study of the reaction mechanism

First we checked CHDO reactivity in function of the pH of the reaction mixture in the presence of catalyst Ru-4.9 and oxygen, at T=90°C. Results are given in Table 26. Reaction products were identified by means of HPLC and ESI-MS.

Table 26. Results of the reactivity experiments starting from CHDO. T=90°C, 3 h reaction time, catalyst Ru-4.9, O₂

pH	X, %	HCPA	AA	GA	SA	Other products (ESI-MS)
6	68	0	traces	0	0	6-hydroxycaprolactone Adipic anhydride aldol condensate 2,2-dihydroxycyclohexanone
12.9	100	0	16	4	19	6-hydroxycaprolactone aldol condensate
13.4	100	61	2	3	0	6-hydroxycaprolactone aldol condensate

After 3 hours of reaction at pH 12.9 and 13.4, CHDO conversion was total, whereas at pH 6 it was 68%. The distribution of products obtained by CHDO oxidation under strongly basic conditions was very similar to that observed starting from CHD. This fact confirms that CHDO is a key intermediate in the reaction of CHD oxidation.

At pH 6 and 12.9 there was no formation of HCPA, and yields to the acids were higher. We also observed the formation of both 6-hydroxycaprolactone and a dimer that forms by CHDO aldol condensation. 6-Hydroxycaprolactone could form from the dione by an intramolecular Cannizzaro-type disproportionation. Further this compound can be oxidized to adipic anhydride, that by hydrolysis forms AA. Actually the presence of adipic anhydride was detected during CHDO oxidation at neutral pH, but there was no formation of AA in this case. This means that the anhydride did not hydrolyse to AA in neutral medium, but this reaction indeed occurred at more basic pH, finally yielding AA.

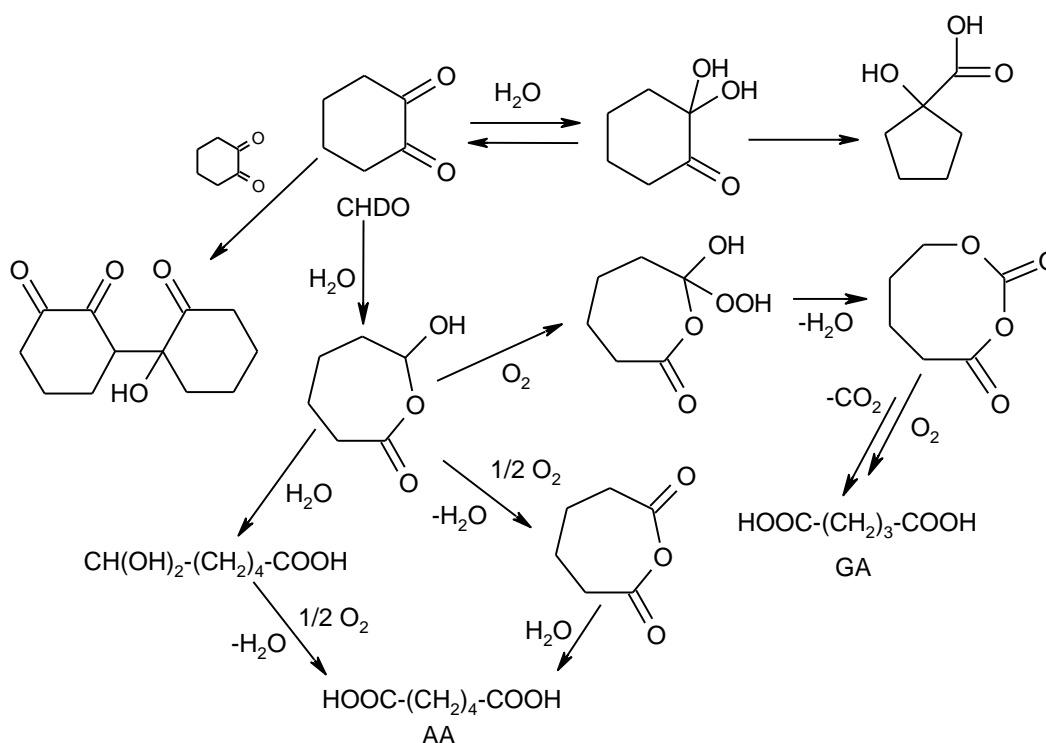
Reactivity of CHDO was checked also in the absence of either the catalyst only, or of both catalyst and oxygen at 90°C and at 45°C (Table 27), under strongly basic conditions.

Table 27. Results of the reactivity experiments starting from CHDO. All experiments were carried out in the absence of catalyst, 3hours, pH=13.4

T, °C	O ₂	X, %	HCPA	AA	GA	SA	Other products (ESI-MS)
90	Yes	100	38	0	28	0	-
90	No	100	61	0	0	0	-
45	No	78	53	0	0	0	aldol condensate

In all cases HCPA was the prevailing reaction product; it can form from 1,2-cyclohexanodione (CHDO) even in the absence of oxygen and at low temperature. Glutaric acid formed only in the presence of oxygen; this indicates that this compound was produced by reaction of CHDO with oxygen, but its formation did not necessitate the presence of the catalyst.

Putting together all data, we can propose the mechanism of CHDO transformation (Scheme 28). The CHDO is the key intermediate compound of CHD oxidation, and its transformations lead to several products, the formation of which occurs under basic conditions, i.e., HCPA, the aldol condensation product, and 6-hydroxycaprolactone. The two first compounds are stable, whereas the 6-hydroxycaprolactone transforms into adipic and glutaric acids; the formation of AA needs the presence of the catalyst to proceed, whereas GA forms without catalyst through the formation of a Criegee type intermediate.



Scheme 28. Transformations of CHDO

The effect of the pH value on HCHN reactivity in the presence of catalyst Ru-4.9 is shown in Table 28.

Table 28. Results of the reactivity experiments starting from HCHN. T=90°C, 3 h reaction time, catalyst Ru-4.9, O₂

pH	X, %	HCPA	AA	GA	SA	Other products (ESI-MS)
12.5	95	0	29	10	traces	6-hydroxycaprolactone aldol condensate
13.4	100	73	9	6	5	-

It is evident that HCHN is a very reactive compound; after 3 hours of reaction it completely, or almost completely at pH 12.5, converted into products. Under strongly basic conditions it rapidly transformed with a high selectivity into HCPA and in a small amount to AA, GA and SA, but at less basic pH it was more selectively converted to AA and did not form HCPA at all.

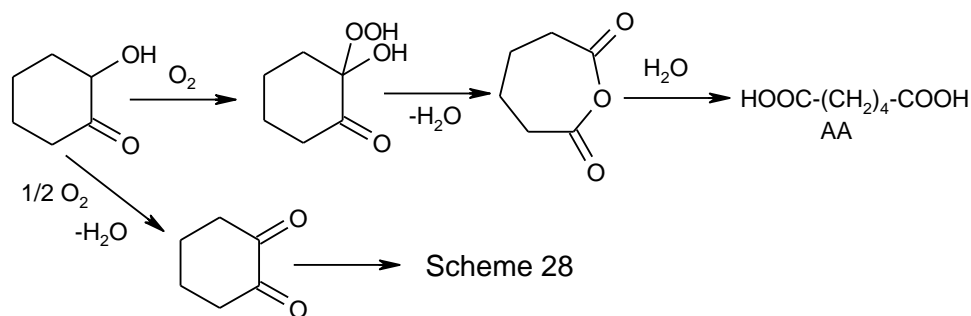
We also performed the experiments starting from HCHN in the absence of any catalyst; results are shown in Table 29.

Table 29. Results of the reactivity experiments starting from HCHN. T=90°C, 3 h reaction time, no catalyst, O₂

pH	X, %	HCPA	AA	GA	SA	Other products (ESI-MS)
10.1	100	0	4	3	0	CHDO (2%)
12.5	100	0	71	6	3	6-hydroxycaprolactone aldol condensate CHDO (2%)
13.4	100	52	20	15	11	Traces

We found that 2-hydroxycyclohexanone is a very reactive compound even in the absence of catalyst; in fact in all cases it was completely converted after 3h. Under strongly basic conditions HCPA was the prevailing product, and yields of AA, GA and SA were higher than those obtained in the presence of catalyst. However, the most interesting results were obtained at pH 12.5: in the absence of catalyst HCHN transformed with high selectivity (71%) to AA. Other products found were GA, SA, 6-hydroxycaprolactone, aldol condensate and CHDO (2%).

Based on results obtained, the reaction scheme for HCHN oxidation was drawn (Scheme 29).



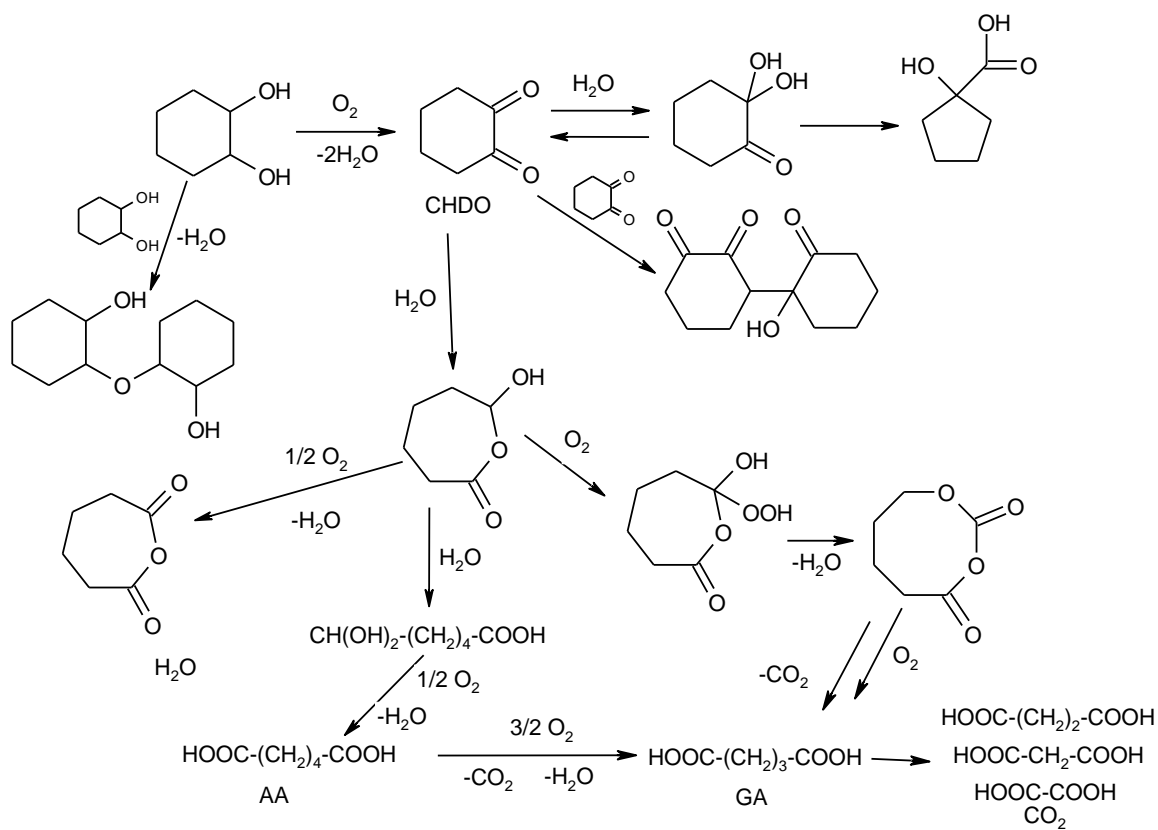
Scheme 29. Transformation of HCHN

The hydrogen atom on the α C atom, holding the hydroxyl moiety, can be easily eliminated giving a radical species, which quickly forms a quaternary carbon by reaction with O_2 , finally giving a hydroperoxide–hydroxide species [157, 158], resembling a Criegee-type compound. The latter may dehydrate and rearrange producing the lactone (adipic anhydride), which as we know is the precursor of AA.

The results obtained from all experiments allowed us to draw some conclusions concerning the mechanism of CHD oxidation:

1. The reaction takes place only under strongly basic conditions.
2. HCHN is the more selective intermediate compound to produce AA. However, we never observed it in reaction mixtures. This could happen due to the following reasons: (a) under strongly basic conditions the oxidative dehydrogenation is very fast and HCHN is immediately oxidized to CHDO; (b) CHD is oxidized directly to CHDO because the Ru^{n+} species coordinates both hydroxyl groups of CHD and transform them into carbonyls at the same time. And, actually, accordingly to the literature [159, 160] a similar situation is described with $Ru(IV)$ oxo complexes, which are able to perform the oxidation of cyclohexene to AA in water solution, through the formation of CHD.
3. CHDO is formed very fast from CHD, and then quickly transforms into aldol condensation product, 6-hydroxycaprolactone and HCPA. The first two compounds need the presence of the catalyst to form, whereas HCPA forms from CHDO under basic conditions even in the absence of both catalyst and oxygen. Due to this fact HCPA is one of the prevailing reaction products, but unfortunately it is not a precursor of AA formation.
4. SA and other lighter compound are formed by decarboxylation and oxidation of AA and GA.

The overall reaction mechanism is given in Scheme 30.



Scheme 30. The reaction mechanism of 1,2-cyclohexanediol oxidation with oxygen in the presence of $\text{Ru(OH)}_x/\text{Al}_2\text{O}_3$

9.4. Au-based catalysts

Experiments with the $\text{Ru}(\text{OH})_3$ catalyst allowed us to conclude the $\text{Ru}^{\text{n+}}$ species coordinates both hydroxyl groups of CHD and transform both of them into carbonyls at the same time, yielding directly CHDO. Moreover, we also found that 2-hydroxycyclohexanone can be very selectively transformed to AA. Therefore, this indicates that this reaction requires a catalyst which oxidizes the two vicinal hydroxyl groups in sequence, in order to obtain HCHN as the first reaction intermediate and allow the latter to become the starting point for a selective route leading to AA. Moreover, the optimal catalyst should be active under mildly basic conditions, in order to avoid the fast formation of CHDO, precursor of HCPA under strongly basic conditions.

From literature, we found that gold-based catalysts do not coordinate both hydroxyl groups in glycols, and hence show the characteristics which are needed for our reaction. For example, in the oxidation of 1,2-propanediol, depending on the conditions, Au nanoparticles either oxidize the primary hydroxyl-group to form lactic acid, or oxidize them in sequence starting from the secondary hydroxyl group, with the formation of pyruvic acid, which is then oxidized to acetic acid and CO_2 [161].

In recent years, the study of gold-based catalysts has grown considerably due to the experimental evidence that its reactivity increases significantly if gold is used in the form of nanosized particles.

Several studies have shown that the supported gold nanoparticles are good catalysts for the liquid phase oxidation of alcohols and diols with oxygen in basic medium. For example, Christensen et al. have studied gold nanoparticles supported on TiO_2 and MgAl_2O_4 in ethanol oxidation to acetic acid with air (150°C , 35 bar of air; selectivity to acetic acid was 92%) [162, 163] and Au/TiO_2 in 5-hydroxymethyl-2-furfural oxidation into 2,5-furandicarboxylic acid (FDCA) with oxygen (30°C , 20 bar of oxygen, different amounts of NaOH; maximum selectivity to FDCA was 71%) [164].

Corma et al. also studied gold nanoparticles supported on ceria and titania in the oxidation of 5-hydroxymethyl-2-furfural into FDCA with air. The reaction was carried out under mild conditions (air pressure 10 bar, T $65\text{--}130^\circ\text{C}$) in water as solvent; the selectivity to FDCA achieved was almost 100% [165].

In this work, gold nanoparticles supported on titania and magnesia have been synthesized and studied in the reaction of CHD oxidation with oxygen.

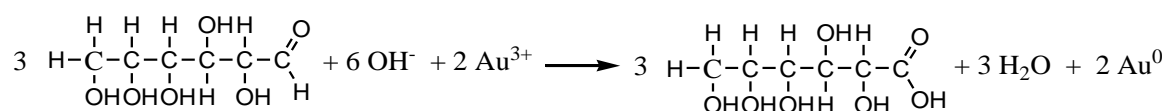
9.5. Experimental part

9.5.1. Synthesis of the catalysts

First, we performed the synthesis of the suspension of gold nanoparticles.

The choice of the method of nanoparticles synthesis is very important because it allows to modulate their characteristics such as shape, size and its distribution, composition and degree of agglomeration (in the case of colloidal systems). For this reason, it is important to follow the method very carefully, in order to ensure reproducibility of the results.

The suspension of gold nanoparticles was prepared by synthesis in water according to the method described in the literature and patented [166, 167]; the procedure provides the reduction of Au (III) by glucose in a basic environment of NaOH and stabilization of the nanoparticles with PVP (polyvinylpyrrolidone) for steric hindrance.



Scheme 31. Reduction of gold with glucose in basic medium

The alkaline environment is necessary to increase the reducing power of sugar that allows to obtain smaller particles of gold, because there are more nucleation sites, and the excess of glucose covers the cluster preventing its aggregation. The addition of PVP allows to stabilize the suspension.

First, 10mL of the gold-containing solution was prepared by dissolving a measured amount of HAuCl₄ to get the concentration of final solution equal to 5·10⁻³ mol/L.

The molar ratios of the reagents used for the synthesis of nanoparticles were the following:

- Au:PVP = 1:2.75
- Au:NaOH = 1:8
- Au:Glucose = 1:2

The PVP and sodium hydroxide were dissolved in 90 mL of distilled water in a three-necked round bottom flask. After the solution was heated to 95°C, glucose was added; the mixture was warmed up to 95°C again. After reaching the desired temperature the solution of HAuCl₄ was added. When exactly 2.5 minutes had passed, the reaction was stopped by fast cooling in bath with ice and water down to room temperature. The final solution showed a dark red color. To check the quality of nanoparticles it is necessary to measure the hydrodynamic diameter by DLS (Dynamic light scattering).

The catalysts were prepared by means of Incipient Wetness Impregnation of a suspension of gold nanoparticles on a support, in our case TiO₂, Mg(OH)₂ or MgO.

Before starting the impregnation, the required amount of solution needed to impregnate the support should be calculated based on the required weight percentage of metal in the catalyst and the amount of the support to be impregnated. Before the

impregnation, we concentrated the solution of nanoparticles carrying out a centrifugation in test tubes fitted with filters of cellulose (50 kDa Amicon Ultra filters (Millipore)) at 1700 rpm for no more than 25 minutes, because longer centrifugation time might lead to the aggregation of nanoparticles.

The Incipient Wetness Impregnation method provides the solution of the metal to drip on the support until reaching the “point of mud”: the volume of the used liquid is equal to that of the pores of the support; next step is a drying in oven to remove the imbibed liquid. We used the same procedure with the suspension of Au nanoparticles. This procedure should be repeated no more than four times, until the nanoparticle solution is finished. The catalyst was finally dried in an oven at 120°C overnight, washed for 30 minutes in boiling distilled water to remove the adsorbed PVP, and finally calcined in static air at 200°C for 3 hours. This treatment is also necessary to prevent the leaching of the catalyst during its use in the reaction.

Following this procedure, we synthesized catalysts Au/TiO₂, Au/Mg(OH)₂ and Au/MgO containing 1.5 wt% of Au.

9.5.2. Characterization of the suspension of gold nanoparticles by means of DLS

The DLS (Dynamic light scattering) technique was used for the analysis of the suspension of gold nanoparticles in order to determine their hydrodynamic diameter, that is the diameter of the particles in motion in a solution that includes the coordination sphere and any adsorbed species on its surface (e.g. surfactants, polymers).

The technique is based on the scattering by a laser beam ($\lambda = 633 \text{ nm}$) that invests a colloidal suspension with a particles size between 0.6 nm and 6 μm : the Brownian motion of particles moving with speed inversely proportional to their size. The intensity of the scattered light after interaction with the particles has a frequency of fluctuation that depends on their rate of diffusion; therefore, it is possible to derive the size of particles from the analysis of fluctuations.

Before each measurement, the suspension was diluted (20 drops of the suspension in 20 mL of distilled water) to avoid the interactions between the particles that may change the rate of diffusion and therefore the estimation of the size.

The instrument is able to provide a statistical distribution of the nanoparticles size based on the intensity of scattering. It is possible to obtain two types of size distributions with respect:

- a) to the volume occupied by the particles, or
- b) to the number of particles.

During the measurement we can get a curve that shows a distribution of the particle size and an index of polydispersity of the particle size in the suspension (PDI).

The value of PDI is between 0 and 1: the more the index is close to zero, the more the size distribution is mono-disperse:

- for the mono-dispersed suspension it is ≤ 0.2 ;

- if the index is between 0.2 and 0.5, the suspension is average poly-dispersed;
- for values greater than 0.6, the distribution is definitely poly-dispersed.

The instrument Nanoseries Zetasizer (Malvern Instruments) was used for the DLS analysis.

Synthesized suspension of the gold nanoparticles was characterized by this technique. Figures 36 and 37 show the results of the analysis.

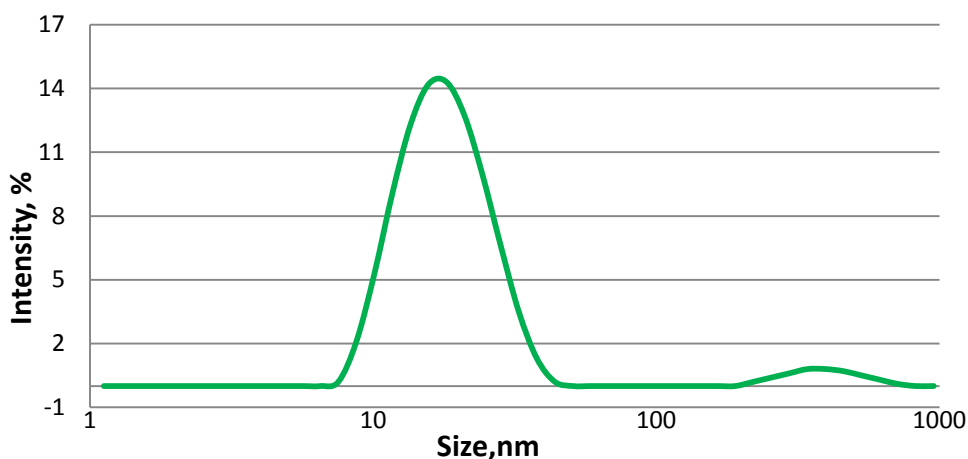


Figure 36. Distribution of the nanoparticles size by the intensity

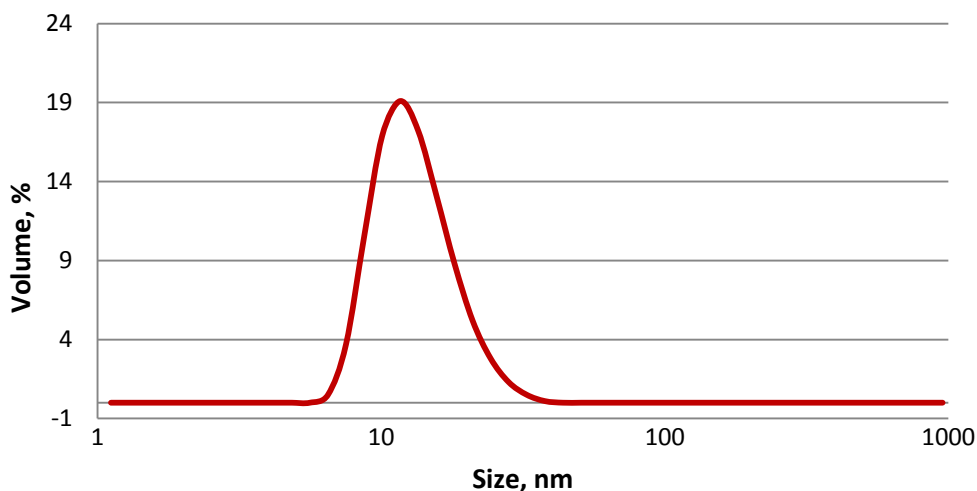


Figure 37. Distribution of the nanoparticles size with respect to the volume occupied

The average hydrodynamic diameter of the particles was 19 nm with the value of PDI index of 0.33, which corresponds to an average poly-disperse distribution of the nanoparticles size.

9.5.3. Characterization of the catalysts

The catalysts were characterized by means of X-ray diffraction (XRD) and High-Resolution transmission electron microscopy (HR-TEM), in order to determine the size of the crystallites of Au nanoparticle.

9.5.3.1. XRD analysis

X-ray diffraction (XRD) patterns of catalysts were recorded on a diffractometer Gragg/Brentano X'pertPro PANalytical, the X-ray source is a Cu anode ($K\alpha$ radiation with $\lambda=0.15418$ nm). All the samples were analyzed between 5 and $80^\circ 2\theta$, with acquisitions of $2s$ every $0.1^\circ 2\theta$. Before analysis the samples were put in the form of powder on a glass slide and dried at 120°C for a few minutes.

XRD pattern of Au nanoparticles supported on titanium oxide is shown in Figure 38.

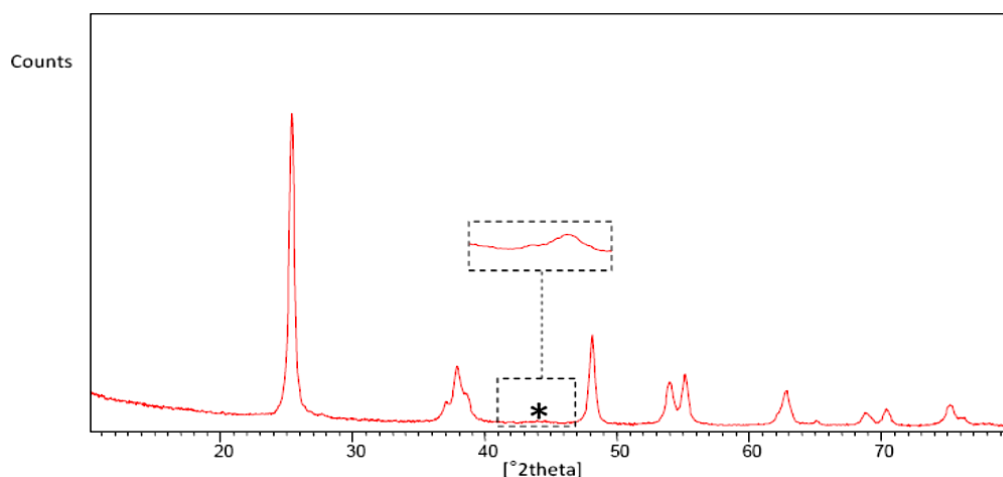


Figure 38. XRD pattern of Au/TiO₂

The reflections in the diffractogram are all relative to the support with the exception of the weak reflection at $44^\circ 2\theta$. The latter, as expected, is almost imperceptible due to the fact that the XRD signals are the more enlarged and flattened when the size of the crystallites are close to the detection limit of $2\text{-}3$ nm. In this case, to increase the signal at $44^\circ 2\theta$ an accumulation for $10s$ every $0.1^\circ 2\theta$ from 42 to $46^\circ 2\theta$ was performed.

To calculate the size of the crystallites we used the Debye-Scherrer equation :

Equation. Debye-Scherrer equation for the determination of the crystallites size of less than micrometer

$$d = \frac{K\lambda}{W_{1/2h} \cos \theta}$$

where:

K = factor of crystallinity (depends on the type of crystal, usually 0.9);

λ = wavelength of the used radiation;

$W_{1/2h}$ = width at half height of the reflection;

θ = angle of incidence of the beam on the surface.

Through this equation we calculated an average particle diameter of 6 nm.

In conclusion, as a result of the analysis, it can be stated that the synthesis of the catalyst has led to Au nanoparticles dispersed on the surface of titania.

XRD patterns of Au nanoparticles supported on MgO and Mg(OH)₂ are shown in Figures 39-40. In these cases the detection of the Au reflection was not possible, because of the presence of strong reflections attributable to MgO or Mg(OH)₂.

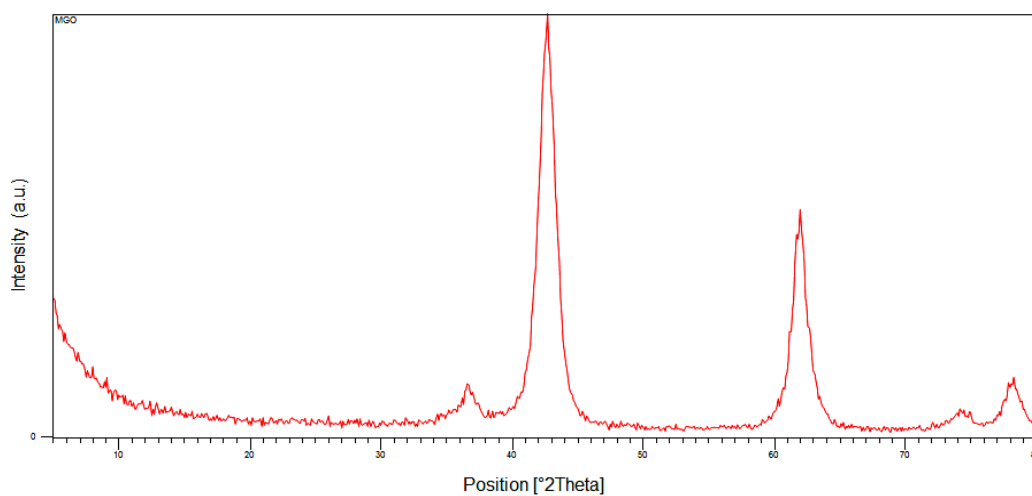


Figure 39. XRD pattern of Au/MgO

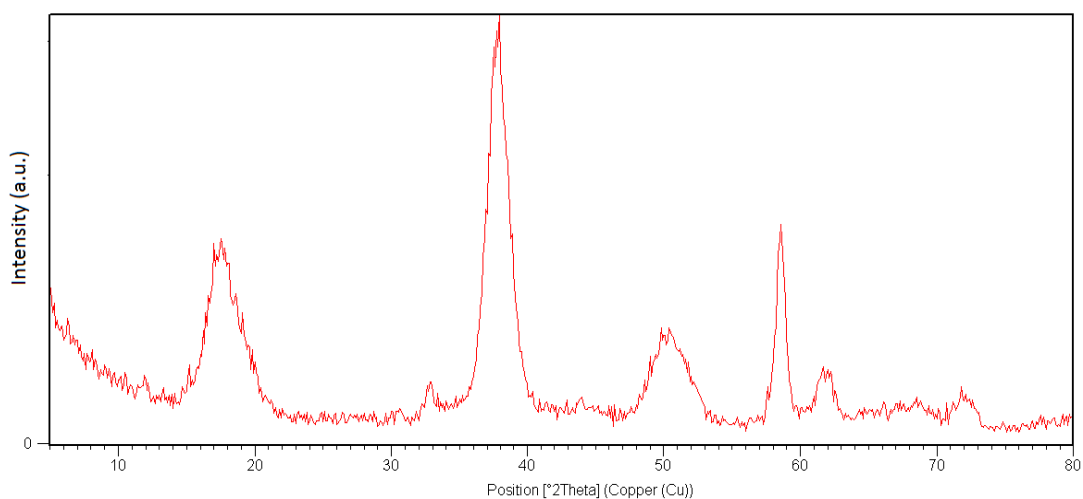


Figure 40. XRD pattern of Au/Mg(OH)₂

9.5.3.2. HR-TEM

Analysis by High-Resolution transmission electron microscopy of the samples was done with a microscope TEM/ STEM FEI TECNAI F20 at 200 keV.

HR-TEM pictures of Au/Mg(OH)₂ catalyst are reported in Figure 41, which show the presence of Au nanoparticles on the surface of the support.

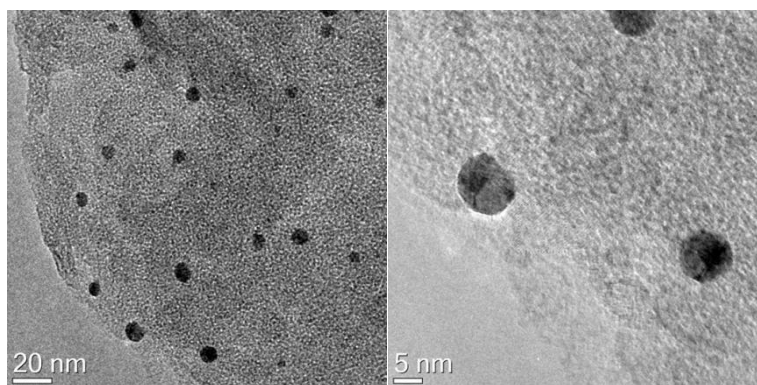


Figure 41. HR-TEM pictures of Au/Mg(OH)₂ catalyst

By means of this technique the average size of the supported nanoparticles has been also measured. For the catalyst based on gold nanoparticles supported on TiO₂ it was 6.6 nm, and for the Au/Mg(OH)₂ – 6.5 nm.

These data are consistent with results obtained by means of XRD.

9.5.4. Catalytic measurements

The experiments to measure the catalytic activity were carried out in the same reactor and in the same way as for experiments done with Ru-based catalysts. The description of the procedure is given in chapter 9.2.3.

9.5.5. Treatment of the reaction mixture

Procedure for the treatment of the reaction mixture is given in chapter 9.2.4.

9.5.6. Analysis of the reaction products

The mixtures were analyzed by means of HPLC and some of them also by means of ESI-MS spectroscopy.

Description of the analysis method is given in chapter 6.4.

9.6. Results and discussion

9.6.1. Au/TiO₂ catalyst

First we carried out some experiments varying the reaction conditions in order to evaluate the effect of some parameters on the selectivity (S) to AA.

The experiments were conducted by varying one of the following parameters:

- Ratio between Au supported on TiO₂ and CHD at a constant temperature of 90°C;
- Ratio between NaOH and CHD at a constant temperature of 90°C;
- Temperature.

The main reaction products were AA, GA, SA and we also detected small amount of the 2-hydroxycyclohexanone (HCHN) and 1,2-cyclohexanedione (CHDO).

9.6.1.1. Effect of the Au:CHD ratio

First, we have determined the optimal ratio between Au and CHD by changing the amount of loaded catalyst (Table 30). Other reaction conditions were: molar ratio NaOH:CHD=1:1, T=90°C, 3 hours of reaction time, oxygen flow 300 mL/min.

Table 30. The amount of catalyst and CHD (purity 98%), and the molar ratio Au:CHD used for the experiments

m(Au/TiO ₂), g	m(CHD), g	Au:CHD, mol/mol
1.1	1	1:100
0.22	1	1:500
0.11	1	1:1000
0.022	1	1:5000

Results of the experiments (yields to the main products and value of CHD conversion) are given in Table 31. Shown in Figure 42 is a comparison of CHD conversions, value of yields and selectivity of AA in function of the Au/CHD ratio.

Table 31. Results of the experiments with different ratio Au:CHD

Au:CHD, mol/mol	X(CHD), %	Y(AA), %	Y(GA), %	Y(SA), %	S(AA), %
1:100	70	21	3	1	30
1:500	52	22	7	3	42
1:1000	35	18	5	3	51
1:5000	33	5	1	0	15

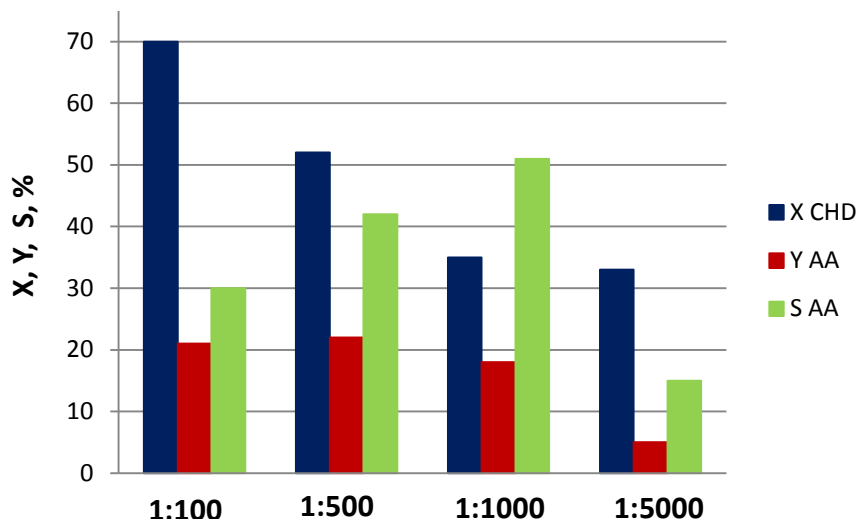


Figure 42. Results of the experiments with different ratio Au:CHD

The yields to HCHN and CHDO were not higher than 1%.

The best selectivity to AA was obtained using Au:CHD=1:1000 mol/mol. It is also shown that the conversion of CHD was not much affected by variations in the range between Au:CHD=1:1000 and 1:5000, while the selectivity to AA was significantly higher in the first case. The latter reaction mixture was analyzed by ESI-MS and we detected the formation of CHD self-condensation compounds, which were the primary products formed at the beginning of the reaction time.

In the case of reactions with ratio Au:CHD=1:100 and 1:500 mol/mol, CHD conversion was greater, especially in the former case. However, the selectivity to AA was lower, because of the oxidative degradation reactions that led to the formation of lighter by-products.

For further experiments, we decided to use the ratio between Au and CHD equal to 1:1000.

9.6.1.2. Effect of the NaOH:CHD ratio

First, we carried out the experiment without NaOH and the results obtained were: conversion of CHD 30%, no formation of dicarboxylic acid, only HCHN and CHDO formed in a small amount (yield < 0.5%).

Next step was to perform the experiments by varying the CHD: NaOH molar ratio in order to determine the best pH value for the reaction mixture (Table 32). Other reaction conditions were: molar ratio Au:CHD=1:1000, T=90°C, 3 h reaction time, oxygen flow 300 mL/min.

Table 32. The amount of NaOH and CHD (purity 98%) and the molar ratio NaOH:CHD used for the experiments

m(NaOH), g	m(CHD), g	NaOH:CHD, mol/mol
0.17	1	1:2
0.34	1	1:1
0.50	1	1.5:1
0.68	1	2:1

Results of the experiments (yields to the main products and value of CHD conversion) are given in Table 33. Figure 43 shows a comparison of CHD conversions, value of yields and selectivity to AA in function of the NaOH/CHD ratio.

Table 33. Results of the experiments with different NaOH:CHD ratio

NaOH:CHD, mol/mol	X(CHD), %	Y(AA), %	Y(GA), %	Y(SA), %	S(AA), %
1:2	38	11	2	1	29
1:1	35	18	5	3	51
1.5:1	52	18	7	4	35
2:1	50	15	15	4	30

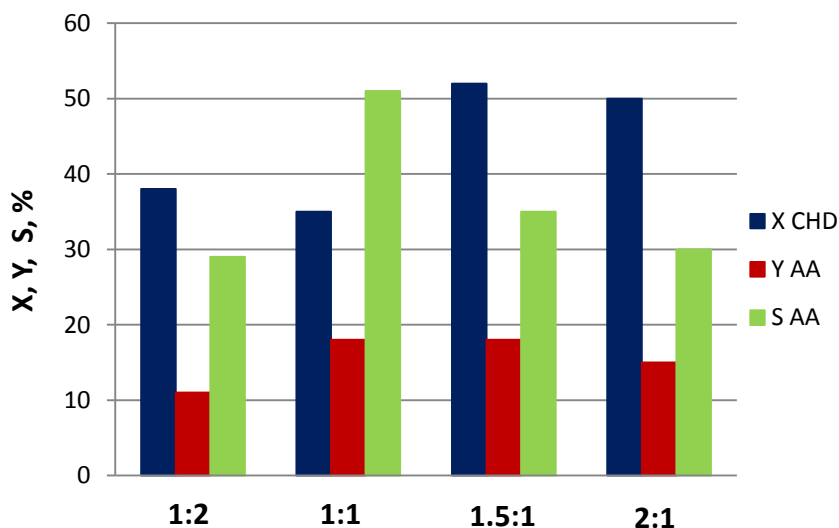


Figure 43. Results of the experiments with different NaOH:CHD ratios

In these reactions HCHN and CHDO were also present in small quantities (yields were <1%).

The conversion of CHD was not strongly affected by the NaOH/CHD ratio, and the maximum AA selectivity was obtained with the 1:1 ratio.

For further experiments we used the NaOH/CHD molar ratio equal to 1:1.

9.6.1.3. Effect of temperature

The last step was to find an optimal value of temperature to perform the reactions (Table 34). Other reaction conditions were: molar ratios Au:CHD=1:1000, NaOH:CHD=1:1, 3 h reaction time, oxygen flow 300 mL/min.

Table 34. Results of the experiments performed at different temperatures

Temperature, °C	X(CHD), %	Y(AA), %	Y(GA), %	Y(SA), %	S(AA), %
60	38	3	0,1	0	8
80	40	9	2	2	22
90	35	18	5	3	51

Figure 44 shows a comparison of CHD conversions, value of yields and selectivity to AA in function of temperature.

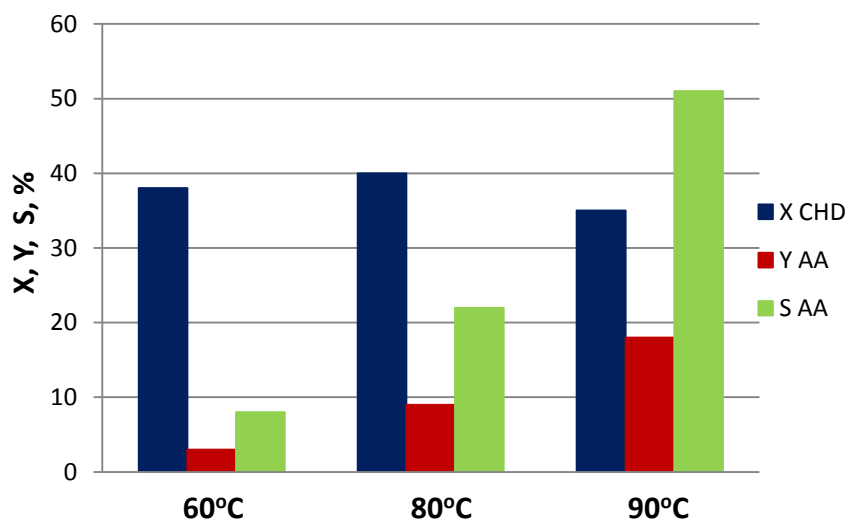


Figure 44. Results of the experiments performed at different temperatures

The maximum selectivity to AA was obtained at 90°C, while the conversion of CHD was not strongly affected by the temperature at which the reaction was carried out. This phenomenon probably takes place due to the presence of the equilibrium reaction of CHD etherification. The etherification reaction, which is an exothermal, equilibrium-limited reaction, prevailed at low temperature (in fact, main products were ethers), while at high temperature CHD oxidation was kinetically more preferred. The combination of these two effects led to the result that conversion was substantially independent from the temperature of reaction.

Thus, we found the optimal conditions to perform experiments:

- 1 g of CHD;

- 0.11 g of Au nanoparticles supported on TiO₂, that corresponds to the molar ratio Au:CHD=1:1000;
- 0.34 g of solid NaOH, that corresponds to the molar ratio NaOH:CHD=1:1;
- 50 ml of distilled water;
- oxygen flow 300mL/min;
- Temperature 90°C.

9.6.1.4. Stability of the catalyst under reaction conditions

To check the stability of the catalyst under reaction conditions we carried out two types of experiments:

- leaching experiments: to check if a leaching of Au into the reaction mixture had occurred;
- recyclability experiments: to check if the catalyst maintained its initial activity or deactivated during the reaction.

9.6.1.4.1. Leaching experiments

Leaching experiments were carried out using the following procedure: first, the reaction was carried out during 3 h, then the catalyst was filtered off, the mixture was loaded back into the reactor and the reaction was continued for 3 h more in the absence of the catalyst. Results are shown in Figure 45.

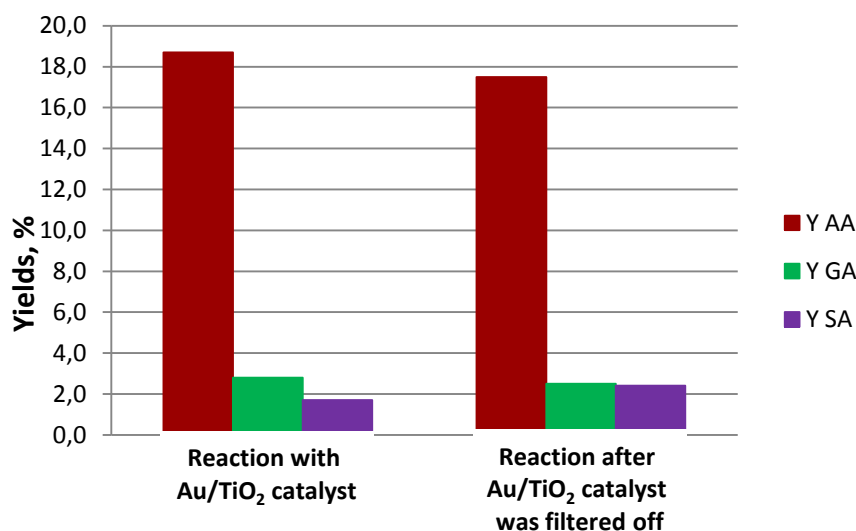


Figure 45. Results of leaching experiments. T=90°C, Au:CHD=1:1000, NaOH:CHD=1:1

As we can see from Figure 45, the yield of the products did not change and the amount of residual CHD was the same in the two mixtures. Therefore, the Au/TiO₂ catalyst did not undergo any leaching phenomena.

9.6.1.4.2. Recyclability experiments

Recyclability experiments were performed using the following procedure: first, the 3 h reaction was carried out, then the catalyst was filtered off, washed with water and reloaded with fresh reagents for the 3 h more of reaction. The procedure was repeated two times. The results are shown in Figure 46.

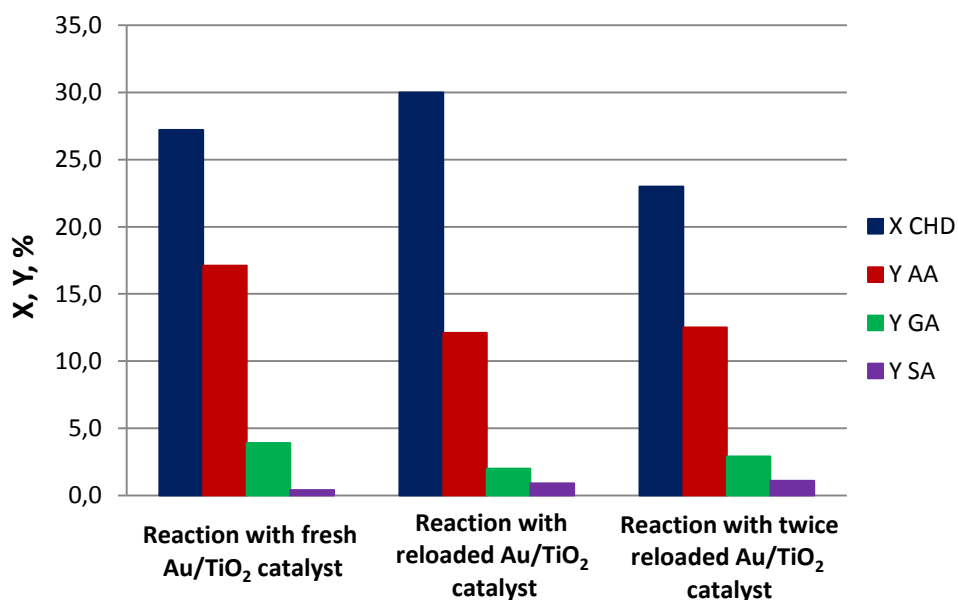


Figure 46. Results of the recyclability experiments. $T=90^{\circ}\text{C}$, $\text{Au}:\text{CHD}=1:1000$, $\text{NaOH}:\text{CHD}=1:1$

A small increase of CHD conversion was detected after the first reloading, but then it decreased to the value of about 23%. At the same time, the amount of products decreased after the first use, but then remained stable. Therefore we can conclude that the catalyst underwent a loss of selectivity after the first use, but then it did not undergo further deactivation in AA synthesis.

9.6.1.5. Activity of the catalyst as a function of reaction time

We performed the experiments in function of reaction time; reaction products were AA, GA, and SA; we also detected the formation of small amounts of 2-hydroxycyclohexanone (HCHN) and 1,2-cyclohexanedione (CHDO) (yields were <1% in all cases). Results are shown in Table 35 and Figure 47.

Table 35. Results of the reactivity experiments in function of time. Catalyst Au/TiO₂, T=90°C, Au:CHD=1:1000, NaOH:CHD=1:1, oxygen flow

Time of reaction, h	X(CHD), %	Y(AA), %	Y(GA), %	Y(SA), %	S(AA), %
0	23	0	0	0	0
0.5	29	4	1	0	14
1	36	10	2	0,3	28
3	39	18	4	2	46
5	35	24	6	2	69
7	35	25	5	3	71

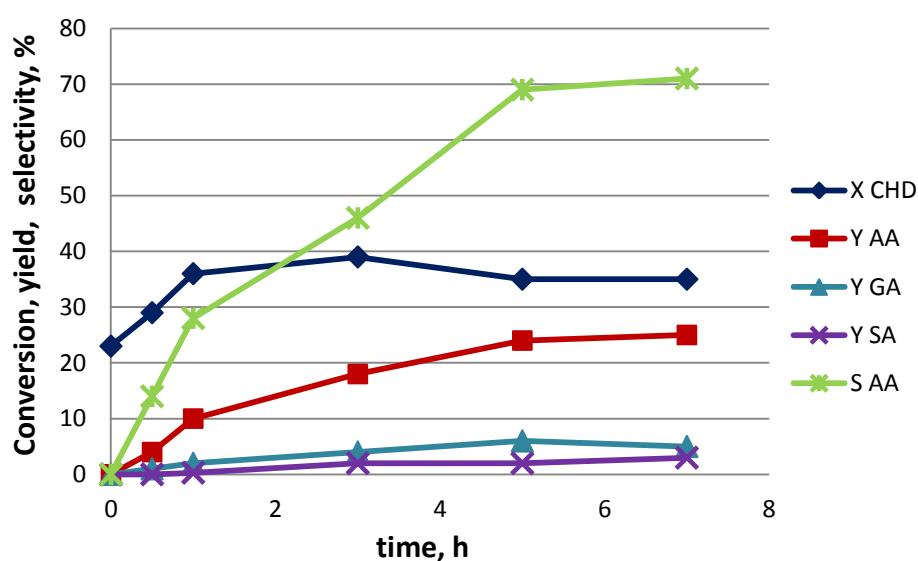


Figure 47. Results of the reactivity experiments. Catalyst Au/TiO₂, T=90°C, Au:CHD=1:1000, NaOH:CHD=1:1, oxygen flow

At the very beginning of the reaction (0 h), we observed CHD conversion of 23% due to formation of CHD self-condensation compounds (Scheme 27). In the reaction mixture obtained after 3h, the ESI-MS analysis showed the presence of 6-hydroxycaprolactone besides the other main products. The yield and selectivity of AA increased with increasing the reaction time, while CHD conversion became constant already after 1 hour. First we thought that this effect was due to the deactivation of the catalyst, but recyclability experiments proved the absence of any deactivation phenomenon. Probably during the oxidation of CHD reaction products were adsorbed on the surface of the catalyst, thereby blocking the active centers of the catalyst, while during the recyclability experiments catalyst was washed before each reloading, thus active centers were set free for catalytic activity again. An alternative explanation is that the formation of the condensation compound is very rapid, soon reaching the equilibrium, whereas the oxidation is much slower (as also demonstrated by the slower increase of AA yield). The second reaction overlaps to the first one, but since the first reaction is at equilibrium, the condensation

restores the original reactant. The two phenomena of conversion decrease (due to the reverse formation of CHD from the dimer) and increase (due to the slower oxidation of CHD) combine, giving a trend of conversion which in overall is constant. This hypothesis is supported by the fact that the yield to the CHD condensation compound decreased during time, as demonstrated by ESI-MS analysis of the reaction mixture.

Considering the conditions under which the reaction takes place and the products identified, probably the mechanism of the reaction was similar to that obtained using supported $\text{Ru}(\text{OH})_x$ as a catalyst. If this hypothesis is true, even in this case HCHN or CHDO should act as key intermediate compounds. In order to better understand the mechanism, some tests were performed using these two compounds as the starting reagents.

9.6.1.6. Reactivity of the CHDO and HCHN. Study of the reaction mechanism

The results of the reactivity experiments carried out starting from CHDO and HCHN in the presence of Au/TiO_2 , and without any catalyst as well, are presented in Table 36. Experiments were carried out at 90°C during 3 h, under oxygen flow. In the case of CHDO, we performed two reactions with different amounts of sodium hydroxide; in the reactions with Au nanoparticles supported on titanium oxide the molar ratio between Au and reagent was 1:1000.

Table 36. Reactivity of the CHDO and HCHN in the presence of Au-based catalyst. $T=90^\circ\text{C}$, Au:reagent=1:1000, 3 hours, oxygen flow

Reagent	pH	Catalyst Au/TiO_2	X, %	Y(HCPA), %	Y(AA), %	Y(GA), %	Y(SA), %	S(AA), %
CHDO	12.5	+	99	0	14	36	5	14
CHDO	6.3	+	64	0	9	47	1	15
CHDO	13.4	-	100	38	0	28	0	0
HCHN	12.5	+	99	0	73	7	3	74
HCHN	12.5	-	100	0	71	6	3	71
HCHN	10	-	100	0	4	3	0	4
HCHN	13.4	-	100	52	20	15	11	20

We did not observe the formation of HCPA, because the latter forms from CHDO only under strongly basic conditions. In the reaction with HCHN we noticed the formation of a small amount of CHDO, with yield however not higher than 1%.

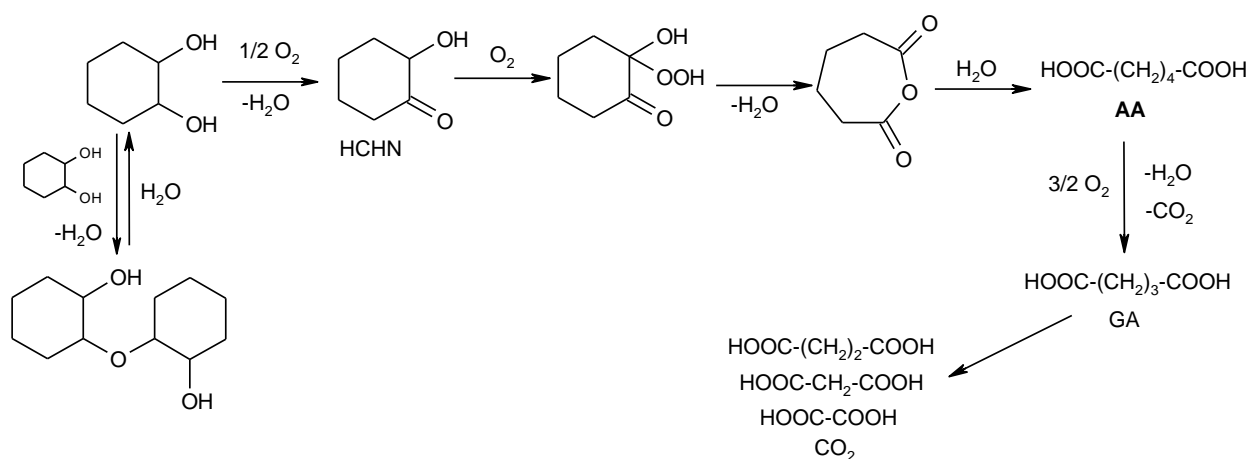
From the obtained data, we can draw the following conclusions:

- the Au-based catalyst promotes AA formation from CHDO (compared to the reaction without catalyst), but the yield is low;
- GA is the prevailing product in the oxidation of CHDO;

- the formation of AA is highly selective when HCHN is used as the reagent; however, this reaction does not require the presence of the catalyst to occur;
- high selectivity of AA starting from HCHN is guaranteed only in the presence of a basic environment, but strongly basic pH are not necessary.

Putting together all the data we can conclude that the key intermediate compound in CHD oxidation in the presence of Au/TiO₂ catalyst is 2-hydroxycyclohexanone; the latter allows to get high yield to AA. The data obtained point out that CHDO is a reaction intermediate which gives rise to several side reactions and only minimally contributes to AA formation. Using Au/TiO₂ as the catalyst allowed to perform the reaction at less basic pH, compared to the Ru-based catalyst, and thereby to avoid or limit the formation of CHDO.

Proposed reaction mechanism for the aerobic oxidation of CHD catalyzed by Au nanoparticles supported on titanium oxide is shown in Scheme 32.



Scheme 32. The overall reaction scheme of the aerobic oxidation of 1,2-cyclohexanediol in the presence of Au/TiO₂

9.6.2. Au/MgO and Au/Mg(OH)₂

Investigation of the reaction in the presence of Au/TiO₂ catalyst has shown the need for a controlled basicity of the reaction environment, in order to activate the hydroxyl group of CHD and avoid side-reactions. Therefore, it was decided to support the nanoparticles of Au on magnesia hydroxide and magnesia, which hold a certain basicity (pKa = 10.3).

As in the case of the Au/TiO₂ catalyst, first we carried out some experiments to check the effect of some parameters on AA selectivity (S).

The experiments were conducted by changing one of the following parameters:

- Molar ratio between NaOH and CHD at a constant temperature of 90°C;
- Molar ratio between Au and CHD at a constant temperature of 90°C.

The main reaction products were AA, GA, and SA; we also detected small amounts of 2-hydroxycyclohexanone and 1,2-cyclohexanedione.

9.6.2.1. Effect of the NaOH:CHD ratio

First, we performed the experiments by varying the NaOH:CHD molar ratio in order to understand if the presence of the sodium hydroxide was anyway necessary even with the basic support, and to determine the best value of pH for the reaction mixture (Table 37). Other reaction conditions were: catalyst Au/Mg(OH)₂, molar ratio Au:CHD=1:1000, T=90°C, 3 h reaction time, oxygen flow 300 mL/min.

Table 37. Effect of the amount of NaOH and CHD (purity 98%) used for experiments and of NaOH:CHD molar ratio

m(NaOH), g	m(CHD), g	NaOH:CHD, mol/mol
0	1	0:1
0.17	1	1:2
0.34	1	1:1
0,8	1	2:1

Results of the experiments (yields to the main products and CHD conversion) are given in Table 38. Figure 48 shows a comparison of CHD conversions and AA yields and selectivity.

Table 38. Results of the experiments with different ratio NaOH:CHD

NaOH:CHD, mol/mol	X(CHD), %	Y(AA), %	Y(GA), %	Y(SA), %	S(AA), %
0:1	13	1	1	1	8
1:2	18	9	0.4	0.6	50
1:1	18	9	1	1	50
2:1	16	7	2	1	44

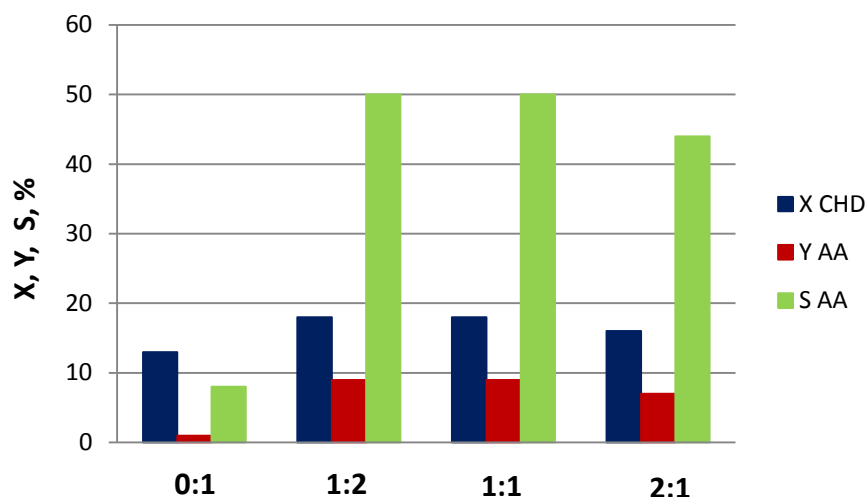


Figure 48. Results of the experiments with different ratio NaOH:CHD

HCHN and CHDO also formed in small quantities (yields <0.1%), except in the case of the reaction carried out without NaOH (HCHN yield 3 %).

By comparing the results, it can be seen that the basicity of the support did not seem to be sufficient to activate CHD. However, when NaOH was added the yield of AA significantly increased. It can then be concluded that even for Au/MgO catalysts the addition of a base is required in order to activate the reagent. The conversion of CHD was not strongly affected by the NaOH/CHD ratio, similar AA selectivity was obtained with NaOH:CHD 1:2 and 1:1 ratios.

Therefore, we chose the ratio of 1:1 in order to compare the data obtained with the Au/TiO₂ catalyst, which showed the highest AA selectivity (50%) using this ratio.

9.6.2.2. Effect of the Au:CHD ratio

Then we determined the optimal ratio between Au and CHD by changing the amount of loaded catalyst (Table 39). Other reaction conditions were: catalyst Au/Mg(OH)₂, molar ratio NaOH:CHD=1:1, T=90°C, 3 hours of reaction time, oxygen flow 300 mL/min.

Table 39. The amount of catalyst and CHD (purity 98%) used for the experiments and the molar ratio Au:CHD

m(Au/MgO), g	m(CHD), g	Au:CHD, mol/mol
1.1	1	1:100
0.11	1	1:1000

Results of the experiments (yields to the main products and CHD conversion) are given in Table 40. Figure 49 shows the comparison of CHD conversions and AA yields and selectivity.

Table 40. Results of the experiments with different ratio Au:CHD

Au:CHD, mol/mol	X(CHD), %	Y(AA), %	Y(GA), %	Y(SA), %	S(AA), %
1:100	28	20	2	2	71
1:1000	18	9	1	1	50

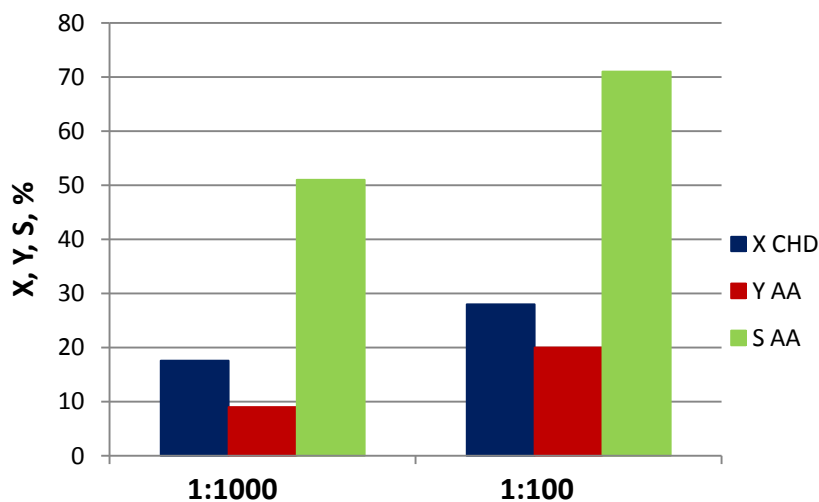


Figure 49. Results of the experiments with different ratio Au:CHD

The yields to HCHN and CHDO were around 0.1%.

It can be noted that the increase of molar ratio led to an effective increase in AA production, both in terms of yield and selectivity. However, the improvement was not so high to justify this molar ratio, which involves the use of more than 1 g of catalyst for each test.

For further experiments we used the ratio between Au and CHD equal to 1:1000.

9.6.2.3. Stability of the catalyst under reaction conditions

Next step was to check the stability of the catalyst under reaction conditions. we carried out two types of experiments:

- leaching experiments: to check if the leaching of Au into the reaction mixture had occurred;
- recyclability experiments: to check if the catalyst maintained its initial activity or underwent deactivation during reaction.

9.6.2.3.1. Leaching experiments

For the leaching experiments this procedure was used: first, the reaction was carried out during 3 h, then the catalyst was filtered off, the mixture was loaded back into the reactor and the reaction was continued for 3 h more in the absence of catalyst. Results for Au/MgO and Au/Mg(OH)₂ catalysts are shown in Figures 50 and 51, respectively.

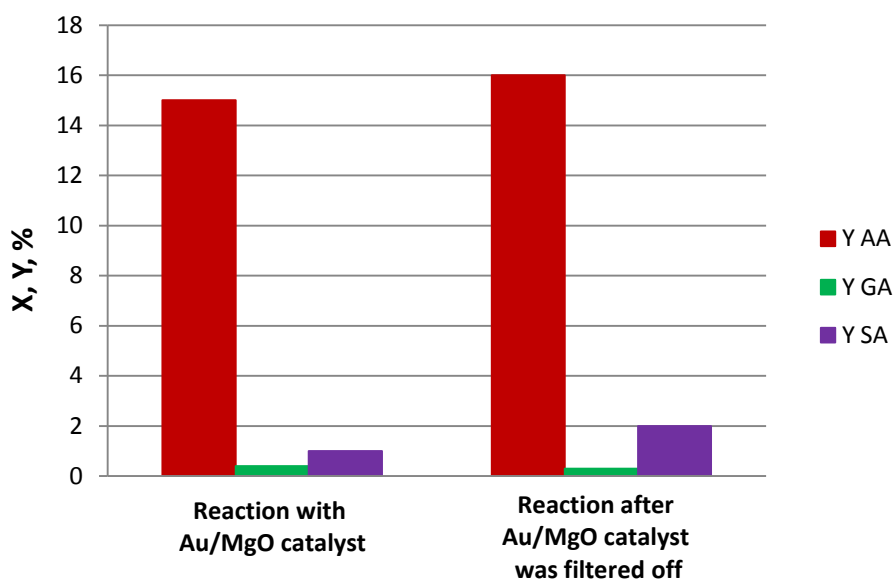


Figure 50. Results of the leaching experiments with Au/MgO

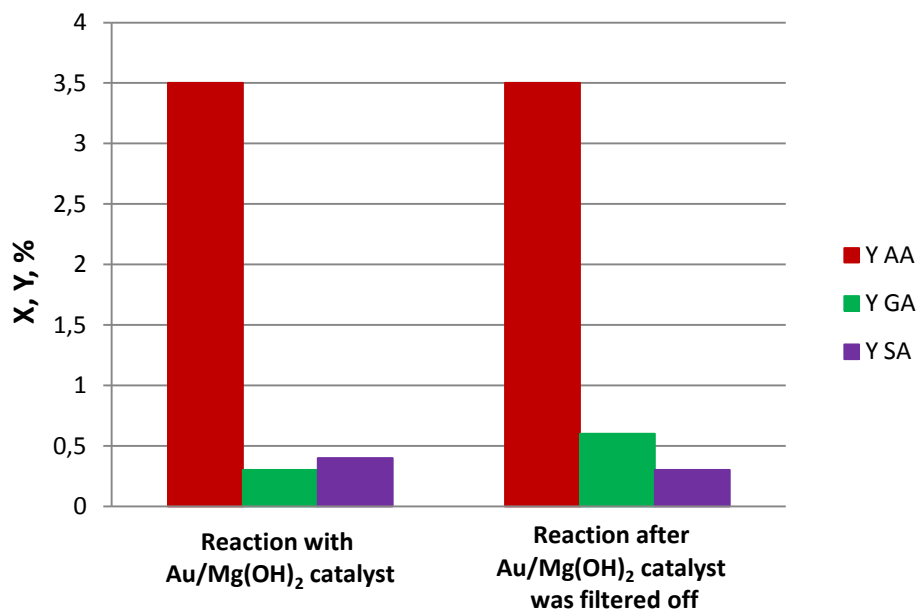


Figure 51. Results of the leaching experiments with Au/Mg(OH)₂

It is shown that the yield of products did not change; the amount of CHD was the same in both mixtures. This data indicate that the Au/MgO and Au/Mg(OH)₂ catalysts did not undergo any leaching phenomena.

9.6.2.3.2. Recyclability experiments

Recyclability experiments were performed following this procedure: first, the 3h reaction was carried out, then the catalyst was filtered off, washed with water and reloaded with fresh reagents for 3 h more. The procedure was repeated two times. The results are shown in Figure 52.

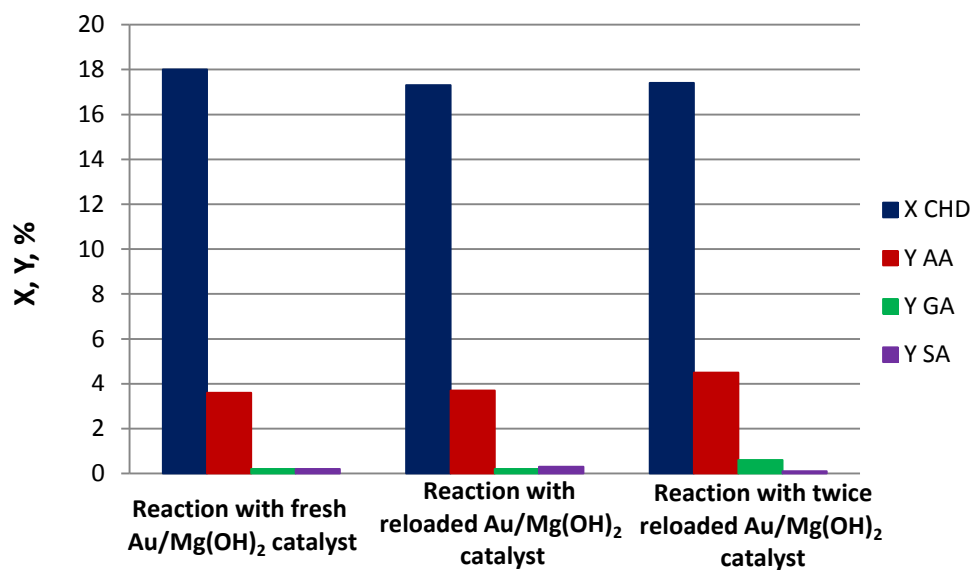


Figure 52. Results of the recyclability experiments for Au/Mg(OH)₂

A small decrease of CHD conversion was measured after the first use, but it was within the error of measurement. The amount of AA increased after the second use. Therefore we can conclude that the catalyst did not undergo significant deactivation.

9.6.2.4. Activity of the catalyst as a function of reaction time

We carried out the experiments in function of time. We calculated CHD conversion, yields to the main products and AA selectivity. Reaction products were AA, GA, and SA; we also detected small amounts of 2-hydroxycyclohexanone (HCHN) and 1,2-cyclohexanedione (CHDO) (yields were <1% in all cases). Table 41 and Figure 53 report the results obtained for Au/MgO, Table 42 and Figure 54 report the results obtained for Au/Mg(OH)₂.

Table 41. Results of the reactivity experiments. Catalyst Au/MgO, T=90°C, Au:CHD=1:1000, NaOH:CHD=1:1, oxygen flow

Time of reaction, h	X(CHD), %	Y(AA), %	Y(GA), %	Y(SA), %	S(AA), %
0	0	0	0	0	0
0.5	18	2	0.2	0	11
1	19	6	0.5	0.3	31
3	22	15	1.5	1	68
5	29	21	3	2	72

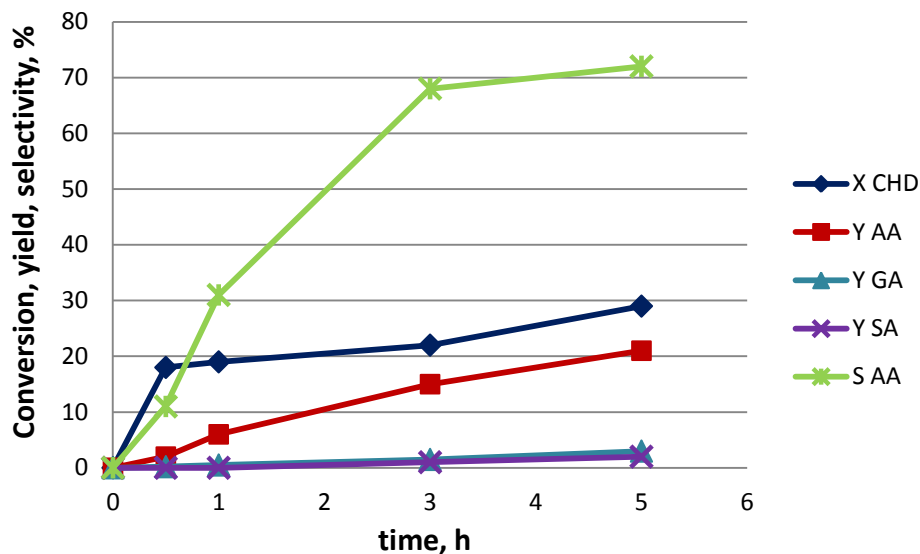


Figure 53. Results of the reactivity experiments. Catalyst Au/MgO, T=90°C, Au:CHD=1:1000, NaOH:CHD=1:1, oxygen flow

Table 42. Results of the reactivity experiments. Catalyst Au/Mg(OH)₂, T=90°C, Au:CHD=1:1000, NaOH:CHD=1:1, oxygen flow

Time of reaction, h	X(CHD), %	Y(AA), %	Y(GA), %	Y(SA), %	S(AA), %
0	12	0	0	0	0
0.5	18	0.3	0	0	2
1	19	1	0	0	5
3	18	4	0.3	0.3	22
5	16	6	1	0.5	38
7	18	9	1	1	50

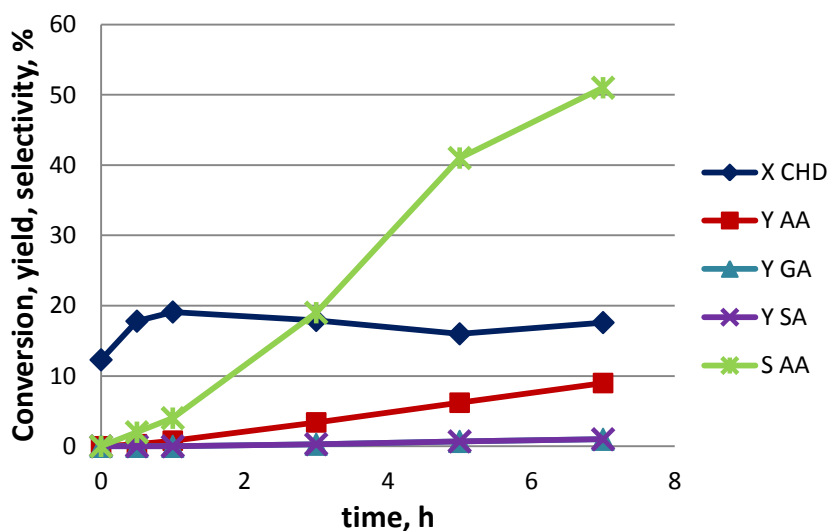


Figure 54. Results of the reactivity experiments. Catalyst Au/Mg(OH)₂, T=90°C, Au:CHD=1:1000, NaOH:CHD=1:1, oxygen flow

The behavior was not much different from that shown by Au/TiO₂; in fact, CHD conversion first increased rapidly, then more slowly and then finally increased again, which can be attributed to the overlapping of the two reactions contributing to CHD conversion. Au/MgO catalyst was more active and more selective to AA than Au/Mg(OH)₂. Selectivity to AA in the presence of Au/MgO catalyst was 70%, whereas for Au/Mg(OH)₂ it was 40% after 5 h reaction time.

9.7. Polyoxometalates

Next catalysts that we used for the oxidation of CHD with oxygen were polyoxometalates, in particular Keggin-type P/Mo/V heteropolyacids.

Polyoxometalates (POMs) are polyatomic ions with general formula $[M_mO_y]^{p-}$. The ion consists of oxygen and transition metals, usually of group 5 and 6 at their highest oxidation states. Also POMs can contain different heteroatoms such as P, Si, V, and in this case they belong to the heteropolyanions with the general formula of $[X_xM_mO_y]^{q-}$ ($x \leq m$).

The most known structural form for heteropolyacids is the Keggin structure. It has the general formula $[XM_{12}O_{40}]^{n-}$, where M is the addenda atom (usually Mo or W) and X is the heteroatom, such as P^{5+} , or B^{3+} . The structure is made of a heteroatom bounded to four oxygen forming a tetrahedron, surrounded by 12 octahedral MO_6 -units. Tetrahedron is linked to each octahedron through the oxygen atoms, and each octahedron is linked to four adjacent octahedra via an edge and corners forming a bridge -M-O-M- [168].

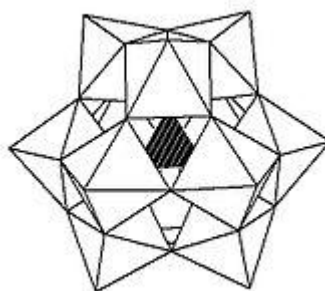


Figure 55. The structure of heteropolyacid with Keggin structure

In P/Mo/V heteropolyacids, those that we studied, one or two atoms of Mo were replaced by V atoms and had the formula $H_5PMo_{10}V_2O_{40}$ and $H_4PMo_{11}VO_{40}$ (POMV2 and POMV1 respectively).

The mixed Mo-V Keggin-type catalytic systems have interesting applications as oxidation catalysts in reactions carried out with air or molecular oxygen. In fact, their redox potential is such that they can establish catalytic cycles where the mixed Mo-V POM first is reduced while oxidizing the substrate, and then is re-oxidized by oxygen. These cycles are not possible with the vanadate or metavanadate individually, because once reduced they can no longer be re-oxidized by oxygen.

In addition, the Keggin-type POMs, if prepared properly, can also function as strong acid systems, and in this way the resulting catalyst presents dual functionality: redox and acid. However, a big practical disadvantage of this class of compounds is that POMs are generally soluble in most solvents and the separation from the reaction mixture is very difficult.

The catalytic activity of POM-V in oxidation reactions and oxidative cleavage is already known and this type of catalyst is amongst the most active ones [169, 170, 171].

For instance, Brégeault et al performed the oxidative cleavage of CHD using a P/Mo/V heteropolyacid catalyst in ethanol at 75°C, and obtained 90% selectivity to the diethyl ester of AA with 62% CHD conversion[172].

9.8. Experimental part

9.8.1. Synthesis of the catalyst

The Keggin-type heteropolyacids were synthesized following a procedure described by Matveev and co-workers [173].

First, we prepared a solution by dissolving V_2O_5 in 5% solution of HP at 4°C during 1 hour. Despite the fact that total dissolution of vanadium oxide was achieved within this time, we left the mixture in the ice bath overnight. The second solution was prepared by dissolving MoO_3 and 85% solution of phosphoric acid in excess of water at a temperature around 100°C (but avoiding boiling). Dissolution of the MoO_3 took about 15h.

The solution of Mo was heated to 90°C , and then the first solution was added dropwise to the second one. Resulted mixture was then stirred for 8h at 90°C to evaporate most of the solvent. Finally, the solution was left at 80°C for a night in order to evaporate the rest of the solvent. The obtained wet solid was then dried in the oven, at 110°C for 4 hours. The dried solid showed an orange color.

9.8.2. Characterization of the catalyst

The obtained solid was characterized by means of FT-IR spectroscopy in order to prove the formation of the Keggin structure.

9.8.2.1. FT-IR spectroscopy

Spectrophotometer FT-IR PerKin–Elmer was used for the characterization of the samples. The instrument was equipped with ATR sampling for the registration of the spectrum in attenuated total reflectance.

The IR spectrum of POMV2 is shown in Figure 56.

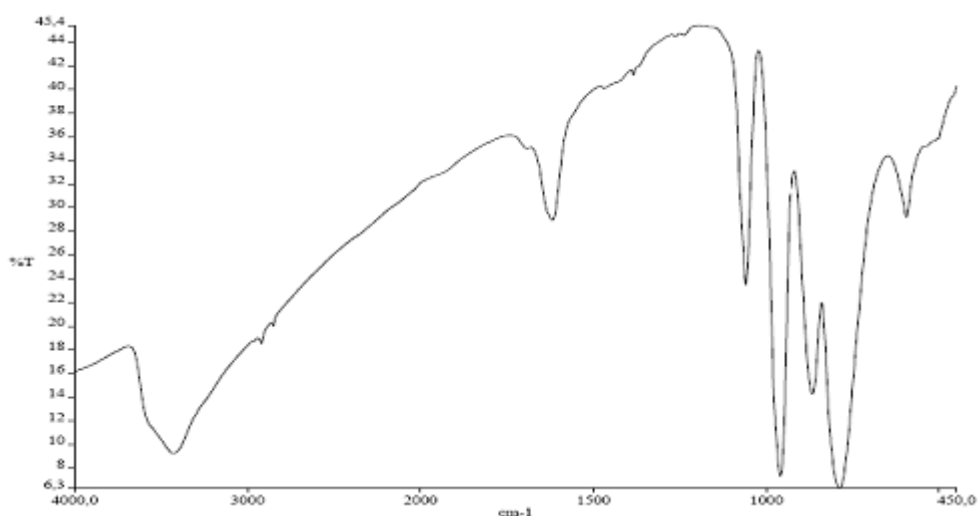


Figure 56. The FT-IR spectrum of POMV2

According to the literature, the Keggin-type structure is characterized by some typical vibration bands, that were also present in our samples [174, 175, 176].

Table 43. Assignment of IR bands to the main vibrational modes of the POM-V2

Wavenumber of the IR band, cm^{-1}	Bonding and vibrational mode
1619; 596	Stretching P=O
1058	Asymmetric stretching P-O
957	Asymmetric stretching Mo=O
869; 787	Asymmetric stretching Mo-O-Mo
3500-3000	Crystallized H_2O

Between 1100 and 700 cm^{-1} we can note two shoulders (Figure 57):

- at 957 cm^{-1} due to vibration of VO bond;
- at 1050 cm^{-1} due to a partial shift and widening of the band of PO, due to the interaction of this group with the atoms of vanadium.

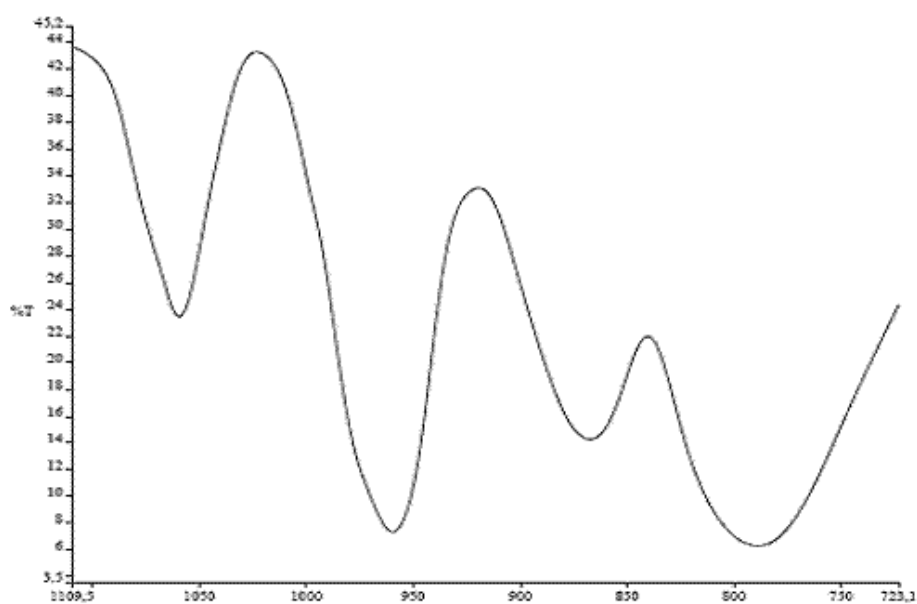


Figure 57. Magnification of the IR spectrum which ranges from 1100 to 700 cm^{-1}

In conclusion, the spectrum shows the presence of the bands typical for the Keggin-type structures based on Mo. The presence of V embedded in the structure is confirmed by the presence of some shoulders in the IR spectrum and by the intense orange color of the solid obtained, typical of these compounds.

The same characterization was done for the POMV1 catalyst. The analysis of obtained data showed that POMV1 also had a Keggin-type structure.

9.8.3. Catalytic measurements

The experiments to measure the catalytic activity of POMs were performed in the same reactor and with the same procedure already used for both Ru- and Au-based catalysts. The description of the procedures used are described in chapter 9.2.3.

Main differences in the use of POMs, compared to the Ru- and Au- based catalyst were:

- POMs were completely soluble in the reaction mixture;
- NaOH was not added; the reaction medium had acid pH because of the POMs, which are stable compounds only under strongly acid conditions.

9.8.4. Treatment of the reaction mixture

After the sample had been picked up from the reaction mixture, it was necessary to separate the catalyst. Since the POMs are soluble, the separation was performed by adding of a concentrated solution of CsCl to the reaction mixture, with the consequent formation of a precipitate, consisting of the insoluble cesium salt $\text{Cs}_5\text{PMo}_{10}\text{V}_2\text{O}_{40}$ or $\text{Cs}_4\text{PMo}_{11}\text{VO}_{40}$. After precipitation, the separation of the solid was done by centrifugation. The obtained mixture could be directly used for the analysis by means of HPLC. For the analysis by means of ESI-MS, the mixture was diluted with methanol.

To carry out the analysis of the reaction mixture by means of GC-MS, we first carried out the esterification of the dicarboxylic acids, using the following procedure:

- 1) 5 mL of the reaction mixture were pulled in a dry 50 mL flask and put in a rotavapor in order to evaporate the solvent;
- 2) a solution of 14% BF_3 in methanol was added to the flask (reagent for the formation of methyl esters);
- 3) the closed flask was heated at 70°C for 1h;
- 4) The obtained mixture was extracted 5 times with 5 mL of *n*-hexane;
- 5) 10 μL of decane was added as an internal standard to 25 ml of the extract.

9.8.5. Analysis of the reaction mixture

The quantitative analysis of the components of the reaction mixture was performed by means of HPLC and GC-MS, while the qualitative analysis was carried out also by means of ESI-MS spectroscopy.

Description of HPLC and ESI-MS techniques is given in chapter 6.4.

9.8.5.1. GC-MS

The instrument used is a Gas chromatograph Agilent Technologies 6890N coupled to a mass spectrometer Agilent Technologies 5973 Inert system with ionization filament EI (electron impact) and quadrupole mass analyzer-photomultiplier.

The capillary column was a Agilent HPS model, consisting of 5% phenyl-95% dimethyl polysiloxane, length 30 m and diameter of 1.025 mm.

The injector was a splitless, maintained at a temperature of 250°C, while the separation took place under temperature gradient according to the following program: 2 minutes at 50°C, then ramp 10°C/min up to 250°C.

The mobile phase was an Ar flow, with rate of 1.0mL/min; the injection is performed by introducing 5µL of solution with a syringe.

9.9. Results and discussion

First we conducted experiments in order to determine the activity of the POMs catalysts.

Typical conditions were:

- 2.4 g of CHD;
- 0,7 g of catalyst;
- 30 ml of distilled water;
- 90°C;
- oxygen flow 300 mL/min.

9.9.1. Activity of the POMs catalysts

Two reactions were conducted with duration of 3 and 6 hours in the presence of POMV2 catalyst, and were analyzed by means of HPLC. We obtained a CHD conversion of 48 and 36%, respectively; however, we did not detect the formation of any product. In order to understand this incongruence, the ESI-MS analysis of the reaction mixtures was done. We found peaks with molecular weights that correspond to the esters formed by the condensation of AA and CHD. Esters are shown in Figure 58.

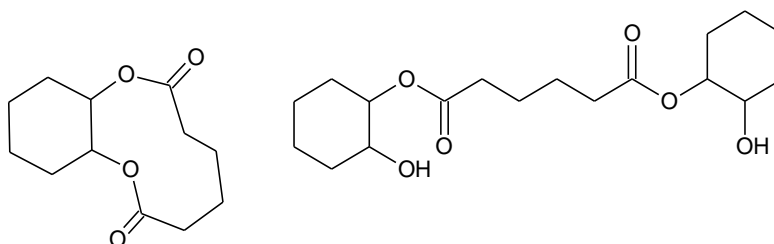


Figure 58. Esters of AA and CHD

These data indicate that AA indeed formed; however, in acid medium it fast reacted with unconverted CHD yielding the esters. The same problem was also detected in the case of the POMV1 catalyst.

In order to calculate the amount of the reaction products, we carried out a transesterification of the reaction mixture with a large excess of methanol (method of this procedure is described in chapter 9.8.5.1). The resulting mixture was then analyzed by means of GC-MS and the yield of methyl esters of dicarboxylic acids were calculated.

The results of the experiments with POMV1 And POMV2 are shown in Table 44. Reactions were carried out at 90°C, during 6 h, with oxygen flow, using water as the solvent. The conversion of CHD was calculated by means of HPLC whereas the yields to the dimethyl esters of acids by means of GC-MS.

Table 44. Experiments with POMV1 and POMV2

Catalyst	t, h	T, °C	X (CHD), %	Yield to AA, GA & SA dimethyl esters, %
POMV1	6	90	36	12, traces, traces
POMV2	6	90	37	9.5, 0.4, 0.1

We did not detect the formation of any of by-products that had formed in the reaction under basic conditions (with Ru-based catalyst, for example). However, CHD conversion was higher than the total yield of dimethyl esters. This can be explained by taking into account the formation of the esters between acids and unconverted CHD: for each mole of dicarboxylic acid we need one mole of CHD and one or even two moles of CHD is necessary to form the corresponding esters. To confirm this hypothesis we carried out an experiment with AA and CHD as reagents without the catalyst, in the absence of oxygen and in acid medium. We measured a AA conversion of 11% and a CHD conversion of 14%; moreover, by ESI-MS we detected the formation of the esterification products. We also detected the formation of CHD self-condensation compounds, which amount decreased with increasing the reaction time.

In the presence of the POMV2 catalyst, selectivity to AA was lower and the formation of the lighter dicarboxylic acids was greater.

As a conclusion we can say that POM catalysts were high selective to AA from CHD due to the absence of the side-reactions that take place under basic conditions; moreover, also the formation of lighter compounds was low.

Unfortunately, the use of POMs catalysts leads to some problems. One drawback is related to the reaction of AA with unconverted CHD giving the corresponding esters; in order to obtain pure AA it is necessary to perform the hydrolysis of the esters. Another problem is the solubility of POMs in the reaction medium; the only way to separate the catalyst is by means of the formation of an insoluble salts the of POMs, which can then be filtered off. The precipitation was carried out adding large amounts of CsCl. We checked the activity of the formed salt in the same reaction, but the POM Cs-salt was much less active than the initial acid POM.

After the reactivity experiments, we performed some tests to understand the mechanism of CHD oxidation in the presence of POMs.

9.9.2. Reactivity of the CHDO and HCHN. Study of the reaction mechanism

When we used CHDO as the reagent, complete conversion was achieved after 1 h of reaction. However, no AA formed, the only products were GA, SA and other degradation compounds. Worthy of note, that starting from CHD we did not detect the formation of these compounds in a big amount. This fact indicates that CHDO is not an intermediate product of the reaction.

To detect possible reaction intermediates we performed the reaction starting from CHD, with POMV2 catalyst, but in the absence of oxygen. The color of the catalyst in the end of the reaction was black, whereas initially it was orange; this means that the POM was reduced during the reaction and since there was no oxygen fed, it could not be re-oxidized. We observed the formation of 2-hydroxycyclohexanone (HCHN), which was produced by oxidative dehydrogenation of CHD, and was not further oxidized to CHDO, but transformed into AA.

In order to prove that HCHN is the intermediate product for AA formation, we carried out the experiments using HCHN as the starting reactant. Reaction conditions were: catalyst POMV2, 90°C, oxygen flow.

Table 45. Results of the experiment with HCHN as the starting compound

t, h	X (HCHN), %	Y (AA), %	Y (GA), %	Y (SA), %	Other products (detected by ESI-MS)
0	32	0	0	0	6-hydroxycaprolactone, condensation compounds
0.08 (5min)	46	0	5	0	adipic anhydride, 6-hydroxycaprolactone, condensation compounds, light dicarboxylic acids
0.17 (10 min)	47	0	10	traces	adipic anhydride, 6-hydroxycaprolactone, condensation compounds, light dicarboxylic acids
0.33 (20min)	63	24	12	traces	6-hydroxycaprolactone, light dicarboxylic acids
0.5	79	32	9	traces	6-hydroxycaprolactone, light dicarboxylic acids
1	96	34	4	8	light dicarboxylic acids
2	99.8	34	4	9	light dicarboxylic acids
3	100	32	2	11	light dicarboxylic acids

2-Hydroxycyclohexanone was very reactive, more than CHD, in fact after 1 h of reaction its conversion was greater than 90%. However, AA started to form only after 20 minutes of reaction, and reached the maximum of 34% after 2 hours. GA formed already after 5 minutes of reaction, before the formation of AA, which means that the mechanism of GA formation was different from that leading to AA. SA and other light dicarboxylic acids formed by consecutive degradation of AA and GA.

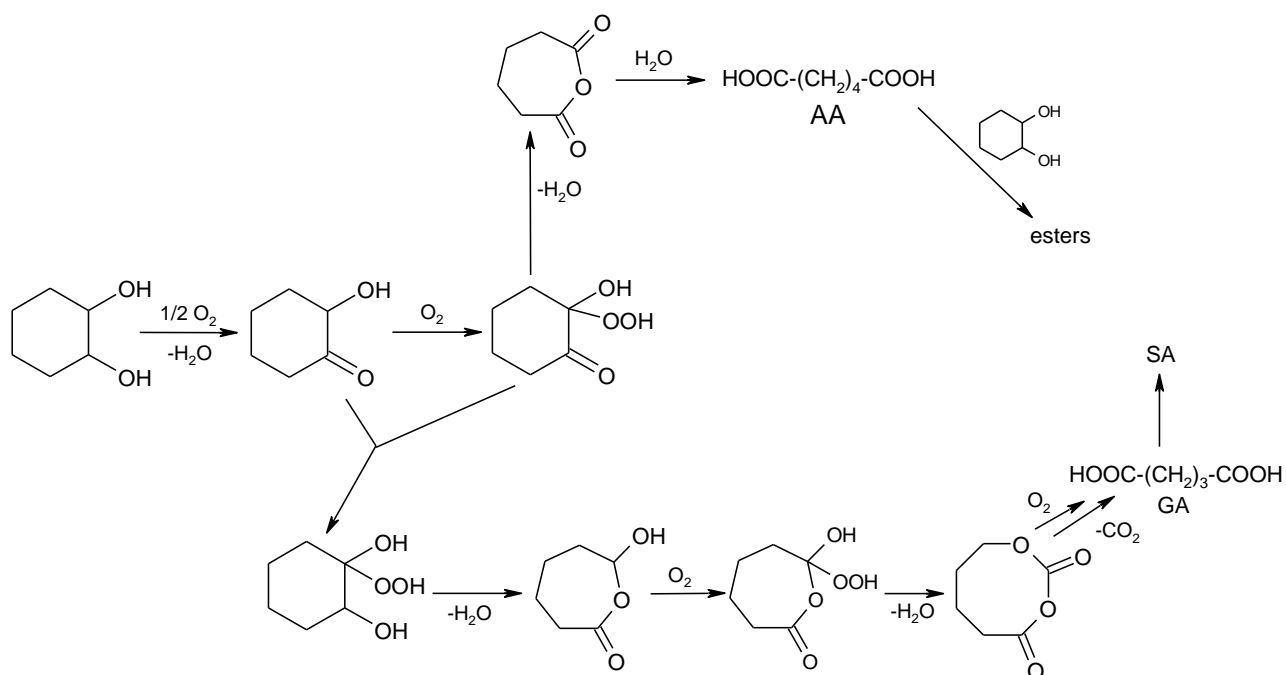
By means of ESI-MS technique we determined the formation of other products, such as 6-hydroxycaprolactone, adipic anhydride and condensation compounds of HCHN. Adipic anhydride was detected only during the first 20 minutes of reaction and then it disappeared forming AA by hydrolysis. The reaction starting from HCHN under acid conditions (but without the POM) was slower than that one with POMV2; after 3h the conversion of HCHN was only 15%.

As it was shown in the previous chapter, in the reaction starting from CHD its conversion was lower than that of HCHN, while the selectivity to AA was higher.

Putting together the results we can conclude that:

- the oxidative dehydrogenation of CHD to 2-hydroxycyclohexanone was slower than the further transformation of the latter;
- in the oxidation of HCHN, GA formed before AA; therefore the oxidation of HCHN occurs along two pathways leading to different products;
- The formation of AA showed an induction period due to the slow hydrolysis of adipic anhydride;
- SA formed by oxidative degradation from both AA and GA.

The proposed mechanism of CHD oxidation under acid conditions using Keggin-type heteropolycompounds as homogeneous catalysts, is shown in Scheme 33.



Scheme 33. Mechanism of CHD oxidation under acid conditions using Keggin-type heteropolycompounds as the catalyst

Conclusions

The aim of my PhD work was to investigate new catalytic processes, more sustainable compared to the traditional ones, for the production of adipic acid. Two processes have been studied, in which various substrates (cyclohexene, 1,2-cyclohexanediol, cyclohexanone) were used with different oxidants (hydrogen peroxide and molecular oxygen) in the presence of homogeneous (tungstic acid, Keggin-type polyoxometalates) or heterogeneous ($\text{Ru}(\text{OH})_x$ supported on alumina, Au-nanoparticles supported on titanium oxide or magnesium oxide, etc.) catalytic systems.

It was shown that in the two-step process of cyclohexene oxidation into adipic acid via trans-1,2-cyclohexanediol it is possible to achieve very high selectivity to the glycol. We could achieve 97.2% yield with complete conversion of the substrate using a stoichiometric amount of hydrogen peroxide in presence of a phase transfer catalyst; no organic solvent was used. Regarding the second step of this process, the oxidation of the 1,2-cyclohexanediol with oxygen into adipic acid, we investigated different catalysts, both homogeneous and heterogeneous. The use of $\text{Ru}(\text{OH})_x$ -based catalyst for this reaction was quite problematic because under strongly basic conditions, at which the catalyst is active, the reaction is poorly selective, due to the simultaneous coordination of both C-OH groups of the reactant by Ru species and the direct formation of 1,2-cyclohexanedione as the key intermediate. The latter transforms to by-products which are not precursors for AA formation. Au-based catalysts are more selective to produce AA because the oxidation of 1,2-cyclohexanediol yields 2-hydroxycyclohexanone, which is oxidized into adipic acid even in the absence of the catalyst with good selectivity. Keggin-type POMs were quite selective to adipic acid, but the main drawback of this type of catalyst is related to its recovery.

We studied also the Baeyer-Villiger oxidation of cyclohexanone with aqueous solution of hydrogen peroxide, at 50°C, as the first step on the way to produce adipic acid, using several heterogeneous catalysts with different structures and compositions and also simply by means of thermal activation, that is in the absence of any catalyst. The Lewis acid properties of the catalysts affected the distribution of products, addressing the reaction pathway to the formation of either 1-hydroperoxycyclohexan-1-ol (the Criegee compound), as an intermediate product on the way to ϵ -caprolactone, or 1-[(1-hydroperoxycyclohexyl)hydroperoxy]cyclohexanol. We also found that cyclohexanone reacts very rapidly with hydrogen peroxide to yield a dioxirane compound, never reported before in the literature. The reactant and the dioxirane rapidly equilibrate, and the latter is likely the precursor for the formation of a bis-hydroperoxide compound.

References

- 1 ULLMANN'S Encyclopedia of Industrial Chemistry, Wiley-VCH, 2nd edition (2002)
- 2 F. Cavani, G. Centi, S. Perathoner, F. Trifirò, Sustainable Industrial Processes, Wiley-VCH, 1st edition (2009)
- 3 A. Castellan, J.C.J. Bart et al., Catal. Today 9 (1991) 237
- 4 U. Schuchardt, D. Cardoso et al., Appl. Catalysis A 211 (2000) 1
- 5 I. Belkhir, A. Germain, F. Fajula, E. Fache, J. Chem. Soc., Faraday Trans. 94 (1998) 1761
- 6 R.A. Sheldon, J.K. Kochi, Adv. Catalysis 25 (1976) 272
- 7 A. Castellan, J.C.J. Bart et al., Catal. Today 9 (199) 255
- 8 W. J van Asselt, D. W. van Krevelen, Rec. Trav. Chim. des Pays-Bas, 82 (1963) 429
- 9 W. J van Asselt, D. W. van Krevelen, Chem. Eng. Science 18 (1963) 471
- 10 S.E. Manahan, Chimica dell'ambiente, Piccin
- 11 C.M. Fu, V.N. Korchak, V.K. Hall, J. Catal 68 (1981) 166
- 12 A. Shimizu, K. Tanaka et al., Chemosphere – Global Change Science 2 (2000) 425
- 13 S. Alini, E. Frigo et al., Eur Patent 2002, 1,413,349 (Assigned to Radici Chimica SpA)
- 14 S. Alini, E. Frigo et al., Eur Patent 2003, 1,488,845 (Assigned to Radici Chimica SpA)
- 15 W.D. McGhee, US Patent 1998, 5,808,167 (assigned to Solutia)
- 16 J. Teles et al., WO Patent Appl 2005/030689 (assigned to BASF)
- 17 N. Mizuno, N. Nozaki, et al., J. Mol. Catalysis A 117 (1997) 159
- 18 T. Hayashi, A. Kishida et al., Chem. Communications 5 (2000) 381
- 19 S.I. Murahashi, N. Komyia et al., Pure and Appl. Chemistry 73 (2001) 311
- 20 G.B. Shul'pin, E.R. Lachter, J. Mol. Catalysis A 197 (2003)
- 21 G. Lu, D. Ji, G. Qian, Y. Qi, X. Wang, J. Suo, Appl. Catal. A, 280 (2005) 175
- 22 G. Lu, R.Zhao, G. Qian, Y. Qi, X. Wang, J. Suo, Cat. Letters, 97 (2004) 115
- 23 L.X. Xu, C.H. He, M.Q. Zhu, S. Fang, Catal. Lett, 114 (2007) 202
- 24 R. Raja, P. Ratnasamy, Catal. Lett., 48 (1997) 1
- 25 E.L. Pires, J.C. Magalhaes, U. Schuchard, Appl. Catal., 203 (2000) 231
- 26 C.S. Yao, H.S. Weng, Ind. Eng. Chem. Res., 37 (1998) 2647
- 27 P. Selvam, S.K. Mohapatra, Microporous Mesoporous Mater., 73 (2004) 137
- 28 A. Sakthivel, P. Selvam, J. Catal., 211 (2002) 134
- 29 S. Samanta, N.K. Mal, A. Bhaumik, J. Mol. Catalysis A 236 (2005) 7
- 30 S.K. Mohapatra, F. Hussain, P. Selvam, Catal. Lett., 85 (2003) 217
- 31 A. Shimizu, K. Tanaka et al., Bull. Chem. Soc. Jpn. 76 (1993) 2001
- 32 A. Atlamsani, J.M. Bregeault et al., J. Org. Chem. 58 (1993) 5663
- 33 J.M. Bregeault, B. El Ali et al., Patents FR 88-11075; EP0355075 B1; US 4 983 767; CA 1 322 762; JP 1 8932-55, 1988
- 34 Y. Ishii, A. Adachi, R. Imai, M. Ogawa, Chem. Lett. (1978) 611
- 35 Y. Usui, K. Sato, Green Chemistry 5 (2003) 373
- 36 K. Tanaka, Shokubai 17 (1975) 197
- 37 K. Tanaka, CHEMTECH (1974) 555

-
- 38 K. Tanaka, A. Shimizu, JP 20011253845 (assigned to Asahi Chem Co)
- 39 A. Onopchenko, J.G.D. Schulz, US Patent 1977, 4,032,569, (assigned to Gulf R&D)
- 40 J.G.D. Schulz, A. Onopchenko, US Patent 1981, US 4,263,453 (assigned to Gulf R&D)
- 41 C.M. Park, N. Goroff, US Patent 1993, 5,221,800 (assigned to Amoco Corp)
- 42 Y. Ishii, *J. Mol. Catalysis A* 117 (1997) 123
- 43 Japan Chemical Week, 30 Aug 2007, 48 (2430) 1
- 44 M. Roper, *Stud. Surf. Sci. Catal.* 64 (1991) 381
- 45 http://www.chemweek.com/sections/business_finance/europe_mideast/6951.html
- 46 H. S. Bruner, Jr., S. L. Lane et al., US Patent 1998, 5,710,325 (assigned to Du Pont de Nemours, DSM N.V.)
- 47 P. Denis, C. Patois, R. Perron, US Patent 1997, 5,625,096 (assigned to Rhone-Poulenc Chimie)
- 48 E. Drent, W.W. Jager, US Patent 2004, 6,706,912 (assigned to Shell Oil Co)
- 49 J. C.L.J. Suykerbuyk, E. Drent, P.G. Pringle, US Patent 2000, 6156934 (assigned to Shell Oil Co)
- 50 G. Tavoularis, M.A. Keane, *J. Mol. Catalysis A* 142 (1999) 187
- 51 N. Mizuno, D. K. Lyon et al., *J. Catalysis* 128 (1991) 84
- 52 R. Neumann, M. Dahan, *J. Chem. Soc., Chem. Commun.* (1995) 171
- 53 U. R. Pillai, E. Sahle-Demessie et al., *Green Chem.* 4 (2002) 495
- 54 N. Mizuno, H. Weiner et al., *J. Mol. Catalysis* 114 (1996) 15
- 55 Y. Liu, K. Murata et al., *Chem. Lett.* 33 (2004) 200
- 56 Y. Kim, H. Kim et al., *J. Appl. Catalysis A* 155 (1997) 15
- 57 M.S. Melgo, A. Lindner, U. Schuchardt, *Appl. Catal. A* 273 (2004) 217
- 58 B. Notari, *Stud. Surf. Sci. Catal.* 37 (1988) 413
- 59 M.G. Clerici, *App. Catalysis* 68 (1991) 249
- 60 O.A. Kholdeeva, N.N. Trukhan, *Russ. Chem. Rev.* 75 (2006) 411
- 61 O.A. Kholdeeva, R.I. Maksimovskaya, *J. Mol. Catalysis A* 262 (2007) 7
- 62 R. Neumann, *Prog. Inorg. Chem.* 47 (1998) 317
- 63 C.L. Hill, C.M. Prosser-McCartha, *Coord. Chem. Rev.* 143 (1995) 407
- 64 M. Schröder, *Chem. Rev.* 80 (1980) 187
- 65 K.B. Sharpless, K. Akashi, *J. Am. Chem. Soc.* 98 (1976) 1986
- 66 V. VanRheenen, R.C. Kelly et al., *Tetrah. Lett.* (1976) 1973
- 67 H.C. Kolb, M.S. VanNieuwenhze et al., *Chem. Rev.* 94 (1994) 2483
- 68 W.A. Hermann, R.W. Fischer et al., *Angew. Chem. Int. Ed.* 30 (1991) 1638
- 69 V. Singh, P.T. Deota, *Synth. Commun.* 18 (1988) 617
- 70 C. Venturello, M. Gambaro, *Synthesis* (1989) 295
- 71 W. A. Herrmann, R.W. Fischer et al., *Angew. Chem. Int. Ed. Engl.* 300 (1991) 1638
- 72 T. Tatsumi, K.Yamamoto et al., *Chem. Letters* (1992) 815
- 73 A. Corma, M.A. Camblor et al., *J. Catalysis* 145 (1994) 151
- 74 T. Tatsumi, K.A. Noyano et al., *Chem. Commun.* (1998) 325

-
- 75 J. Xin, J. Suo et al., *New J. Chem.* 24 (2000) 569
- 76 M. Shimizu, H. Orita et al., *J. Mol. Catal. A* 114 (1996) 217
- 77 T. Iwahama, S. Sakaguchi et al, *Tetrahedron Lett.* 36 (1995) 1523
- 78 G.P. Schindler, P. Bartl et al., *Appl. Catalysis. A* 166 (1998) 267
- 79 K. Sato, M. Aokil, R. Noyori, *Science* 281 (1998) 1646
- 80 R. Noyori, M. Aoki et al., *Chem. Commun.* (2003) 1977
- 81 Y. Deng, Z. Ma et al., *Green Chemistry* (1999) 275
- 82 C.Y. Cheng, K.J. Link et al., *Catal. Comm.* 8 (2007) 1060
- 83 S.O. Lee, R. Raja et al., *Angew. Chem. Int. Ed.*, 42 (2003) 1520
- 84 G. Lapisardi, F. Chiker et al., *Catal. Communications* 5 (2004) 277
- 85 G. Lapisardi, F. Chiker et al, *Micr. Mes. Materials* 78 (2005) 289
- 86 M. Draths, J.W. Frost, *J. Am. Chem. Soc.* 116 (1994) 399
- 87 K.M. Draths, J.W. Frost, in "Green Chemistry: Frontiers in Benign Chemical Synthesis and Processes", P.T. Anastas and T.C. Williamson, Ed., Oxford University Press, Inc., New York, N.Y., (1998) 150
- 88 W. Niu, K.M. Draths, J.W. Frost, *Biotechnolog. Prog.* 18 (2002) 201
- 89 A. Baeyer, V. Villiger, *Ber. Dtsch. Chem. Ges.* 32 (1899) 3625
- 90 J.J. ten Brink et al., *Chem. Rev.* 104 (2004) 4105
- 91 G. Strukul *Angew. Chem. Int. Ed.*, 37 (1998) 1198
- 92 http://worldaccount.basf.com/wa/NAFTA/Catalog/ChemicalsNAFTA/doc4/BASF/PRD/30062055/pdf?title=&asset_type=pds/pdf&language=EN&urn=urn:documentum:eCommerce_sol_EU:09007bb280063b37.pdf
- 93 P. Zhang, M. Yang, et al., *Chem. Eng. Journal* 121 (2006) 59
- 94 J. Fischer, W. Hoelderich, *Appl. Catal. A* 180 (1999) 435
- 95 R.A. Steffen, S. Teixeira et al., *J. Mol. Catal. A* 287 (2008) 41
- 96 L. Balbinot, U. Schuchardt et al., *Catal. Commun.* 9 (2008) 1878
- 97 C. Jimenez-Sanchidrian, J.M. Hidalgo et al., *Appl. Catal. A* 312 (2006) 86
- 98 C Li, J. Wang et al., *Catal. Commun.* 8 (2007) 1202
- 99 A. Lambert, D.J. Macquarrie et al., *New J. Chem.* 24 (2000) 485
- 100 C. Palazzi, F. Pinna et al., *J. Mol. Catal. A* 151 (2000) 245
- 101 R. Llamas, C. Jimenez-Sanchidrian et al., *Appl. Catal. B* 72 (2007) 18
- 102 A. Bhaumik, P. Kumar et al., *Catal. Lett.* 40 (1996) 47
- 103 A. Corma, L.T. Nemeth *Nature* 412 (2001) 423
- 104 N.N. Trukhan, V.N. Romannikov, E.A. Paukshtis, A.N. Shmakov, and O.A. Kholdeeva, *J. Catal.* 202 (2001) 110
- 105 O.V. Zalomaeva, N.N. Trukhan, I.D. Ivanchikova, A.A. Panchenko, E. Roduner, E.P. Talsi, A.B. Sorokin, V.A. Rogov, O.A. Kholdeeva, *J. Mol. Catal. A: Chemical* 277 (2007) 185
- 106 O.A. Kholdeeva et al., *Catal. Today* 91–92 (2004) 205
- 107 O.A. Kholdeeva et al., *J. Catal.* 236 (2005) 62
- 108 L. Li, T.I. Korányi, B.F. Sels, P.P. Pescarmona, *GreenChem.* 14 (2012) 1611

-
- 109 L. Li, C. Stroobants, K. Lin, P.A. Jacobs, B.F. Sels, P.P. Pescarmona, *Green Chem.* 13 (2011) 1175
- 110 W. Lueangchaichaweng et al. *Catalysis Today* 203 (2013) 66
- 111 M. Taramasso, G. Perego, B. Notari, US Patent 4 410 501, (1983)
- 112 M.J. Frisch, G.W. Trucks, H.B. Schlegel, G.E. Scuseria, M.A. Robb, J.R. Cheeseman, G. Scalmani, V. Barone, B. Mennucci, G.A. Petersson, H. Nakatsuji, M. Caricato, X. Li, H.P. Hratchian, A.F. Izmaylov, J. Bloino, G. Zheng, J.L. Sonnenberg, M. Hada, M. Ehara, K. Toyota, R. Fukuda, J. Hasegawa, M. Ishida, T. Nakajima, Y. Honda, O. Kitao, H. Nakai, T. Vreven, J.A. Montgomery Jr., J.E. Peralta, F. Ogliaro, M. Bearpark, J.J. Heyd, E. Brothers, K.N. Kudin, V.N. Staroverov, R. Kobayashi, J. Normand, K. Raghavachari, A. Rendell, J.C. Burant, S.S. Iyengar, J. Tomasi, M.R. Cossi, N.J. Millam, M. Klene, J.E. Knox, J.B. Cross, V. Bakken, C. Adamo, J. Jaramillo, R.E. Gomperts, O. Stratmann, A.J. Yazyev, R. Austin, C. Cammi, J.W. Pomelli, R. Ochterski, R.L. Martin, K. Morokuma, V.G. Zakrzewski, G.A. Voth, P. Salvador, J.J. Dannenberg, S. Dapprich, A.D. Daniels, O. Farkas, J.B. Foresman, J.V. Ortiz, J. Cioslowski, D.J. Fox, Gaussian 09, Revision A.1: Gaussian, Inc., Wallingford, CT, (2009)
- 113 A.D. Becke, *J.Chem.Phys.* 98 (1993) 5648
- 114 P.J. Stephens, F.J. Devlin, C.F. Chabalowski, M.J. Frisch, *J.Phys.Chem.* 98 (1994) 11623
- 115 J.A. Montgomery Jr., M.J. Frisch, J.W. Ochterski, and G.A. Petersson, *J. Chem. Phys.* 110 (1999) 2822
- 116 A.V. Marenich. C.J. Cramer, D.G. Truhlar, *J. Phys. Chem. B* 13 (2009) 16378
- 117 S. Benson, *Thermochemical Kinetics*; New York, (1968) 8
- 118 M. Boron, A. Corma, M. Renz, P.M. Viruela, *Chem. Eur. J.* 12 (2006) 7067
- 119 A. Prechter, M.R. Heinrich, *Synthesis* 10 (2011) 1515
- 120 R.W. Murray, M. Singh, R. Jeyaraman, *J. Am. Chem. Soc.* 114 (1992) 1346
- 121 Italian patent, MI2009A001842, (assigned to Radici Chimica SPA)
- 122 K.B. Sharpless, K. Akashi, *J. Am. Chem. Soc.* 98 (1976) 1986
- 123 M. Schröder, *Chem. Rev.* 80 (1980) 187
- 124 K. Bergstad, S.Y. Jonsson, J.E. Bäckvall, *J. Am. Chem. Soc.* 121 (1999) 10424
- 125 M. Schwegler, M. Floor, H. Van Bekkum, *Tetrahedron Lett.* 29 (1988) 823
- 126 W.A. Herrmann, R.W. Fischer, D.W. Marz, *Angew. Chem. Int. Ed.* 30 (1991) 1638
- 127 C. Venturello, M. Gambaro, *Synthesis* 4 (1989) 295
- 128 R. Noyori, M. Aoki, K. Sato, *J. Chem. Soc. Chem. Commun.* 16 (2003) 1977
- 129 A. Corma, M.A. Camblor, P. Esteve, A. Martinez, J. Perez-Pariante, *J. Catal.* 145 (1994) 151
- 130 J. Xin, J. Suo, X. Zhang, Z. Zhang, *New J. Chem.* 24 (2000) 569
- 131 M.N. Timofeeva, O.A. Kholdeeva, S.H. Jung, J.-S. Chang, *Appl. Catal. A* 345 (2008) 195
- 132 A. Corma, M.A. Camblor, P. Esteve, A. Martinez, J. Perez-Pariante, *J. Catal.* 145 (1994) 151
- 133 Y. Usui, K. Sato, M. Tanaka, *Angew. Chem. Int. Ed.* 42 (2003) 5623

-
- 134 J.M. Fraile, J.I. Garcia, J.A. Mayoral, E. Vispe, *J. Catal.* 189 (2000) 40
135 B.S. Lane, K. Burgess, *Chem. Rev.* 103 (2003) 2457
136 C. Venturello, R. D'Aloisio, *J. Org. Chem.* 53 (1988) 1553
137 Y. Ishii, K. Yamawaki, T. Ura, H. Yamada, T. Yoshida, M. Ogawa, *J. Org. Chem.* 53 (1988) 3587
138 D.C. Duncan, R.C. Chambers, E. Hecht, C.L. Hill, *J. Am. Chem. Soc.* 117 (1995) 681
139 N.V. Maksimchuk, K.A. Kovalenko, S.S. Arzumanov, Y.A. Chesalov, M.S. Melgunov, A.G. Stepanov, V.P. Fedin, O.A. Kholdeeva, *Inorg. Chem.* 49 (2010) 2920
140 O.A. Kholdeeva, B.G. Donoeva, T.A. Trubitsina, G. Al-Kadamany, U. Kortz, *Eur. J. Inorg. Chem.* 34 (2009) 5134
141 N. Mizuno, K. Kamata, K. Yamaguchi, *Top. Catal.* 53 (2010) 876
142 K. Kaneda, T. Yamashita, T. Matsushita, K. Ebitani, *J. Org. Chem.* 63 (1998) 1750
143 K. Motokura, T. Mizugaki, K. Ebitani, K. Kaneda, *Tetrahedron Lett.* 45 (2004) 6029
144 Z. Opre, J.-D. Grunwaldt, T. Mallat, A. Baiker, *J. Mol. Catal. A* 242 (2005) 224
145 M. Matsumoto, N. Watanabe, *J. Org. Chem.* 49 (1984) 3436
146 D.V. Bavykin, A.A. Lapkin, S.T. Kolaczkowski, P.K. Plucinski, *Appl. Catal. A* 288 (2005) 175
147 K. Yamaguchi, N. Mizuno, *Chem. Eur. J.* 9 (2003) 4353
148 N. Mizuno, K. Yamaguchi, *Catal. Today* 132 (2008) 18
149 M. Totani, T. Koike, K. Yamaguchi, N. Mizuno, *Green Chem.* 8 (2006) 741.
150 F. Vocanson, Y.P. Guoa, J.L. Namya & H.B. Kagan, *Synth. Commun.* 28 (1998) 2577
151 K. Yamaguchi, J. Won Kim, J. He, N. Mizuno, *J. Catal.* 268 (2009) 343
152 T.R. Felthouse, *J. Am. Chem. Soc.* 109 (1987) 7566
153 T. Mallat, A. Baiker, *Chem. Rev.* 104 (2004) 3037
154 C. Donze, P. Korovchenko, P. Gallezot, M. Besson, *Appl. Catal. B* 70 (2007) 621
155 K. Yamaguchi, T. Koike, J. Won Kim, Y. Ogasawara, N. Mizuno, *Chem. Eur. J.* 14 (2008) 11480
156 O. Wallach, *Jus. Lieb. Annalen der Chemie* 437 (1924) 193
157 I. Hermans, J. Peeters, P.A. Jacobs, *Top. Catal.* 48 (2008) 41
158 I. Hermans, J. Peeters, P.A. Jacobs, *Top. Catal.* 50 (2008) 124
159 Y. Hirai, T. Kojima, Y. Mizutani, Y. Shiota, K. Yoshizawa, S. Fukuzumi, *Angew. Chem., Int. Ed.* 47 (2008) 5772
160 Y. Shiota, J.M. Herrera, G. Juhasz, T. Abe, S. Ohzu, T. Ishizuka, T. Kojima, and K. Yoshizawa, *Inorg. Chem.* 50 (2011), 6200
161 Y. Ryabenkova, P.J. Miedzak, N.F. Dummer, S.H. Taylor, N. Dimitratos, D.J. Willock, D. Bethell, D.W. Knight and G.J. Hutchings, *Topics in Catal.* 55 (2012) 1283
162 C.H. Christensen, B. Jørgensen, J. Rass-Hansen, K. Egeblad, R. Madsen, S.K. Klitgaard, S.M. Hansen, M.R. Hansen, H.C. Andersen, A. Riisager, *Angew. Chem. Int. Ed.* 45 (2006) 4648

-
- 163 B. Jørgensen, S.E. Christiansen, M.L.D. Thomsen, C.H. Christensen, *J. Catal.* 251 (2007) 332
- 164 Y.Y. Gorbanev, S.K. Klitgaard, J.M. Woodley, C.H. Christensen, A. Riisager, *ChemSusChem* 2 (2009) 672
- 165 O. Casanova, S. Iborra, A. Corma, *ChemSusChem* 2 (2009) 1138
- 166 M. Blosi, S. Albonetti, M. Dondi, G. Bardi, A. Barzanri, PTC/EP2010/052534/2010
- 167 T. Pasini, M. Piccinini, M. Blosi, R. Bonelli, S. Albonetti, N. Dimitratos, J.A. Lopez-Sanchez, M. Sankar, Q. He, C.J. Kiely, G.J. Hutchings, F. Cavani, *Green Chem.* 13 (2011) 2091
- 168 M. Ammam, *J. Mater. Chem. A* 1 (2013) 6291
- 169 B. El Ali, J.-M. Bregeault, J. Martin, C. Martin, *New J. Chem.* 13 (1989) 173
- 170 A. Atlamsani, J.-M. Bregeault, M. Ziyad, *J. Org. Chem.* 58 (1993) 5663
- 171 L. El Aakel, F. Launay, A. Atlamsani, J.-M. Bregeault, *Chem. Commun.* 21 (2001) 2218
- 172 J.-M. Brégeault, *Dalton Trans.* (2003) 3289
- 173 V.F. Odyakov, E.G. Zhizhina, R.I. Maksimovskaya, K.I. Matveev, *Kinet. Catal.* 36 (1995) 733
- 174 J.K. Lee, J. Melsheimer et al., *App. Catalysis A* 214 (2001) 125
- 175 S. Benadji, P. Eloy, A. Leonard, B.-L. Su, C. Rabia, E.M. Gaigneaux, *Microporous and Mesoporous Mat.* (2012) 153
- 176 A.N. Kharat, S. Moosavikia, B.T. Jahromi, A. Badiei, *J. Mol. Catal. A-Chem.* 348 (2011) 14